PHASES OF SUPERSYMMETRIC GAUGE THEORIES AND GALOIS INVARIANTS

BY ELEONORA DELL'AQUILA

A dissertation submitted to the

Graduate School—New Brunswick

Rutgers, The State University of New Jersey

in partial fulfillment of the requirements

for the degree of

Doctor of Philosophy

Graduate Program in Physics and Astronomy

Written under the direction of

Professor Duiliu-Emanuel Diaconescu

and approved by

_____

_____

_____

_____

_____

New Brunswick, New Jersey

May, 2007

ABSTRACT OF THE DISSERTATION

Phases Of Supersymmetric Gauge Theories And Galois Invariants

by Eleonora Dell'Aquila

Dissertation Director: Professor Duiliu-Emanuel Diaconescu

This thesis deals with the problem of understanding the vacuum structure of supersymmetric gauge theories. More precisely, the theories considered here are $\mathcal{N} = 1$ supersymmetric gauge theories obtained through breaking of part of the supersymmetry from $\mathcal{N} = 2$ gauge theories. The space of vacua of these theories has a very interesting and rich structure, only partly understood. This work proposes a new point of view on this problem, conjecturing a relation between the classification of certain special phases of $\mathcal{N} = 1$ supersymmetric gauge theories and the mathematical problem of classifying a certain kind of graphs - Grothendieck's "dessins s'enfants" - according to the corresponding Galois invariants. The Seiberg-Witten solution of the parent $\mathcal{N} = 2$ theory plays a crucial role in establishing this correspondence.

Acknowledgements

There are a lot of people without whose help and support I would not have been able to do the work that led to this thesis. Sujay, for his confidence in me. Emanuel, who was my first guide to string theory. Emiliano, for his help in navigating the world of physicists. Daniel, for his understanding and encouragement when it was most needed. Freddy, for the nice collaboration that led to the work presented in this thesis.

More people from Rutgers that I would like to thank are Diane, Kathy, Benjamin, Pedro, Rouven, Bogdan, Greg, Mike, Dima, Diwakar, Pankaj, Indrani and Sridhar.

Most of the work in this thesis was done during several visits to Perimeter Institute, Waterloo, Canada. I would like to thank everybody at PI for their warm hospitality. In particular Christian, Jaume, Amihay, little Ella, Freddy, the staff of the Black Hole bistro, Chanda and Filippo.

Finally, I am thankful to my family for accepting my choices, as much as it was possible to them.

Dedication

To B. and L. O.

Table of Contents

Chapter 1

Introduction

The interest in $\mathcal{N} = 2$ supersymmetric gauge theories is especially due to the seminal work of Seiberg and Witten in the mid nineties [46, 47]. They showed that the low energy action and infrared dynamics of the gauge theory on the Coulomb branch can be completely solved and that all the relevant information about the low energy theory is encoded in a hyperelliptic curve and in an associated meromorphic differential. This work led to a tremendous amount of progress in the understanding of the physical aspects of $\mathcal{N} = 2$ gauge theories, including the vacuum structure of related $\mathcal{N} = 1$ theories. At the same time, there have also been fascinating connections between Seiberg-Witten theory and mathematics, especially to the Donaldson theory of four manifolds [53].

The study of the phase structure of $\mathcal{N} = 1$ theories obtained by supersymmetry breaking from $\mathcal{N} = 2$ theories was initiated in [12]. In that paper it was shown that the moduli space of $\mathcal{N} = 1$ vacua obtained this way is composed of several branches that meet at special points. These branches can be distinguished introducing appropriate order parameters. The purpose of this thesis, based on [5,6], is to discuss the possibility that the physical problem of characterizing the vacuum structure of these $\mathcal{N} = 1$ theories might be related to the mathematical problem of classifying "dessins d'enfants" (or "children's drawings") into Galois orbits. The mathematical terminology will be explained in Chapter 2 and in Appendix A

As an introduction, we will give a general review of supersymmetric gauge theory, with particular attention to Seiberg-Witten theory, which will be the main focus of what follows. The discussion in this chapter follows closely [46] and the reviews [1, 34].

In Chapter 2 we will give a pedagogical introduction to the theory of Grothendieck's

dessins d'enfants. We will introduce Belyi maps and show how such maps are related to specific Seiberg-Witten curves. We will also discuss in some detail the order parameters introduced in [12] and construct a dictionary between these order parameters and the Galois invariants used to classify the children's drawings.

We will make the discussion more concrete in Chapter 3, where we will discuss some examples. We will mostly focus on the $\mathcal{N} = 2$ $U(6)$ pure gauge theory without matter and show how the phase structure can be understood from both a physical and a mathematical point of view. We will also discuss briefly some examples of gauge theory with flavour. This latter is probably the most interesting case from a physical point of view, but it is also the least understood so far.

Chapter 4 contains a summary of the discussion of the previous chapters and a list of open questions. Some technical or only marginally relevant material is collected in the appendices.

1.1 Overview Of Supersymmetric Gauge Theories

Supersymmetry has not yet been observed in nature, however there are several reasons for studying supersymmetric theories:

- Supersymmetry is the only extension of Poincaré invariance allowed for an interacting four-dimensional quantum field theory with non-trivial scattering amplitudes[1].

- It is generally recognized that the standard model of particle physics, which is very successful in describing particle physics at the energies probed so far, will need to be extended or replaced by a more complete theory at higher energies. For phenomenological reasons, a supersymmetric extension of the standard model is considered a good candidate for describing the physics that will be observed in the upcoming accelerator experiments.

[1]This statement is known as the Coleman-Mandula theorem [16]

- Supersymmetry leads to fascinating mathematical structures, which are interesting in their own right. Morse theory, Donaldson theory of four-manifolds, etc. are some of the examples in which supersymmetric quantum field theories have played an important role.

- Supersymmetry is also very helpful from a computational point of view, because it makes it possible to obtain non-perturbative results for many quantities of interest. In particular, the supersymmetric version of non-abelian gauge theories is more tractable than the non-supersymmetric counterpart and one can hope to learn more about general phenomena such as asymptotic freedom and chiral symmetry breaking.

Supersymmetric theories are classified according to the number of supersymmetry generators. For our purposes, we will only be interested in $\mathcal{N} = 1$ and $\mathcal{N} = 2$ supersymmetry in four dimensions.

1.1.1 $\mathcal{N} = 1$

The $\mathcal{N} = 1$ supersymmetry algebra in four dimensions contains one spinor supercharge and its conjugate. We write the spinor of the four-dimensional Lorentz group $SL(2,\mathbb{C}) \sim SU(2)_L \times SU(2)_R$ with dotted and undotted components $\psi_\alpha, \psi_{\dot\alpha}$. The spinor indices are raised and lowered with the ϵ-tensor $\epsilon^{\alpha\beta} = \epsilon^{\dot\alpha\dot\beta} = i\sigma_2$, with σ_μ denoting the standard Pauli matrices. Occasionally, when the expression is unambiguous, the indices will be omitted. The four-dimensional metric is $\eta_{\mu\nu} = \mathrm{diag}(1,-1,-1,-1)$. With these conventions, the $\mathcal{N} = 1$ supersymmetry algebra takes the form

$$\begin{aligned} &\{Q_\alpha, \overline{Q}_{\dot\alpha}\} = 2\,(\sigma^\mu)_{\alpha\dot\alpha} P_\mu\,, \\ &\{Q_\alpha, Q_\beta\} = 0 \qquad \{\overline{Q}_{\dot\alpha}, \overline{Q}_{\dot\beta}\} = 0\,, \end{aligned} \tag{1.1}$$

where P_μ is the four-dimensional momentum operator.

The fields of a supersymmetric theory can be arranged in multiplets, according to the representations of the supersymmetry algebra. The supercharges commute with

P_μ, and therefore with P^2, so all states in a given representation have the same mass. For $\mathcal{N}=1$ there are two kinds of mutiplets:

- *Vector multiplet*, containing gauge fields A_μ and a fermion λ, the "gaugino";
- *Chiral multiplets*, containing a scalar field A and a fermion ψ.

It is convenient to use the superspace notation. This is done by introducing one anticommuting spinor coordinate θ_I for each supercharge Q_I. For $\mathcal{N}=1$, the superspace is parametrized by the spacetime coordinates x^μ and the spinors θ_α and $\overline{\theta}_{\dot\alpha}$. We further introduce $y^\mu \equiv x^\mu + i\theta\sigma^\mu\overline{\theta}$. Now we can rearrange the fields in a chiral multiplet in the form of a *chiral superfield*

$$\Phi \equiv A(y) + \sqrt{2}\theta^\alpha\psi_\alpha(y) - \theta^\alpha\theta_\alpha F(y)\,. \tag{1.2}$$

Here F is an auxiliary field required for the off-shell closure of the algebra, which can be eliminated from the action by using the equations of motion. A chiral superfield satisfies the condition

$$\overline{D}_{\dot\alpha}\Phi = 0 \qquad \Big(\text{or} \quad D_\alpha\Phi^\dagger = 0\Big)\,, \tag{1.3}$$

with

$$D_\alpha \equiv \frac{\partial}{\partial\theta^\alpha} + i\sigma^\mu_{\alpha\dot\alpha}\theta^{\dot\alpha}\partial_\mu\,, \qquad \overline{D}_{\dot\alpha} \equiv -\frac{\partial}{\partial\overline{\theta}^{\dot\alpha}} - i\sigma^\mu_{\alpha\dot\alpha}\theta^\alpha\partial_\mu\,. \tag{1.4}$$

The generic action for a chiral superfield can be written in the compact form

$$S_{matter} = \int \mathrm{d}^4x\,\mathrm{d}^4\theta\ K(\Phi,\Phi^\dagger) + \int \mathrm{d}^4x\,\mathrm{d}^2\theta\ f(\Phi) + \int \mathrm{d}^4x\,\mathrm{d}^2\overline{\theta}\ \overline{f}(\Phi^\dagger)\,. \tag{1.5}$$

In this expression K is the *Kähler potential*, which is a real function of the superfield Φ and its complex conjugate. This term gives rise to the kinetic part of the action, with a metric $g_{ij} = \partial^2 K/\partial\Phi_i\partial\Phi_j^\dagger$. A metric of this kind is known as a Kähler metric. Supersymmetry constrains the configuration space to be a Kähler manifold [56]. For flat space, $K(\Phi,\Phi^\dagger) = \Phi^\dagger\Phi$, which gives rise to a free action for massless fields. The other two terms in (1.5) determine the interactions and they depend on the choice of a *superpotential* f, which is a holomorphic function of Φ. The action (1.5) is automatically supersymmetric and can be written in terms of the fields A and ψ by expanding the superfields in $\theta,\overline{\theta}$ and performing the integration over these variables.

A similar discussion can be repeated for the fields in the vector multiplet. We introduce a real vector superfield[2]

$$W = W^\dagger \equiv -\theta\sigma^\mu\overline{\theta}A_\mu + i\theta^2\overline{\theta}\,\overline{\lambda} - i\overline{\theta}^2\theta\,\lambda + \frac{1}{2}\theta^2\overline{\theta}^2 D\,, \tag{1.6}$$

where D is an auxiliary field. The abelian gauge transformations for the fields in the vector multiplet are implemented by

$$W \to W + \Lambda + \Lambda^\dagger\,, \tag{1.7}$$

with Λ a chiral superfield. The abelian field strength is defined as

$$\mathcal{W}_\alpha \equiv -\frac{1}{4}\overline{D}^2 D_\alpha W\,, \qquad \overline{\mathcal{W}}_{\dot\alpha} \equiv \frac{1}{4}D^2\overline{D}_{\dot\alpha}W\,, \tag{1.8}$$

with D and $\overline{D}$ as defined in (1.4). Note that $\mathcal{W}$ is a chiral superfield. In the non-abelian case W belongs to adjoint representation of the gauge group: $W = W_A T^A$. The gauge transformation is then implemented by

$$e^{-2W} \to e^{-i\Lambda^\dagger}e^{-2W}e^{i\Lambda}\,, \qquad \text{with} \qquad \Lambda = \Lambda_A T^A\,. \tag{1.9}$$

The non-abelian field strength is

$$\mathcal{W}_\alpha \equiv \frac{1}{8}\overline{D}^2 e^{2W} D_\alpha e^{-2W}\,. \tag{1.10}$$

A gauge invariant and supersymmetric action for the vector multiplet can be written in the form

$$S_{gauge} = \frac{1}{8\pi}\int \mathrm{d}^4x\,\mathrm{Im}\left(\tau\,\mathrm{d}^2\theta\,\mathrm{Tr}\mathcal{W}_\alpha\mathcal{W}^\alpha\right)\,, \tag{1.11}$$

where the dimensionless coupling

$$\tau = \frac{\theta}{2\pi} + i\frac{4\pi}{g^2} \tag{1.12}$$

combines the coupling constant and the theta angle of the gauge theory. Written in components, the action (1.11) becomes

$$S_{gauge} = \int \mathrm{d}^4x\,\left(\frac{1}{4\pi g^2}F^A_{\mu\nu}F^{A\mu\nu} + \frac{\theta}{32\pi^2}F^A_{\mu\nu}\tilde{F}^{A\mu\nu} + \frac{1}{2g^2}(D^AD^A - 2i\lambda^A\sigma^\mu D_\mu\overline{\lambda}^A)\right)\,, \tag{1.13}$$

[2]This is the expression in the so called Wess-Zumino gauge.

where D_μ is the usual covariant derivative.

Finally, a general $\mathcal{N}=1$ action for a vector multiplet coupled to a chiral multiplet can be written as

$$S_{total} = \int \mathrm{d}^4x \left[\frac{1}{8\pi} \mathrm{Im}\,\tau\,\mathrm{Tr} \int \mathrm{d}^2\theta\, \mathcal{W}_\alpha \mathcal{W}^\alpha + \int \mathrm{d}^4\theta\, \Phi^\dagger e^{-2W} \Phi + \int \mathrm{d}^2\theta\, f + \int \mathrm{d}^2\overline{\theta}\, \overline{f} \right], \tag{1.14}$$

where Φ is chosen to belong to some representation of the gauge group, for example the fundamental representation.

1.1.2 $\mathcal{N}=2$

The $\mathcal{N}=2$ supersymmetry algebra in four dimensions contains two spinor supercharges and their conjugates. The general supersymmetry algebra, including a central charge [54], is

$$\begin{aligned} \{Q^I_\alpha, \overline{Q}_{\dot\beta J}\} &= 2\,(\sigma^\mu)_{\alpha\dot\beta}\, P_\mu\, \delta^I_J\,, \\ \{Q^I_\alpha, Q^J_\beta\} &= 2\sqrt{2}\,\epsilon_{\alpha\beta}\,\epsilon^{IJ}\,Z\,, \\ \{\overline{Q}_{\dot\alpha I}, \overline{Q}_{\dot\beta J}\} &= 2\sqrt{2}\,\epsilon_{\dot\alpha\dot\beta}\,\epsilon_{IJ}\,Z\,, \end{aligned} \tag{1.15}$$

where Z is the central charge. One finds that for representations containing massless states the central charge has to vanish. For massive states, there is a bound on the mass $M \geq \sqrt{2}|Z|$. The inequality is satisfied by states in the so called *BPS* or *short representations*, which give rise to multiplets that contain fewer states than a generic massive multiplet [54].

$\mathcal{N}=2$ theories contain two kinds of multiplets:

- *Vector multiplets*, containing gauge fields A_μ, two Weyl fermions λ and ψ and a scalar A. In terms of $\mathcal{N}=1$ representations these fields form a vector multiplet $(A_\mu,\, \lambda)$ and a chiral multiplet $(A,\, \psi)$.

- *Hypermultiplets*, containing two Weyl fermions ψ_q and $\psi^\dagger_{\tilde q}$ and two complex bosons q and $\tilde q^\dagger$. In terms of $\mathcal{N}=1$ representations these fields make up two chiral multiplets $(q,\, \psi_q)$ and $(\tilde q^\dagger,\, \psi^\dagger_{\tilde q})$.

Pure Super-Yang-Mills

It is possible to introduce $\mathcal{N}=2$ superfields and write a supersymmetric action in a very compact form. However, we can also use the $\mathcal{N}=1$ notation and write the action in terms of the $\mathcal{N}=1$ superfields that make up the $\mathcal{N}=2$ multiplets. If we denote by Φ and W_α the chiral and vector superfileds that compose an $\mathcal{N}=2$ vector multiplet, we can write an action of the form

$$S_{\text{gauge}} = \frac{1}{4\pi}\text{Im}\int \mathrm{d}^4x\,\mathrm{d}^4\theta\,(\Phi^\dagger e^{2gW})^A\,\frac{\partial\mathcal{F}(\Phi)}{\partial\Phi^A} + \frac{1}{8\pi}\text{Im}\int \mathrm{d}^4x\,\mathrm{d}^2\theta\,\frac{\partial^2\mathcal{F}(\Phi)}{\partial\Phi^A\partial\Phi^B}\mathcal{W}^{A\alpha}\mathcal{W}^B_\alpha\,, \tag{1.16}$$

where $\mathcal{F}$ is a function of Φ known as *prepotential*. Note that in this case the Kähler potential is $K = \Phi^{\dagger A}\mathcal{F}_A(\Phi)$. The corresponding metric in this case is known as a special Kähler metric. Thus $\mathcal{N}=2$ supersymmetry further constrains the geometry of the configuration space to be special Kähler [18, 24, 51]. All the fields appearing in (1.16) must be in the adjoint representation of the gauge group, since they belong to the same $\mathcal{N}=2$ multiplet as the gauge field. The capital letters are used for the Lie algebra indices.

The action S_{gauge} possess $\mathcal{N}=2$ supersymmetry only if the coefficients in front of the two terms are related as in (1.16). In addition, the superpotential for the chiral superfield Φ needs to be set to zero. Turning on a superpotential $f(\Phi)$ would break supersymmetry from $\mathcal{N}=2$ to $\mathcal{N}=1$.

For the analysis to follow in Section 1.2, we will need some information about the supersymmetric vacua of $\mathcal{N}=2$ super-Yang-Mills theory, in particular with gauge group $SU(2)$. First, note that the bosonic part of (1.16) simply describes a charged scalar field A coupled to a gauge field A_μ. A model of this kind contains magnetic monopoles, if the scalar acquires a nonzero expectation value in the vacuum and the gauge field has a topologically nontrivial configuration [27, 41, 52]. In term of the component fields, choosing $\mathcal{F} = \tau\Phi^2$, the action (1.16) takes the form

$$\begin{aligned} S_{\text{gauge}} = \frac{1}{g^2}\int \mathrm{d}^4x\ \text{Tr}\big(&-\frac{1}{4}F^{\mu\nu}F_{\mu\nu} + g^2\frac{\theta}{32\pi^2}F^{\mu\nu}\tilde{F}_{\mu\nu} + (D_\mu A)^\dagger D^\mu A \\ &-\frac{1}{2}[A^\dagger, A]^2 - i\lambda\,\sigma^\mu D_\mu\overline{\lambda} - i\overline{\psi}\,\overline{\sigma}^\mu\ D_\mu\psi - i\sqrt{2}\,[\lambda,\psi]A^\dagger - i\sqrt{2}\,[\overline{\lambda},\overline{\psi}]A\big)\,. \end{aligned} \tag{1.17}$$

The scalar potential is

$$V = -\frac{1}{2g^2}\mathrm{Tr}[A^\dagger,\, A]^2\,, \tag{1.18}$$

and the minimum of the potential is determined by the condition

$$[A^\dagger, A] = 0\,. \tag{1.19}$$

In addition, the condition $D_\mu A = 0$ needs to be satisfied in the vacuum, so the Higgs vacuum is parametrized by non-zero constant configuration of A such that A commutes with $A^\dagger$.

The general solution of the condition (1.19) for a gauge group $G = SU(N)$ is discussed in [**?**, 2, 3, 22, 33]. From (1.19) it follows that A takes value in the Cartan subalgebra $H$of the gauge group, so generically the gauge group is broken to G/H. The correct parametrization of the moduli space of vacua, taking into account the gauge redundancy, is given by the Weyl invariant[3] functions constructed from from A, usually denoted as u_k. In Section 1.2 we will mostly focus on the $SU(2)$ example discussed in [46]. In this case we can take $A = \frac{1}{2}a\sigma_3$ and the unique Weyl invariant function is $u \equiv \langle \mathrm{Tr}A^2\rangle = \frac{1}{2}a^2$.

When a is nonzero one can check [54] that the central charge Z in the supersymmetry algebra takes the value

$$Z = ae(n + m\tau)\,, \tag{1.20}$$

where e is the electric charge, and n and m are the units of electric and magnetic charge respectively. The inequality $M \geq \sqrt{2}|Z|$ then becomes the well known Bogomol'nyi bound [9, 42].

Super-Yang-Mills With Flavour

If we want to couple (1.16) with $SU(N_c)$ gauge group to N_f matter fields in the fundamental representation, to write a supersymmetric version of QCD, we can introduce

[3]Here Weyl invariant means invariant under the Weyl reflections of the Lie algebra, which are the transformations that change A preserving the condition (1.19).

N_f hypermultiplets and add to S_{gauge} a matter component of the form

$$S_{\text{matter}} = \int \mathrm{d}^4x\, \mathrm{d}^4\theta \sum_{i=0}^{N_f} (Q_i^\dagger e^{-2W} Q_i + \tilde{Q}_i e^{2W} \tilde{Q}_i^\dagger) + \int \mathrm{d}^4x\, \mathrm{d}^2\theta \sum_{i=0}^{N_f} (\sqrt{2}\, \tilde{Q}_i \Phi Q_i + m\, \tilde{Q}_i Q_i) + \, c.c. \quad (1.21)$$

where Q_i and $\tilde{Q}_i$ are two $\mathcal{N} = 1$ superfields that make up a hypermultiplet. The coefficients of the various terms in (1.21) are chosen to ensure $\mathcal{N} = 2$ supersymmetry.

The vacuum structure is more complicated than in the case without flavour, because the scalars q_i and $\tilde{q}_i$ can also acquire a vacuum expectation value. If all the quark masses are zero, then it is found that the vacuum expectation value of these scalars must vanish and the earlier discussion still applies. However, if some quarks are massive, we need to distinguish two cases:

- $N_f < N_c$: the gauge group $SU(N_c)$ is broken to $SU(N_c - N_f)$. $2N_fN_c - N_f^2$ quark superfileds become heavy and the remaining N_f^2 remain massless.
- $N_f \geq N_c$: the gauge group is completely broken.

The formula (1.20) for the central charge is modified by including an additional term depending on the quark masses.

1.2 The Seiberg-Witten Solution Of The $\mathcal{N} = 2$ Super-Yang-Mills Theory

In this section we give a very brief review of the work of Seiberg and Witten, following [1]. We focus on $SU(2)$ Super-Yang-Mills theory without flavour, as in the the original Seiberg-Witten article [46]. The more general results will be summarized at the end of the section.

1.2.1 Low-Energy Effective Action

We consider the $\mathcal{N} = 2$ super-Yang-Mills theory in the vacuum discussed in Section 1.1.2. This vacuum is supersymmetric, so the low-energy effective description of the

theory can be given in terms of an $\mathcal{N}=2$ supersymmetric effective action. This will contain only the massless fields and in principle it can be obtained by integrating out all the modes above a set cutoff. However, as shown in [46], the low-energy effective action can be also determined through some arguments based on supersymmetry.

Since the effective action is $\mathcal{N}=2$ supersymmetric, it is completely determined by the prepotential $\mathcal{F}$. Also, the metric on the moduli space of vacua is

$$\mathrm{d}s^2 = \mathrm{Im}\frac{\partial^2\mathcal{F}}{\partial a^2}. \tag{1.22}$$

Recall that in the classical theory $\mathcal{F}=\tau\Phi^2$, so the metric on the moduli space is $\mathrm{d}s^2=\mathrm{Im}\,\tau a^2$, where a^2 parametrizes the space of vacua, as discussed in Section 1.1.2. What we need to do is determine the quantum corrections to $\mathcal{F}$.

It is known that, because of $\mathcal{N}=2$ supersymmetry, the prepotential does not receive any perturbative correction at more than one loop [39, 44]. The one loop computation can be bypassed using an argument based on the behaviour of the effective action under an R-symmetry transformation. The result is [44]

$$\mathcal{F}_{1-\mathrm{loop}}(\Phi) = \frac{i}{2\pi}\Phi^2\ln\frac{\Phi}{\Lambda} \equiv \tau_{eff}\Phi^2\,, \tag{1.23}$$

where Λ is a dynamically generated scale, like in QCD. In addition, there are non-perturbative corrections due to instantons. A correction from a configuration with instanton number k is weighted by $\exp(-8\pi^2k/g^2)$, and it is found that

$$e^{-8\pi^2k/g^2} = \left(\frac{\Lambda}{a}\right)^{4k}. \tag{1.24}$$

In conclusion, fixing the coefficient of (1.24) by another R-symmetry argument, the final answer is

$$\mathcal{F}(\Phi) = \frac{1}{2\pi}\Phi^2\ln\frac{\Phi^2}{\Lambda^2} + \sum_{k=1}^{\infty}\mathcal{F}_k\,\Phi^2\left(\frac{\Lambda}{\Phi}\right)^{4k}, \tag{1.25}$$

where the coefficients $\mathcal{F}_k$ are constants. Thus the main problem in solving the theory is to find the coefficients $\mathcal{F}_k$. This problem was solved by Seiberg and Witten in [46] and we will discuss the path that leads to their solution in the next sections.

From (1.23) we can calculate, for large $|a|$,

$$\tau(a) \equiv \frac{\partial^2\mathcal{F}}{\partial a^2} = \frac{i}{\pi}(\ln\frac{a^2}{\Lambda^2}+3)\,. \tag{1.26}$$

From this expression one can see that $\tau(a)$ is defined only locally on the moduli space, so we need an alternative description of the theory for the regions where $\tau(a)$ is not well defined. The alternative description can be obtained through electromagnetic duality, which is discussed next.

1.2.2 Electromagnetic Duality

Electromagnetic duality is the statement that a theory has two equivalent descriptions: one with electrically charged particles in the perturbative spectrum and another with magnetically charged particles in the perturbative spectrum [26, 35, 40]. A form of electromagnetic duality holds for $\mathcal{N} = 2$ super-Yang-Mills theory [46].

Classically, the duality transformation replaces the gauge filed which couples to electric charges with a gauge field that couples to magnetic charges and at the same time transforms the gauge coupling as

$$\tau \to \tau_D = -\frac{1}{\tau}\,. \tag{1.27}$$

We will see in what sense the duality holds at the quantum level. The theory is also invariant under $\tau \to \tau + 1$, so the full duality group is $SL(2,\mathbb{Z})$, which acts on the coupling as

$$\tau \to \frac{a\tau + b}{c\tau + d}\,, \quad \text{with} \quad ab - cd = 1\,, \quad a, b, c, d \in \mathbb{Z}\,. \tag{1.28}$$

Because of supersymmetry, the duality transformation also acts on the scalar that belongs to the same multiplet as the gauge field. If we introduce the dual variable $A_D \equiv \frac{\partial \mathcal{F}}{\partial A}$, the action of the duality group on A and A_D is simply

$$\begin{pmatrix} A_D \\ A \end{pmatrix} \to \begin{pmatrix} a & b \\ c & d \end{pmatrix} \begin{pmatrix} A_D \\ A \end{pmatrix}\,. \tag{1.29}$$

In terms of the variables a and a_D the classical metric on the moduli space can be rewritten as

$$\mathrm{d}s^2 = \mathrm{Im}\,\mathrm{d}a_D \mathrm{d}\overline{a} = -\frac{i}{2}(\mathrm{d}a_D \mathrm{d}\overline{a} - \mathrm{d}a \mathrm{d}\overline{a}_D)\,. \tag{1.30}$$

Note that this expression is invariant under the $SL(2,\mathbb{Z})$ transformation above. More precisely, since for the $SU(2)$ gauge theory we haven chosen the coordinate $u = \langle \mathrm{Tr} A^2 \rangle$

on the moduli space, we can write

$$\mathrm{d}s^2 = \mathrm{Im}\,\frac{\mathrm{d}a_D}{\mathrm{d}u}\frac{\mathrm{d}\overline{a}}{\mathrm{d}\overline{u}}\mathrm{d}u\mathrm{d}\overline{u} = -\frac{i}{2}\left(\frac{\mathrm{d}a_D}{\mathrm{d}u}\frac{\mathrm{d}\overline{a}}{\mathrm{d}\overline{u}} - \frac{\mathrm{d}a}{\mathrm{d}\overline{u}}\frac{\mathrm{d}\overline{a}_D}{\mathrm{d}u}\right)\mathrm{d}u\mathrm{d}\overline{u}\,. \tag{1.31}$$

1.2.3 Monodromies

If the moduli space has a nontrivial structures, then there might be a nontrivial monodromy group that acts on (a_D, a) when going around a closed loop on the u plane. Some constraints on what the monodromy group can be come from the formula for the mass of BPS dyons, $M = \sqrt{2}|Z|$. In terms of (a_D, a), it is possible to rewrite the central charge Z as

$$Z = an_e + a_D n_m\,. \tag{1.32}$$

This expression is invariant under the duality transformation, because n_e, n_m transform inversely than in (1.29) and moreover, it has the property of being renormalization group invariant. Since Z determines a physical mass, it has to be also invariant under the monodromies and analyzing this requirement, one finds that the monodromy group must be a subgroup of $SL(2,\mathbb{Z})$.

One point around which we might expect a nontrivial monodromy is $u = \infty$. At large u (and hence large $|a|$), the one-loop formula (1.23) for the prepotential is a good approximation, so we have

$$a_D = \frac{\partial\mathcal{F}}{\partial a} = \frac{2ia}{\pi}\ln\left(\frac{a}{\Lambda}\right) + \frac{ia}{\pi}\,. \tag{1.33}$$

If we make a closed loop around $u = 0$, we get $a_D \to -a_D + 2a$ and $a \to -a$, so we can write a monodromy matrix

$$M_\infty = \begin{pmatrix} -1 & 2 \\ 0 & -1 \end{pmatrix} \tag{1.34}$$

that acts on the column vector $(a_D, a)^T$.

Since there is a monodromy at infinity, there must be other monodromies somewhere else on the u-plane. It turns out that for the gauge group $SU(2)$ there are exactly two other singular points, related by the discrete symmetry $u \to -u$, say at $u = \pm 1$. Physically, these singularities are interpreted in [46] as points where some non-perturbative

states become massless. With this assumption, the corresponding monodromy matrices can be determined. We don't repeat the details of the discussions here, but just give the result:

$$M_1 = \begin{pmatrix} 1 & 0 \\ -2 & 1 \end{pmatrix}, \quad M_{-1} = \begin{pmatrix} -1 & 2 \\ -2 & 3 \end{pmatrix}. \tag{1.35}$$

One can check that $M_1 M_{-1} = M_\infty$.

1.2.4 The Seiberg-Witten Curve

One of the central points of [46] is that the moduli space of the $\mathcal{N} = 2$ super-Yang-Mills theory with gauge group $SU(2)$ can be identified with the moduli space of a genus one Riemann surface, known in this context as the Seiberg-Witten curve. This is crucial in obtaining the complete solution of the theory.

The identification comes from the fact that, as the analysis summarized so far has revealed, the moduli space of vacua can be described as the u-plane with singularities at $1, -1, \infty$, a discrete $\mathbb{Z}_2$ symmetry $u \to -u$ and the monodromies described earlier. In other words, the moduli space is $H/\Gamma(2)$, where H denotes the upper half complex plane and $\Gamma(2)$ is the subgroup of $SL(2,\mathbb{Z})$ generated by the matrices (1.34) and (1.35). The space $H/\Gamma(2)$ also parametrizes the family of curves

$$E_u : \quad y^2 = (x-1)(x+1)(x-u), \tag{1.36}$$

where $u \in H/\Gamma(2)$ and x, y are complex variables. This is the Seiberg-Witten curve for $SU(2)$ super-Yang-Mills theory without matter.

The equation (1.36) describes an elliptic curve, i.e. a genus one Riemann surface. To see this, note that for y to be a single valued function, the x-space must be a double cover of the complex sphere. There are four branching points, connected by two cuts as shown in Figure 1.1. The two sheets that form the x-space are connected through these cuts. One can convince oneself that this kind of structure signals that the x-space is a torus: the a-cycle of the torus corresponds on the complex plane to a contour that circles one of the two cuts; the b-cycle, instead, corresponds to a contour that circles two branch points intersecting both cuts (Figure 1.1). As we will see, many properties of the gauge theory can be encoded in properties of this curve.

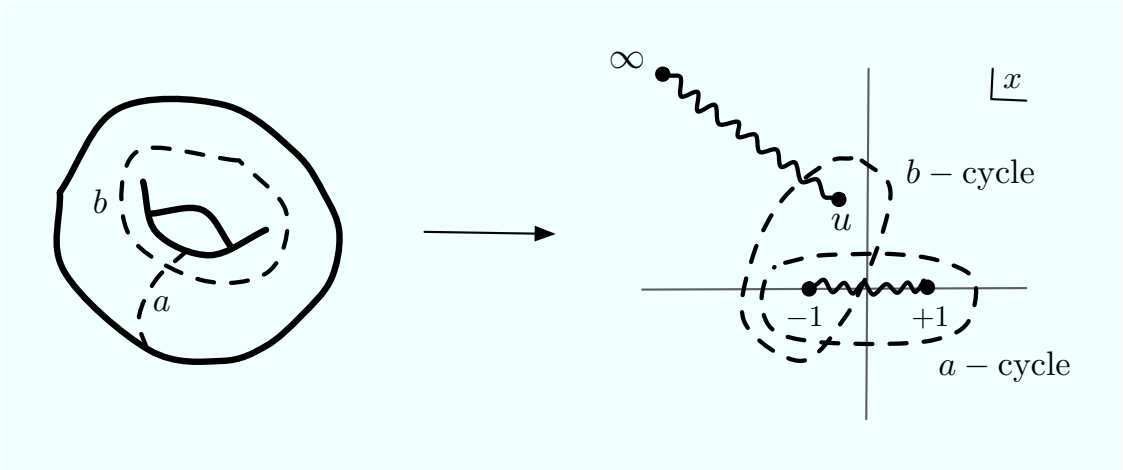

Figure 1.1: Representation of the $SU(2)$ Seiberg-Witten curve on the x-plane.

There are many physically equivalent ways to rewrite the curve (1.36). For example, we can reintroduce the scale Λ, that was previously set to one, and redefine the coordinates so that the branch points are at

$$x_1 = \sqrt{u + 2\Lambda^2} \qquad x_2 = \sqrt{u - 2\Lambda^2}$$
$$x_3 = -\sqrt{u + 2\Lambda^2} \qquad x_4 = -\sqrt{u - 2\Lambda^2}\,. \tag{1.37}$$

Then we can write the equation of the $SU(2)$ Seiberg-Witten curve as

$$y^2 = \prod (x - x_i) = (x^2 - u)^2 - 4\Lambda^4\,. \tag{1.38}$$

As we will see later, this expression is easily generalized to the case of a $SU(N)$ (or $U(N)$) gauge theory.

1.2.5 Monopole Condensation And Confinement

Some features of $\mathcal{N} = 1$ theories can also be understood within the $\mathcal{N} = 2$ Seiberg-Witten formalism. This is usually referred to as the strong coupling analysis [11, 14] and will be very important for the discussion in the next chapters.

As we saw, the $\mathcal{N} = 2$ vector multiplet can be thought of as being made out of a $\mathcal{N} = 1$ vector multiplet A and a$\mathcal{N} = 1$ chiral multiplet Φ. We can break supersymmetry from $\mathcal{N} = 2$ to $\mathcal{N} = 1$ by adding to the action (1.16) a superpotential $W(\Phi)$. For

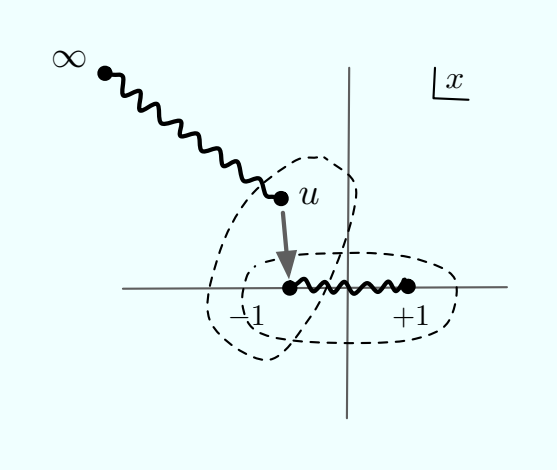

Figure 1.2: When the two branch points collide the corresponding cycle of the Seiberg-Witten curve shrinks to zero. At this point in the moduli space a monopole becomes massless.

example, adding a superpotential $m\mathrm{Tr}\Phi^2$ gives a bare mass to the fields in the chiral multiplet, so that the low energy theory is a pure abelian gauge theory. In the $SU(2)$ case we are considering, the theory exhibits spontaneous chiral symmetry breaking from $\mathbb{Z}_4$ to $\mathbb{Z}_2$ and it is believed to have a mass gap and be confining.

Let us discuss how one can see these features of the $\mathcal{N} = 1$ theory from the point of view of the $\mathcal{N} = 2$ low-energy effective action. For small m, the theory can be simply modified by adding a term $\langle \mathrm{Tr}\phi^2 \rangle$ to the effective action. However, we also need a mechanism that makes the gauge field massive, to realize the expected mass gap. This point was discussed in [46] and the conclusion is that the $\mathcal{N} = 1$ vacuum must correspond to a point in the $\mathcal{N} = 2$ moduli space where a light charged field becomes massless, allowing a form of Higgs mechanism to take place. If the charged field that becomes massless is a monopole, then we have a magnetic Higgs mechanism, with magnetic monopoles condensing in the vacuum. In this case the magnetic equivalent of the Meissner effect gives rise to confinement of electric charges.

As we will see in the next section, the mass of BPS monopoles can be computed as integrals over the b-cycles of the Seiberg-Wittem curve. Therefore the points in the moduli space where massless monopoles appear are those points where such cycles

shrink to zero. In the $SU(2)$ case there is only one degenerate point, where two branch points collide as shown in Figure 1.2. This is the point of the $\mathcal{N}=2$ moduli space that corresponds to the $\mathcal{N}=1$ vacuum.

A similar statement, i.e. the fact that the $\mathcal{N}=1$ vacua correspond to points in the moduli space where the Seiberg-Witten curve degenerates, still holds for more general superpotentials and gauge groups. We will return to this point in Section 1.3.

1.2.6 The Solution Of The Model

Let us now return to the $\mathcal{N}=2$ theory. Solving the model means finding an explicit formula for a and a_D as functions of u. This would give an exact expression for the dyon masses and for the metric on the moduli space. The solution found by Seiberg and Witten involves rephrasing the problem from a geometric point of view, in terms of data of the Riemann surface E_u in (1.36).

The first step is to pick a basis $\{\gamma_1, \gamma_2\}$ of one cycles on E_u, such that their intersection number is one: $\gamma_1 \cdot \gamma_2 = 1$. We also pick a corresponding basis of one-forms

$$\lambda_1 = \frac{\mathrm{d}x}{y}\,, \quad \lambda_2 = \frac{x\mathrm{d}x}{y}\,. \tag{1.39}$$

Then we consider an arbitrary linear combination

$$\lambda = a_1(u)\lambda_1 + a_2(u)\lambda_2\,, \tag{1.40}$$

and make the identification

$$a_D = \oint_{\gamma_1} \lambda\,, \qquad a = \oint_{\gamma_2} \lambda\,. \tag{1.41}$$

The differential λ is called the Seiberg-Witten differential. The explicit form of λ such that (1.41) holds can be determined to be [46]

$$\lambda = \frac{\sqrt{2}}{\pi}\frac{\sqrt{x-u}}{\sqrt{x^2-1}}\,\mathrm{d}x \tag{1.42}$$

and this leads to the following formulae for $a(u)$ and $a_D(u)$:

$$a(u) = \frac{\sqrt{2}}{\pi}\int_{-1}^{1}\mathrm{d}x\,\frac{\sqrt{x-u}}{\sqrt{x^2-1}}\,, \qquad a_D(u) = \frac{\sqrt{2}}{\pi}\int_{1}^{u}\mathrm{d}x\,\frac{\sqrt{x-u}}{\sqrt{x^2-1}}\,. \tag{1.43}$$

These integrals can be written explicitly in terms of elliptic functions, so it is possible to write $a(u)$ and $a_D(u)$ in closed form. We can then obtain the low-energy prepotential, as discussed earlier, and compute from it all quantities of interest.

1.2.7 Generalizations

The Seiberg-Witten approach to $\mathcal{N} = 2$ gauge theories can be applied to theories with any gauge group, with and without matter. In each case it is possible to introduce an appropriate manifold such that all the relevant physical information about the low-energy theory can be recovered from it. We briefly summarize the known results that we will use in the later sections.

For a theory without matter and with $SU(N)$ gauge group[4] the manifold can be represented as [3, 32, 33]

$$y^2 = P_N^2(z) - 4\Lambda^{2N}\,, \tag{1.44}$$

where $P_N(z) = \langle \det(z\mathbb{I} - \Phi) \rangle$. This generalizes the expression (1.38) for the $SU(2)$ Seiberg-Witten curve. The manifold (1.44) is a genus $N-1$ hyperelliptic curve. As before, the curve can be represented by the two-sheeted x-plane, with cuts between the roots of y (Figure 1.3).

Finally, for a theory with N_f flavours and $SU(N)$ gauge group, the equation of the Seiberg-Witten curve is [4, 29]

$$y^2 = P_N^2(z) + B_{N_f}(z)\,, \tag{1.45}$$

with

$$B_{N_f}(z) = -4\Lambda^{2N-L} \prod_{i=1}^{N_f} (z + m_i)\,, \tag{1.46}$$

where the m_i's are the quark masses.

[4]The Seiberg-Witten curve is the same for the $U(N)$ and $SU(N)$ gauge groups, except for an additional constraint (vanishing of the trace) on $\langle \det(z\mathbb{I} - \Phi) \rangle$ in the second case.

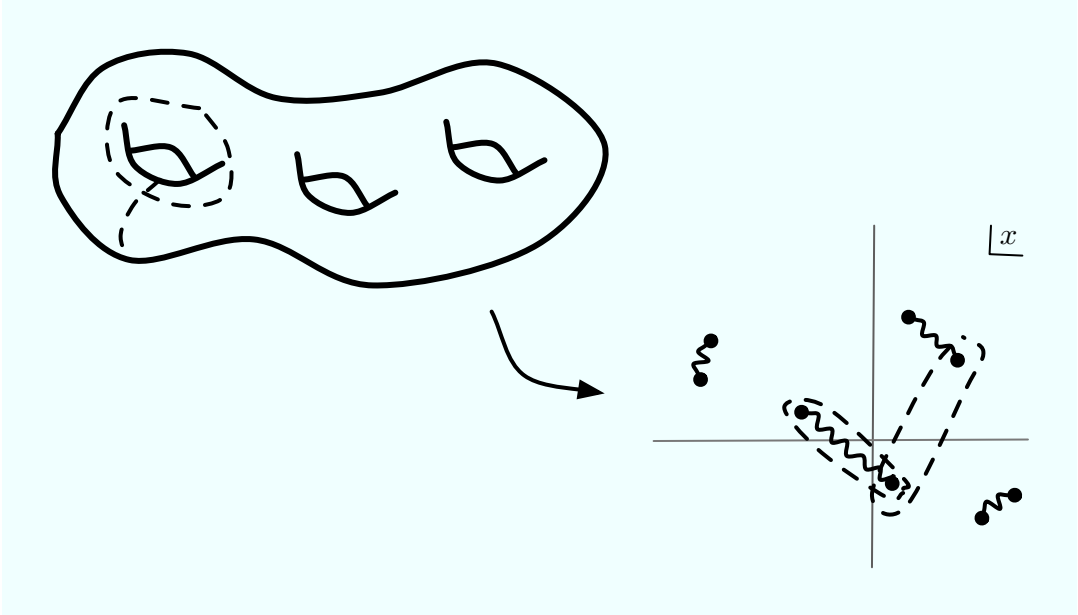

Figure 1.3: The $SU(4)$ Seiberg-Witten curve and its representation on the x-plane. It is a genus three hyperelliptic curve.

1.3 Factorization Of The Seiberg-Witten Curve And Breaking To $\mathcal{N} = 1$

In the Seiberg-Witten solution of $\mathcal{N} = 2$ gauge theories it is natural to study the loci in the moduli space where the SW curve develops singularities. For a pure $U(N)$ gauge theory - the most well studied case - as we saw the curve has the form

$$y^2 = P_N^2(z) - 4\Lambda^{2N}\,, \tag{1.47}$$

with $P_N(z) = \langle \det(z\mathbb{I} - \Phi) \rangle$. One class of degenerate curves that we will study extensively is [12]:

$$P_N^2(z) - 4\Lambda^{2N} = F_{2n}(z)\, H_{N-n}^2(z)\,. \tag{1.48}$$

(For all polynomials we adopt the usual notation, with the subscripts denoting the degree of the polynomials.) Let us briefly discuss the physical information that is encoded in this kind of polynomial equation.

The $\mathcal{N} = 2$ Coulomb moduli space of the gauge theory is parametrized by N parameters $u_k = \frac{1}{k}\langle \mathrm{Tr}\Phi^k \rangle$, constructed from the adjoint scalar Φ. A problem studied in

the physics literature is to find and classify the $\mathcal{N}=1$ supersymmetric vacua obtained by perturbing the $\mathcal{N}=2$ theory by a tree level superpotential

$$W_{\rm tree} = \sum_{k=1}^{n+1} \frac{g_k}{k} \, {\rm Tr}\Phi^k \, . \tag{1.49}$$

It is known [11, 17] that once the tree level potential is introduced, all points in the Coulomb moduli space are lifted except those for which $N-n$ mutually local magnetic monopoles become massless (see also Section 1.2.5). The superpotential triggers the condensation of monopoles and the magnetic Higgs mechanism leads to confinement of the electric charges. The points at which this occurs are precisely those that solve the factorization problem (1.48). At low energies at these points, out of the original $U(1)^N$ only a $U(1)^n$ subgroup remains unbroken and its coupling constants are given by the reduced Seiberg-Witten curve

$$y^2 = F_{2n}(z) \, . \tag{1.50}$$

From a simple counting of parameters, we see that (1.48) defines an n-dimensional subspace of the moduli space. Plugging the u_k's as functions of these n parameters into the superpotential $W_{\rm tree}$, one gets an effective superpotential

$$W_{\rm eff} = \sum_{k=1}^{n+1} g_k \, u_k \tag{1.51}$$

on the moduli space. Thus, given the parameters g_k, one can vary with respect to the coordinates on the moduli space and obtain *all* the u_k's as functions of the g_k's and Λ.

In other words, the form of the superpotential picks out specific points in the $\mathcal{N}=2$ moduli space which correspond to $\mathcal{N}=1$ vacua. It was shown in [11, 14] that this extremization problem can be rephrased as the problem of factorizing the Seiberg-Witten curve in the following manner:

$$P_N^2(z) - 4\Lambda^{2N} = \frac{1}{g_{n+1}^2} \Big((W'_{\rm tree}(z))^2 + f_{n-1}(z) \Big) \, H_{N-n}^2(z) \, . \tag{1.52}$$

Let us denote the critical points of $W_{\rm tree}$ by a_i, i.e., $W'_{\rm tree}(z) = \prod_{i=1}^n \, g_{n+1}(z-a_i)$. We set $g_{n+1}=1$ in what follows.

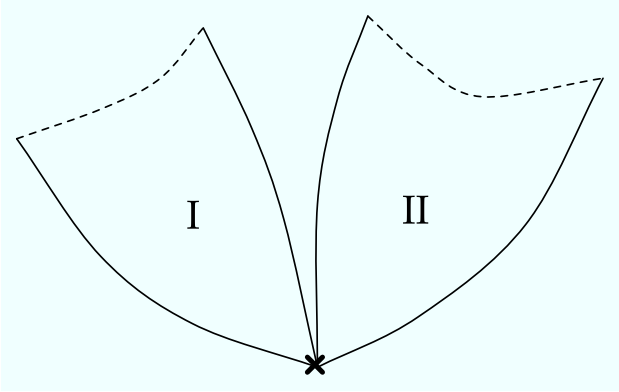

Figure 1.4: Two $\mathcal{N} = 1$ branches of the $U(4)$ gauge theory obtained by deforming the $\mathcal{N} = 2$ theory by a cubic superpotential. Only those branches with two $U(1)$'s in the infrared are shown. The two branches meet at a point where one more monopole becomes massless.

1.3.1 The Moduli Space Of $\mathcal{N} = 1$ vacua.

It is interesting to ask what the "moduli space" of $\mathcal{N} = 1$ vacua is, as the parameters g_k's are varied. The motivation for such a question was explained in [12]: semiclassically, as $\Lambda \to 0$, the gauge group $U(N)$ can be broken to $\prod_{i=1}^{n} U(N_i)$ with $\sum_{i=1}^{n} N_i = N$ by choosing Φ to be a diagonal matrix with N_i entries equal to a_i [5]. It is therefore natural to ask whether it is possible quantum mechanically to interpolate between vacua that have the same n but different N_i's.

This was answered in [12], where it was shown that, for example, vacua with one $U(1)$ factor can be smoothly connected to vacua with any allowed values of the N_i's. All these classical limits are different corners of a single connected subspace of the $\mathcal{N} = 2$ moduli space, which was referred to as an $\mathcal{N} = 1$ branch. However, in [12] it was also discovered that there were other branches distinguished by order parameters such as the expectation values of Wilson loops. Branches meet at points where extra massless mutually local monopoles appear. At these points other branches also emanate which have the same dimension but where some of the N_i's are zero.

The structure of these branches and how they meet can be quite intricate [12].

[5] We assume that all $N_i \neq 0$. See Appendix C for some comments about the case when some of the N_i are zero.

In Figure 1.4 we use the example of a cubic superpotential in a $U(4)$ gauge theory to represent a region close to one of the points with three massless monopoles. At a generic point the low energy group is $U(1)^2$. At the special point where the two branches meet, a third branch (not drawn) emanates which consists of vacua with a single $U(1)$ as the low energy group. Along each of the depicted branches one can take a semiclassical limit and find vacua corresponding to (classically) unbroken $U(N_1) \times U(N_2)$ gauge groups.

In the next chapter we will discuss in greater detail the structure of the moduli space of $\mathcal{N} = 1$ vacua in a theory with a generic gauge group $U(N)$. We will describe the order parameters used to distinguish the different branches and their physical meaning. The goal will be to bring some arguments in favour of the conjecture that the problem of identifying the $\mathcal{N} = 1$ branches in this context might be related to the mathematical problem of classifying "dessins d'enfants" according to their Galois invariants. The relevant mathematical background in also presented in the next chapter.

Chapter 2

A Conjectured Correspondence

The aim of this thesis is to suggest a new connection between a particular class of Seiberg-Witten curves and what Grothendieck called "dessins d'enfants" or "children's drawings". We will refer to these simply as "dessins" in what follows. We will formally define a dessin later on, but for the moment by a dessin we simply mean a connected graph on a two dimensional surface, with vertices of two kinds - say black and white - that alternate along the graph.

The original reason for studying such drawings in mathematics was that there is a natural action of the absolute Galois group $\mathrm{Gal}(\overline{\mathbb{Q}}/\mathbb{Q})$ on them. Moreover, the action is faithful, i.e. there is no group element, other than the identity, that leaves invariant all dessins. The absolute Galois group is one of the central objects of interest in mathematics, especially in number theory. This object has already made its appearance in the physics literature in the context of rational conformal field theory due to work by Moore and Seiberg [36–38]. It has been known that the solutions of the Moore-Seiberg equations lead to a projective representation of the so called Teichmüller tower. As noted by Grothendieck in [28], the absolute Galois group also acts on this tower. In fact, both the Teichmüller tower and the dessins were introduced by Grothendieck in the same letter [28].

In the next few sections we will summarize recent progress made in [12, 13] in understanding the vacuum structure of $\mathcal{N} = 1$ gauge theories obtained by deforming an $\mathcal{N} = 2$ theory by a tree level superpotential. We will see that these gauge theory techniques and the existing results could have implications for the study of the action of the Galois group on the dessins and, conversely, we would like to argue that there is a wealth of information on the mathematical side that could potentially lead to an

improved understanding of the phases of $\mathcal{N} = 1$ gauge theories.

We will conjecture that there is an intimate relation between Grothendieck's programme of classifying dessins into Galois orbits and the physics problem of classifying certain special phases of $\mathcal{N} = 1$ vacua. The precise form of the conjecture is given in Section 2.4.4. The meaning of the different physical and mathematical elements that go into this conjecture will be explained in Section 2.2 (See also Appendix A for a more complete explanation of the mathematical terminology.).

2.1 Dessins From Gauge Theory

Let us continue the analysis of the $U(4)$ example discussed in Section 1.3. In Figure 2.1, we show a typical configuration of the zeroes of the polynomials that appear in the factorization equation

$$P_N^2(z) - 4\Lambda^{2N} = F_{2n}(z)\, H_{N-n}^2(z) \tag{2.1}$$

introduced earlier. This kind of configuration would appear at points near the semi-classical limit in the branches shown in Figure 1.4. The line segments that are drawn represent the branch cuts. Of course, it is not essential to draw the cuts through the zeroes of $P(z)$ (denoted by $\circ$) but this will have a mathematical significance when we formally define a dessin. On the other hand, the cuts naturally pass through the zeroes of $H_2^2(z)$ (denoted by a bivalent $\bullet$ node in the drawing) since a small deformation away from the $\mathcal{N} = 1$ branch will split the double zeroes. As is clear from the figure, these look like disconnected branchless trees.

It turns out that one of the two branches in Figure 1.4 has $U(2) \times U(2)$ as the only semi-classical limit [12]. We now focus our attention on this branch. We further tune the parameters of the superpotential so that the corresponding $\mathcal{N} = 1$ vacuum is an isolated singular point where $H_2(z)$ develops a double root. There is only one such point in the branch we have chosen and it naturally leads to a connected graph. This is shown in Figure 2.2. We have omitted the zeroes of $P_4(z)$ so as to not clutter the figure.

It turns out that such connected trees show up in the moduli space whenever the

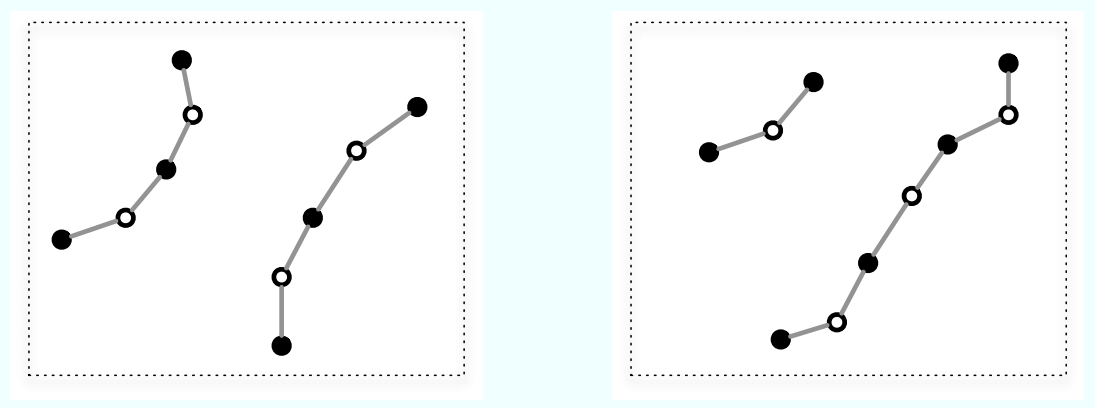

Figure 2.1: Zeroes of $P_4(z)$ (denoted by $\circ$), zeroes of $F_4(z)$ (denoted by univalent $\bullet$) and zeroes of $H_2^2(z)$ (bivalent $\bullet$) near the semi-classical limits with $N_1 = N_2 = 2$ (*left*) and $N_1 = 1$, $N_2 = 3$ (*right*). Edges represent branch cuts.

Seiberg-Witten curve develops isolated singularities. Examples of such "rigid curves" include the maximally confining points [22, 46] and the generalized Argyres-Douglas points [2]. Such singularities arise when some of the zeroes of F_{2n} and H_{N-n} coincide, F_{2n} develops double roots, etc.

The connected trees that appear at such special points in the moduli space are precisely the "dessins d'enfants" that Grothendieck introduced as a tool to study the structure of the absolute Galois group $\mathrm{Gal}(\overline{\mathbb{Q}}/\mathbb{Q})$. This is the group of automorphisms of $\overline{\mathbb{Q}}$ that leave $\mathbb{Q}$ fixed[1]. As mentioned earlier, $\mathrm{Gal}(\overline{\mathbb{Q}}/\mathbb{Q})$ acts faithfully on the dessins. This means that the only element of the group that leaves every dessin invariant is the identity. The set of dessins is then partitioned into orbits under the action of the group. (We exhibit how $\mathrm{Gal}(\overline{\mathbb{Q}}/\mathbb{Q})$ acts on the dessins in Section 2.2.4.) One way of learning about the Galois group is to construct a complete set of invariants that distinguish dessins that belong to distinct Galois orbits. This is one of the goals in the study of dessins in mathematics and we will discuss some of the known Galois invariants in detail in section 2.3.

In the following sections we show that the known order parameters that distinguish

[1]Here $\mathbb{Q}$ is the field of rational numbers and $\overline{\mathbb{Q}}$ is its algebraic closure. For more details see Appendix A.

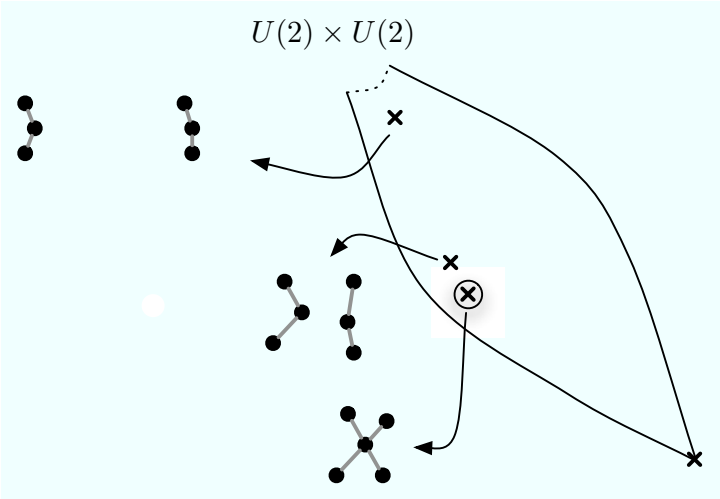

Figure 2.2: Evolution of the two branchless trees in one $\mathcal{N} = 1$ branch of the $U(4)$ gauge theory starting near the $U(2) \times U(2)$ semi-classical limit and reaching an isolated singularity where we get a connected tree.

different branches of $\mathcal{N} = 1$ vacua can be thought of as Galois invariants. In particular we prove that the "confinement index" introduced in [12] is a Galois invariant and can be given a purely combinatorial interpretation. Interestingly, we will find that certain operations on the gauge theory side, such as the "multiplication map" introduced in [11], have a precise interpretation as operations on the dessins. We believe that solving the non-rigid problem in (2.1) before specializing to singular points might lead to a new and useful perspective in the study of dessins d'enfants. Conversely we will also see that this correspondence leads to open questions regarding the interpretation of interesting mathematical invariants in the gauge theory.

More explicitly, we would like to argue that the special points where the dessins make their appearance can be thought of as special phases of the $\mathcal{N} = 1$ gauge theory. This would imply the existence of appropriate order parameters which distinguish these special points from generic points in the $\mathcal{N} = 1$ branch to which they belong. We provide some evidence for this in the examples of Section 3.1.

So far we have seen in an example how dessins can arise at isolated singular points in the moduli space of a Seiberg-Witten curve. We will now show that given a dessin,

one can associate to it a polynomial equation which corresponds to a singular Seiberg-Witten curve, of the type discussed in this section. It turns out that this is precisely equivalent to the content of the Grothendieck correspondence, which we discuss next.

2.2 Grothendieck's "Dessins D'Enfants"

The Grothendieck correspondence is a bijection between classes of dessins and special classes of maps on punctured Riemann surfaces called Belyi maps. At first sight this might seem far removed from gauge theory physics, but we will describe a precise route that leads to a correspondence between Seiberg-Witten theory and the dessins d'enfants.

2.2.1 Mathematical Preliminaries

Let us briefly introduce the concepts that we will discuss in detail in the remainder of the section.

The first ingredient in the correspondence is the Belyi map. A Belyi map [8] is a holomorphic map from any punctured Riemann surface to $\mathbb{P}^1$ with exactly three critical values at $\{0, 1, \infty\}$. In [28] Grothendieck showed that any dessin can be constructed from a Belyi map. For the purposes of our discussion, we will restrict to dessins drawn on a Riemann sphere[2]. We show two simple examples in Figure 2.3. The key result that makes explicit the relation to Seiberg-Witten theory is that Belyi maps are obtained as solutions to certain polynomial equations.

As we will see, these equations have a natural interpretation as Seiberg-Witten curves that describe particular degenerations of Riemann surfaces, such as those we have already encountered in Section 1.3 and Section 2.1. More generally, we find that whenever the Seiberg-Witten curve factorizes so as to give rise to a "rigid curve", i.e. a curve described by an equation without free parameters, one can associate a dessin to it[3]. Our goal will be to set up a dictionary that maps the relevant quantities in

[2]All the mathematical discussion in this section can be generalized to a general Riemann surface. See for example [43] for more details.

[3]This is up to a shift of z in (2.1). In gauge theory, this corresponds to the overall $U(1)$ degree of

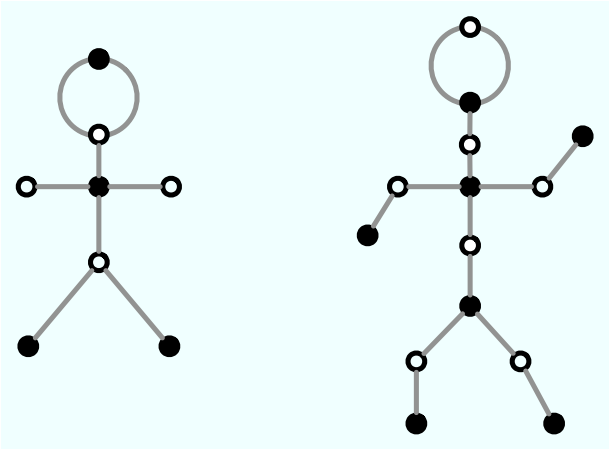

Figure 2.3: Examples of dessins; the bipartite structure of the graph is manifestly shown.

mathematics, related to the Galois group action on dessins, into gauge theory language and vice versa.

2.2.2 Dessins From Belyi Maps

We now state without proof some basic mathematical facts which are crucial to establish the relation between the dessins and Seiberg-Witten theory. See [43] for a thorough discussion and for a full list of references. The main result we will use is the Grothendieck correspondence, which connects the theory of dessins with algebraic curves defined over $\overline{\mathbb{Q}}$, the algebraic closure of $\mathbb{Q}$. Let us see how this comes about.

Consider an algebraic curve X defined over $\mathbb{C}$. Such a curve is defined over $\overline{\mathbb{Q}}$ if and only if there exists a non-constant holomorphic function $f : X \to \mathbb{P}^1$ such that all its critical values lie in $\overline{\mathbb{Q}}$. A theorem by Belyi [8] gives a very striking result: X is defined over $\overline{\mathbb{Q}}$ if and only if there exists a holomorphic map $f : X \to \mathbb{P}^1$ such that its critical values are $\{0, 1, \infty\}$.

A map $\beta : X \to \mathbb{P}^1$ with all its critical values in $\{0, 1, \infty\}$ is therefore called a *Belyi map*. A Belyi map is called *clean* if all ramification degrees over 1 are exactly equal to 2.

---

freedom that decouples from the strong dynamics in the infrared.

Let us give a simple example that will be very relevant in the rest of the chapter. Let $X = \mathbb{P}^1$ and β a polynomial. To guarantee that all critical points that map to 1 have ramification degree 2, we set

$$\beta(z) = 1 - P^2(z)\,, \tag{2.2}$$

where $P(z)$ is a polynomial. Let us see under which conditions β is a clean Belyi map. The critical points are computed as the zeroes of

$$\frac{\mathrm{d}\beta(z)}{\mathrm{d}z} = -2P(z)P'(z). \tag{2.3}$$

This means that the zeroes of $P(z)$ are critical points. Their ramification degree is 2 since $P(z)$ is squared in β and their critical value, i.e., β evaluated at a zero of $P(z)$, is 1. All we need is that the remaining critical points, which are precisely the roots of $P'(z)$, have critical value 0. In other words, they must also be roots of $1 - P^2(z)$. Up to the freedom to shift z, these conditions have only a discrete number of solutions. These are Belyi maps.

We now have the ingredients to formally define a dessin: for the present purposes we define a *dessin d'enfant* on the sphere as the pre-image under a clean Belyi map of the interval joining 0 and 1 in $\mathbb{P}^1$. In other words, the dessin D associated to a clean Belyi map β is $D = \beta^{-1}([0,1]) \subset X$. We show this pictorially in Figure 2.4 for the case $\beta(z) = 1 - P_4^2(z) = F_4(z)\,H_1^4(z)$.

Such a dessin has a natural bipartite structure given by assigning a $\bullet$ to the preimages of 0 and $\circ$ to the preimages of 1. We will refer to a pre-image of 0 as a vertex of the dessin. An edge is a line segment between two vertices that contain exactly one pre-image of 1. For example the second dessin in Figure 2.3 is clean (while the first is not) so that the notion of edges and vertices as we just defined makes sense: it has 7 edges and 7 vertices. In what follows, we will restrict our attention to clean dessins and refer to them simply as dessins. Likewise, the corresponding clean Belyi maps will be simply called Belyi maps.

Also important for characterizing the dessins are the preimages of ∞, denoted by $\times$. There is one pre-image of ∞ for each open cell enclosed by a set of edges. For example, a dessin is a tree if and only if the preimage of ∞ is a single point.

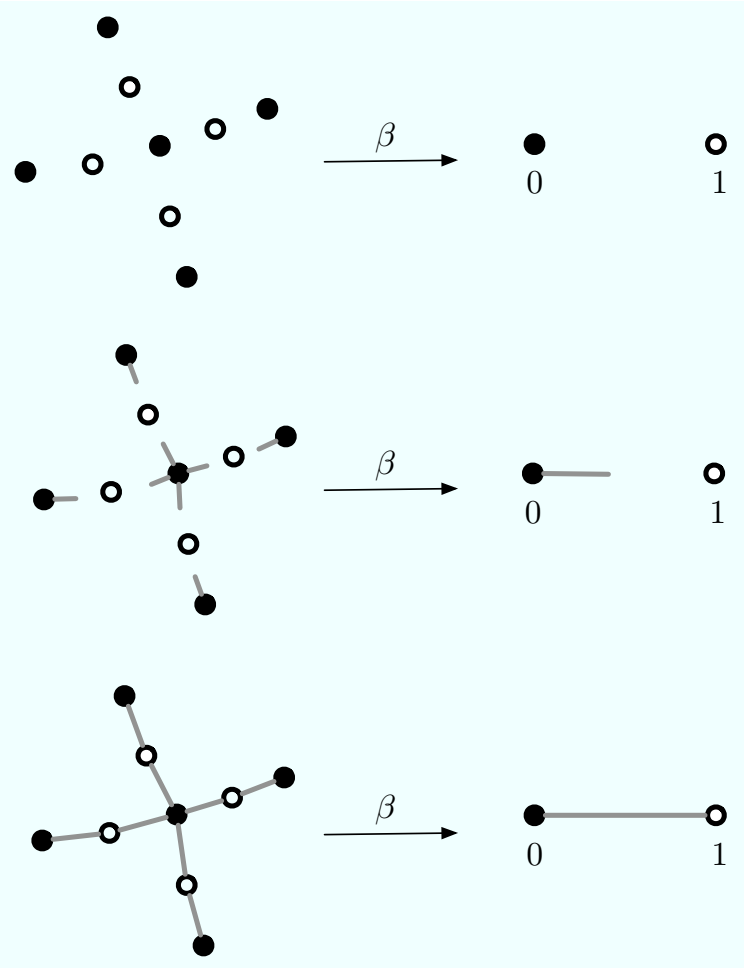

Figure 2.4: We show how the dessin is the pre-image of the interval $[0, 1]$ under the Belyi map. Note that as we move from 0 to 1, the number of lines emanating from a given pre-image of 0 is given by the ramification degree of the map at those points. Since the map is clean, *exactly* two lines meet at each pre-image of 1.

The study of dessins on the sphere is important because the absolute Galois group $\mathrm{Gal}(\overline{\mathbb{Q}}/\mathbb{Q})$ acts faithfully on them. As mentioned before, the absolute Galois group is the group of automorphisms of $\overline{\mathbb{Q}}$ that leaves invariant $\mathbb{Q}$ and it is a remarkably complex object. We give a basic introduction to the Galois group in Appendix A. It can also be shown that not only is the action of $\mathrm{Gal}(\overline{\mathbb{Q}}/\mathbb{Q})$ on genus-0 dessins faithful, but so is the action on the much smaller set of trees.

The main thing to take away from this section is that one can map the problem of classifying dessins to the problem of classifying Belyi maps β. As we have seen, these are a special class of rational functions on the Riemann sphere that satisfy the conditions in the definition above. We now turn to the question of how Belyi maps corresponding to a given dessin can be explicitly constructed. This will naturally lead us to gauge theory physics.

2.2.3 Belyi Maps From Polynomial Equations

Consider a dessin D on the sphere with N edges. Let $V = \{u_1, \ldots, u_k\}$ where u_i is the number of vertices (pre-images of 0) of valence i. We choose k to be the maximum vertex valence in D. Let $C = \{v_1, \ldots, v_m\}$ where v_i is the number of faces with i edges. Again we choose m to be the maximum face valence in D. The lists V and C are called the *valency lists* of D.

Let $G_{v_i}(z)$ and $J_{u_i}(z)$ be polynomials of degree v_i and u_i respectively, with undetermined coefficients. Take one polynomial for each element in V and in C. Pick i_0 to be the valence whose v_{i_0} is the smallest non zero value in C. Then let all polynomials $G_{v_i}(z)$ and $J_{u_i}(z)$ be monic except for $G_{v_{i_0}}(z)$ which we choose to be of the form

$$G_{v_{i_0}}(z) = \alpha(z^{v_{i_0}-1} + \ldots). \tag{2.4}$$

In other words, we have chosen the coefficient of $z^{v_{i_0}}$ to vanish and we have factored out the coefficient of $z^{v_{i_0}-1}$ which we call α.

Now construct the two polynomials

$$A(z) = \prod_{j=1}^{k} J_{u_j}(z)^j\,, \qquad B(z) = \prod_{i=1}^{m} G_{v_i}(z)^i\,. \tag{2.5}$$

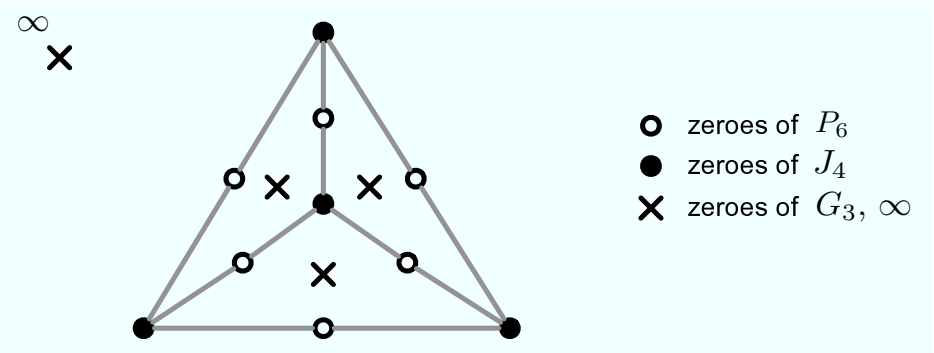

Figure 2.5: Dessin corresponding to the solution of the factorization problem (2.8).

Then if $A(z)$ and $B(z)$ are such that there exists a monic polynomial $P_N(z)$, with N equal to the number of edges of the dessin, and which satisfies the polynomial constraint

$$A(z) - B(z) = P_N^2(z)\,, \tag{2.6}$$

then

$$\beta(z) = 1 + \frac{P_N^2(z)}{B(z)} = \frac{A(z)}{B(z)} \tag{2.7}$$

is a rational clean Belyi map. Note that the polynomial equation is rigid, in the sense that there are no coefficients in the polynomials which are free parameters[4]. There are thus only a finite number of solutions to (2.5). The discussion has been rather abstract so far, so let us illustrate the various concepts with some simple examples.

Consider the dessin in Figure 2.5 which has 6 edges. From the figure, we see that each open cell is bounded by 3 edges and every vertex is trivalent. The valency lists are therefore of the form $V = \{0, 0, 4\}$ and $C = \{0, 0, 4\}$. From the discussion above, we need $A(z) = J_4^3(z)$ and $B(z) = G_3^3(z)$ such that they satisfy the polynomial equation

$$P_6^2(z) + G_3^3(z) = J_4^3(z)\,. \tag{2.8}$$

It turns out that there is only one solution to the polynomial equation (2.8) [5]. However, in general, such polynomial equations have more than one solution. For instance, the polynomial equation

$$P_{10}^2(z) + G_3^5(z) = J_4^3(z)\,\tilde{J}_4^2(z)\,. \tag{2.9}$$

[4]Up to a shift and rescaling of z. We will return to this point in Section 2.2.7.

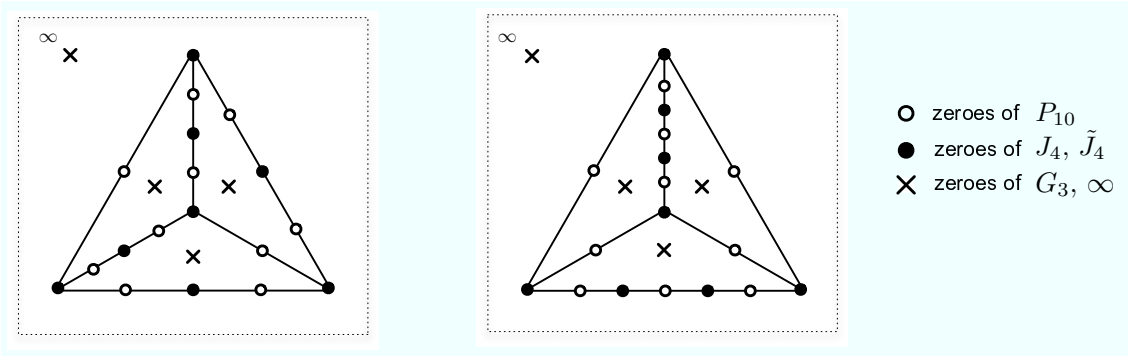

Figure 2.6: Dessin corresponding to the solution of the factorization problem (2.9). The bivalent • vertices are roots of $\tilde{J}_4(z)$ while the trivalent • nodes are the roots of $J_4(z)$.

turns out to have two solutions [5]. This is because for the same valency lists $V = \{0, 4, 4\}$ and $C = \{0, 0, 0, 0, 4\}$ (which we can infer from the polynomial equation), there are two dessins one can draw. These are shown below in Figure 2.6. We shall revisit this specific example in Section 3.2 in much more detail.

The key result which we will use from now on is that for *every* dessin D with valency lists V and C there exists a solution to the factorization problem (2.6) such that the corresponding Belyi function gives $D = \beta^{-1}([0, 1])$. This is a simplified version of the Grothendieck correspondence [28].

2.2.4 Action Of The Galois Group

So far we have mentioned repeatedly that the absolute Galois group $\Gamma = \mathrm{Gal}(\overline{\mathbb{Q}}/\mathbb{Q})$ acts faithfully on dessins. We now show how Γ acts on the dessins via the Belyi map.

Let D be a dessin such that $D = \beta^{-1}([0, 1])$. Furthermore, let β be of the form

$$\beta = \frac{A(z)}{B(z)} = \frac{z^{2N} + a_1 z^{2N-1} + \ldots + a_{2N}}{z^L + b_1 z^{L-1} + \ldots + b_L},$$

where $A(z)$ and $B(z)$ solve the polynomial equation (2.6), N is, as before, the degree of $P(z)$ and $L = \sum_{i=1}^{m} i v_i$. Then Γ acts on D by twisting the coefficients[5] in β. For $g \in \Gamma$,

[5]The a_i (and b_j) are algebraic numbers; i.e. they are solutions to some polynomial equations with coefficients in $\mathbb{Q}$. The solutions to such equations include a_i along with other algebraic numbers which are, by definition, in the Galois orbit of a_i. Twisting by the relevant group element of Γ here refers to choosing another element in the orbit of a_i. For a more formal discussion, refer to Appendix A.

D_g is defined to be the dessin obtained by the action of g on D, i.e. $D_g = \beta_g^{-1}([0,1])$, where

$$\beta_g = \frac{A_g(z)}{B_g(z)} = \frac{z^{2N} + g(a_1)z^{2N-1} + \ldots + g(a_{2N})}{z^L + g(b_1)z^{L-1} + \ldots + g(b_L)} \,. \tag{2.10}$$

Thus, given a solution to the polynomial problem (2.6) it is easy to understand how the dessin changes under the action of the Galois group. However, given two dessins, it is in general very difficult to tell whether they belong to the same Galois orbit or not. This is the central problem associated to the dessins d'enfants. Later we will discuss several Galois invariants that mathematicians have introduced in order to distinguish dessins that belong to distinct Galois orbits by studying the combinatorial data associated to each dessin.

2.2.5 The Identification

Recall that for a $U(N)$ gauge theory with $L < 2N$ massive flavors with masses given by m_i, the Seiberg-Witten curve that captures the infrared dynamics of the gauge theory is the following hyperelliptic Riemann surface [4, 29]:

$$y^2 = \langle \det(z\mathbb{I} - \Phi) \rangle^2 - 4\Lambda^{2N-L} \prod_{i=1}^{L} (z + m_i) \,. \tag{2.11}$$

We would like to propose the following identification and argue that it is a useful one. Let us identify objects in (2.6) and in (2.11) as follows: $P_N(z) = \langle \det(z\mathbb{I} - \Phi) \rangle$, $B(z) = -4\Lambda^{2N-L} \prod_{i=1}^{L} (z - m_i)$. In particular, $\alpha = -4\Lambda^{2N-L}$. In each case, the precise form of $A(z)$ in (2.5) defines the special point in the Coulomb moduli space we are looking at. Since dessins are associated only to rigid factorizations of the Seiberg-Witten curves, they appear at isolated singular points in the moduli space of the $\mathcal{N} = 2$ gauge theory.

At this point, it appears as if the relation to Seiberg-Witten curves is purely at a formal level. We will show in what follows that this is more than a superficial similarity and we exhibit features of the gauge theory that have a natural interpretation as operations on the dessin. For this we have to abandon the $\mathcal{N} = 2$ point of view and deform the theory to $\mathcal{N} = 1$ by a tree level superpotential as reviewed in Section 1.3.

We mentioned earlier that the absolute Galois group acts faithfully on the set of all trees. For most part of this thesis we will restrict our discussion to the set of trees and only in Section 3.2 will we discuss dessins with loops.

2.2.6 Trees On The Riemann Sphere: Refined Valency Lists

Since trees have only one open cell (with the associated vertex at infinity) the Seiberg-Witten curve associated to the dessin is that of the pure $U(N)$ gauge theory:

$$y^2 = P_N^2(z) - 4\Lambda^{2N} \,. \tag{2.12}$$

By itself, the curve in (2.12) does not correspond to any dessin, but if we tune the parameters in $P_N(z)$ so that we are at an isolated singularity in the moduli space, the curve factorizes, and the zeroes of the polynomials involved will describe vertices of a dessin. This also means that the Belyi map (2.7) is a polynomial

$$\beta(z) = \frac{A(z)}{B(z)} = 1 - \frac{P_N^2(z)}{4\Lambda^{2N}} \,, \tag{2.13}$$

where $P_N(z)$ solves the factorization

$$(P_N(z) - 2\Lambda^N)(P_N(z) + 2\Lambda^N) = \prod_{j=1}^{k} (J_{u_j}(z))^j \,. \tag{2.14}$$

From this expression it follows that the two factors on the left cannot have any factors in common. Thus, for trees, the problem always reduces to solving two lower order equations of the form

$$P_N(z) - 2\Lambda^N = \prod_{j=1}^{k} (Q_{u_j^-}(z))^j \tag{2.15}$$

$$P_N(z) + 2\Lambda^N = \prod_{j=1}^{k} (R_{u_j^+}(z))^j \tag{2.16}$$

such that $u_j^- + u_j^+ = u_j$ for every j. One can now define a new bipartite structure on the dessin by assigning a $+(-)$ to every zero of $R_{u_j^+}$ $(Q_{u_j^-})$ such that if a given vertex (pre-image of 0) is of one sign, every one of its neighbors is of the opposite sign. The bipartite structure is unique up to an overall sign flip. This leads to a valency list

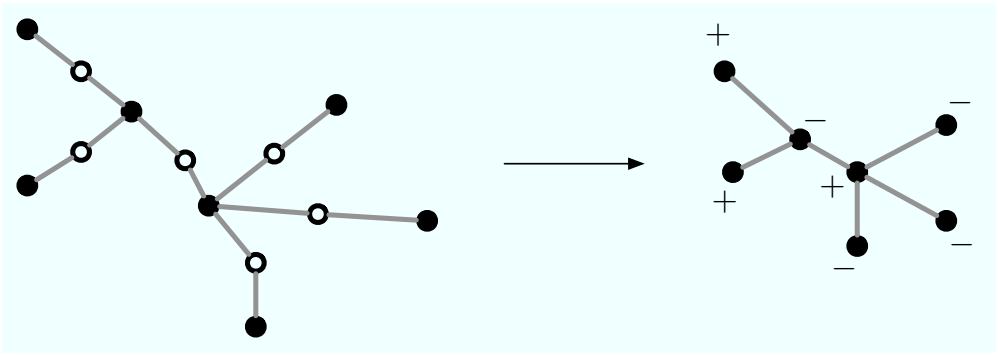

Figure 2.7: Refined valency list for the trees. $V^+ = \{2, 0, 0, 1\}$ and $V^- = \{3, 0, 1\}$ for this case

$\{V^+, V^-\}$ that is more refined than the valency list $\{V, C\}$ introduced earlier[6] where $V_\pm$ denotes the positive/negative valency list. For instance, from (2.15) u_j^+ is the number of j-valent vertices of type "+".

With the refined valency list, the trees can be redrawn as shown in Figure 2.7. Note that in the figure on the right we have removed the preimages of 1 depicted as $\circ$ on the left. This is common practice in the literature when dealing with trees. There is one more common convention which is to depict elements in V^+ by $\bullet$ and elements in V^- by $\circ$; we have not adopted this convention in order to avoid confusion and we simply add $\pm$ to the $\bullet$'s as in Figure 2.7.

Clearly, the dessins that arise from different valency lists belong to distinct Galois orbits; we will comment more about this later.

Interestingly enough, there is a related splitting of the polynomial equation in the gauge theory. In [12] while solving the non-rigid problem (2.1) it was found that the $\mathcal{N} = 1$ branches are classified by the integers (s_+, s_-), where $s_\pm$ refers to the number of double roots in each of the factors on the left hand side of (2.15). This is already a hint that the mathematical goal of classifying dessins according to Galois orbits might be closely related to the more physical problem of studying the branches of $\mathcal{N} = 1$ vacua in gauge theory. We will see this in more detail in Section 2.4.

[6] C contains just one element and is trivial for the case of trees.

2.2.7 Equivalence Classes Of Trees

Let us consider the equations (2.15) in more detail. These equations have two free parameters corresponding to a rescaling and shift of z. In other words, if $P_N^{(1)}(z)$ is a solution then $P_N^{(2)}(z) = P_N^{(1)}(az+b)$ is also a solution. In physics as well as in mathematics, it is natural to consider monic polynomials. This means that a is restricted to be an N^{th} root of unity.

The trees constructed using the Belyi map (2.13) with $P_N^{(1)}(z)$ and $P_N^{(2)}(z)$ are identical except for a displacement or rotation in the z plane. In the mathematical literature such trees are considered equivalent and one considers equivalence classes of the corresponding Belyi maps. The Grothendieck correspondence is in fact an isomorphism between equivalence classes of Belyi maps[7] and children's drawings.

Every tree has an associated number field (see Appendix A for a primer on field extensions) [43], determined by the field of definition of the polynomial $P_N(z)$ that gives the corresponding Belyi map (2.13). This might be a little puzzling at first, since the transformation $z \to az+b$ can in general involve arbitrary algebraic numbers. This means that the number field associated to trees that differ by translations and rotations can be different. On the other hand we have just said that such trees are taken to define an equivalence class on which $\mathrm{Gal}(\overline{\mathbb{Q}}/\mathbb{Q})$ acts.

The resolution to this puzzle is that, although the Galois group acts nontrivially on all these trees, there is always a way of choosing the tree with the simplest number field [48] as a representative of the equivalence class. It turns out that the action of $\mathrm{Gal}(\overline{\mathbb{Q}}/\mathbb{Q})$ on just the representatives of each class is faithful. Therefore, for the purposes of studying the absolute Galois group one uses the shift and scale of z to pick the simplest representative.

All these statements have a counterpart in physics. The freedom to shift by b corresponds to the fact that the underlying theory is $U(N)$, as opposed to $SU(N)$. The overall $U(1)$ decouples in the IR and gives rise to this shift degree of freedom. Just like

[7]The equivalence class of Belyi maps is, in fact, up to any $SL(2,\mathbb{C})$ transformation. However, we have used one of these to put the pole at ∞. Thus only shift and scale transformations remain.

in mathematics, one can use this shift to bring any tree level superpotential to a form that displays the $\mathcal{N}=1$ branches, introduced in Section 1.3, most clearly. We will use this in section 3.1.

More intriguing is the meaning of the rescaling by an N-th root of unity. In physics, this corresponds to different kinds of confinement distinguished by the behavior of combinations of Wilson and 't Hooft loop operators. Roughly speaking, the trivial root of unity corresponds to usual confinement while the other roots correspond to oblique confinement [12]. Quite nicely, the mathematical criterion of choosing the simplest number field corresponds in physics to choosing the phase with usual confinement.

It would be very interesting to explore the connection between the "not-so-simple number fields" and the oblique confining phases. However, since our goal is to establish a connection between dessins (in terms of equivalence classes) and gauge theory, we will restrict our study to physics phases with only usual confinement.

2.2.8 Example: The Maximally Confining $\mathcal{N}=1$ Vacua

For now, let us discuss as an example the simplest tree one can draw: a branchless linear tree with N edges. Such a tree has 2 vertices of valence 1 and $N-1$ vertices of valence 2. From the general discussion above, it is easy to write down the corresponding Seiberg-Witten curve for this case:

$$P_N^2(z) - 4 = (z^2-4)H_{N-1}^2(z)\,. \tag{2.17}$$

Here we have set $\Lambda^N = 1$.

This Seiberg-Witten curve corresponds to points where $N-1$ mutually local monopoles go massless. The $\mathcal{N}=1$ vacua are obtained by perturbing the $\mathcal{N}=2$ theory by a mass term, with $W_{\text{tree}} = \frac{1}{2}\text{Tr}\Phi^2$. The condition $\Lambda^N = 1$ has N different solutions that correspond to the N different maximally confining $\mathcal{N}=1$ vacua[8]. However, as discussed above, we take the simplest solution, i.e. $\Lambda = 1$. The solution to this equation is well known and given in terms of Chebyshev polynomials[9]. In Figure 2.8 the zeroes of $P_N(z)$

[8]The reason for the name is that the low energy gauge group is just $U(1) \subset U(N)$.

[9]Here the shift symmetry is used to set $< \text{Tr}\Phi >= 0$.

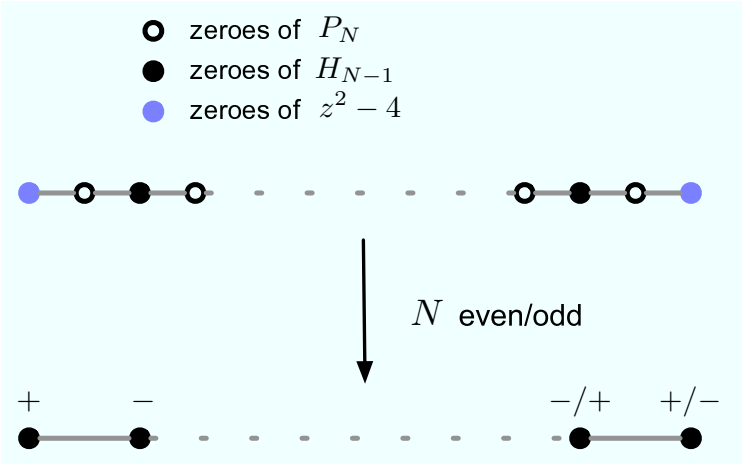

Figure 2.8: The dessin that corresponds to the maximally confining vacuum. Case by case, it is obtained by plotting the zeroes of the polynomials that solve the factorization problem (2.17). See for example Figure 3.8 for the $N = 6$ plot.

and $H_{N-1}(z)$ have been depicted showing how the branchless tree arises.

The importance of the branchless tree lies in the fact that these appear at the intersection of the $\mathcal{N} = 1$ branches, the point marked by a cross in Figure 1.4. They also appear near the semi-classical limits ($\Lambda \to 0$) as shown in Figure 2.1 and Figure **??**. Although these truncated branchless trees cannot be thought of as dessins, they seem to be "building blocks" that come together to create a dessin at an isolated singularity. We will elaborate a bit more on this point in the conclusions.

So far we have been rather loose in the language employed to discuss aspects of the factorization problems. Techniques from both the physics and mathematics literature have been used interchangeably. We now turn to a more systematic discussion of how the dessins are classified from a mathematical point of view. We will follow this up with a review of how the $\mathcal{N} = 1$ vacua are classified from a physics point of view.

2.3 Invariants

2.3.1 Invariants From Mathematics

One way of learning about the structure of the absolute Galois group $\mathrm{Gal}(\overline{\mathbb{Q}}/\mathbb{Q})$ is by constructing a complete set of invariants under the action of $\mathrm{Gal}(\overline{\mathbb{Q}}/\mathbb{Q})$ such that any

two dessins that do not belong to the same Galois orbit will disagree in at least one invariant. Such a complete list of invariants is currently not known although many invariants have been constructed. In this section we review the most basic invariants[10] associated to dessins that are related by the action of $\mathrm{Gal}(\overline{\mathbb{Q}}/\mathbb{Q})$ [43, 55].

- *Valency Lists.* The most intuitive invariants are the valency lists V and C introduced in Section 2.2.3. These are clearly invariants, since as we saw they are determined by the form of the polynomial equation which is invariant under the action of $\mathrm{Gal}(\overline{\mathbb{Q}}/\mathbb{Q})$. It is sometimes possible to define more refined valency lists, corresponding to different ways of solving the polynomial equation. We have already seen this for the case of trees, where we introduced the $\{V^+, V^-\}$ valency lists. As we discussed, this possibility of constructing a new invariant has a nice counterpart in physics; this will be further clarified in the examples that follow. Note that by concentrating on dessins coming from the same factorization problem we can forget about the valency list invariant since all dessins constructed this way have the same valency list. Therefore, the search is for other invariants that will distinguish different Galois orbits.

- *Monodromy Group.* Every dessin is associated to a cover of $\mathbb{P}^1$, defined by the Belyi map

$$\beta : \Sigma \to U \equiv \mathbb{P}^1 \setminus \{0, 1, \infty\},$$

that maps the edges of the graph on the Riemann surface Σ into the open segment $\overline{01}$ on $\mathbb{P}^1$. If the graph has N edges, where we count the number of edges to be equal to the number of pre-images of 1, the map β gives a $2N$-fold cover of U (see Figure 2.9 for an illustration).

Consider $\pi_1(U, \overline{01})$, the homotopy group of paths in U that begin and end on a point of $\overline{01}$. Since a closed path based on $\overline{01}$ in $\mathbb{P}^1$ can be mapped into a path between any two of the $2N$ segments in the fiber over $\overline{01}$, any given element of $\pi_1(U, \overline{01})$ acts on the dessin as a permutation of the half-edges (that go between a

[10] More invariants than those discussed here are known, but for the purpose of our analysis we will concentrate on those that can be most easily computed explicitly.

filled and unfilled vertex in Figure 2.9). Therefore, the covering map β induces a map from $\pi_1(U, \overline{01})$ to S_{2N}. Let us denote by σ_0 the permutation corresponding to circling once the point $z = 0$ on $\mathbb{P}^1$ and by σ_1 the permutation corresponding to circling once the point $z = 1$. Recall that the dessins have a bipartite structure that keeps track of whether a vertex is mapped to 0 or 1 by the Belyi map. One can convince oneself that σ_0 is the element of S_{2N} that permutes cyclically the edges incident on each vertex (that maps to 0) and, similarly, σ_1 is a cyclic permutation of the edges incident on each pre-image of 1. The subgroup of S_{2N} generated by σ_0 and σ_1 is the monodromy group of the dessin and it is a Galois invariant [30].

Let us consider the example of the dessin in Figure 2.9. There are 8 half-edges. The monodromy group is generated by the following permutations:

$$\sigma_0 = (1, 7, 6)(2, 3)(4, 5)\,, \tag{2.18}$$

$$\sigma_1 = (1, 2)(3, 4)(5, 6)(7, 8)\,. \tag{2.19}$$

We will give the explicit monodromy groups for the examples we will encounter later.

- *Belyi Extending Maps.* It is possible to construct new invariants by composing the Belyi map of interest with any Belyi-extending map and then computing the valency lists or the monodromy group of the new dessins obtained this way [55]. A Belyi extending map is a Belyi map $\alpha : \mathbb{P}^1 \to \mathbb{P}^1$ defined over $\mathbb{Q}$, such that its composition with any other Belyi map does not change the associated number field. For our purposes, we relax the definition slightly: by a Belyi extending map here we will mean any map α defined over $\mathbb{Q}$ that can be composed with a Belyi map β to give another Belyi map $\beta_\alpha := \alpha \circ \beta$.

  Let I be any invariant of a dessin D_α, where $D_\alpha = \beta_\alpha^{-1}([0, 1])$; the claim [55] is that I is also an invariant of the dessin $D = \beta^{-1}([0, 1])$. For example, for the Belyi extending map $\alpha_2(z) = 4z(1 - z)$ the monodromy group of D_α is the cartographic group of D, which is known to be another Galois invariant. Later

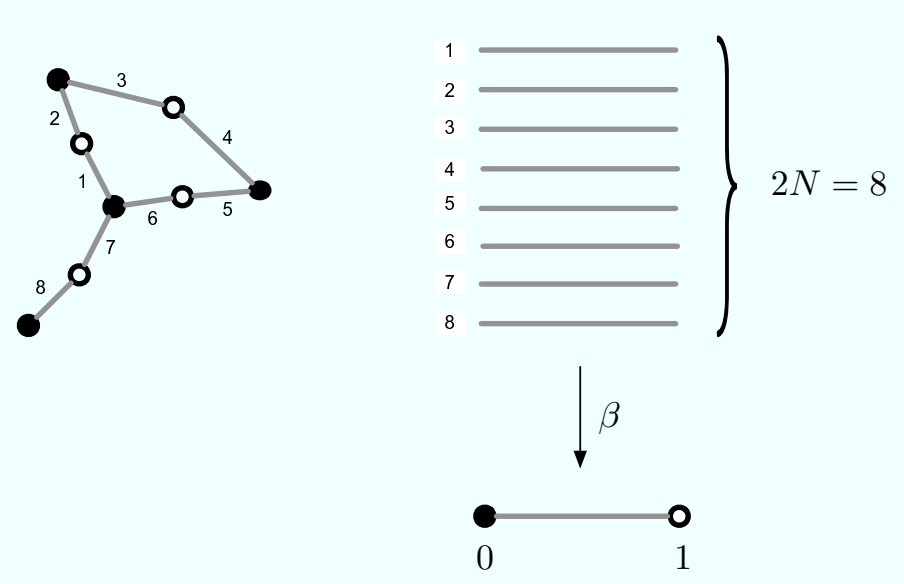

Figure 2.9: Left: Example of a dessin with $N = 4$ edges. Right: The 8 half-edges come from the preimage of the open interval $\overline{01}$, i.e. the preimage of 0 and 1 are not shown.

we will prove that the multiplication map of [11, 12] is the physical realization of the Belyi extending map α_2 .

2.3.2 Invariants From Physics

As discussed in Section 1.3, one problem that is very similar to the classification of dessins using Galois invariants is the problem of classifying branches of $\mathcal{N} = 1$ vacua using order parameters, such as Wilson and 't Hooft loops. We will consider those $\mathcal{N} = 1$ vacua that are obtained in the infrared by starting with an $\mathcal{N} = 2$ gauge theory and adding a tree level superpotential W_{tree} for the adjoint scalar Φ. The discussion of the gauge theory order parameters in this section will closely follow that of [12]. In fact, what follows is just a summary. We refer the reader to [12] for all relevant details and proofs.

- *Confinement Index.* In a $U(N)$ gauge theory a natural order parameter is the expectation value of a Wilson loop W in, say, the fundamental representation. The Wilson loop in the tensor product of r fundamental representations is W^r. Clearly, for $r = N$ there is no area law, for it is equivalent to a singlet representation (due

to electric screening). A measure of confinement is the smallest value of r, which can only be between 1 and N, for which W^r does not exhibit an area law. Such a value is denoted by t and it is called the confinement index. When the gauge group is broken classically to a product of factors $U(N_1) \times U(N_2) \times ... \times U(N_n)$ one has to also use the 't Hooft loop H to determine the confinement index. By embedding a 't Hooft-Polyakov magnetic monopole of the full $U(N)$ theory in any two of the $U(N_i)$ factors, we take into account magnetic screening. If for each $U(N_i)$ we get that $W_i^{r_i} H_i$ has no area law, this implies that in the full $U(N)$ theory $W^{r_i - r_j}$ has no area law. The relative sign comes from the fact that the magnetic monopole sits in both groups with opposite charges.

Therefore, after taking into account electric and magnetic screening, the confinement index is given by the greatest common divisor of the N_i and $b_i = r_i - r_{i+1}$. These two sets of quantities, N_i's and b_i's, will have a very clear combinatorial meaning, which will allow us to compute the confinement index just by inspection of any dessin.

As a preparation for that let us mention that both set of quantities are encoded in the expectation values of the generating function for chiral operators $\mathrm{Tr}\Phi^s$, given by [10]

$$T(z) = \left\langle \mathrm{Tr}\left(\frac{1}{z\mathbb{I} - \Phi}\right)\right\rangle . \tag{2.20}$$

It turns out that the periods of $T(z)dz$, thought of as a meromorphic differential on $y^2 = W'_{\mathrm{tree}}(z)^2 + f_{n-1}(z)$, are related to the N_i's and b_i's as follows: the N_i's are the periods of $T(z)dz$ on the A-cycles and the b_i's are the periods of $T(z)dz$ on the B-cycles (for an appropriate choice of basis). The b_i's measure the relative theta angle of $U(N_i)$ and $U(N_{i+1})$. Moreover, one can show that in the $\mathcal{N} = 1$ branch with confinement index t, $T(z)\,dz = t\,\tilde{T}(z)\,dz$, where $\tilde{T}(z)\,dz$ is the generating function for chiral operators in a Coulomb vacuum (which have $t = 1$) of a $U(\frac{N}{t})$ theory [12]. The fact that the two generating functions are related by a multiplication by t has an important consequence: all confining vacua with confinement index t are obtained from Coulomb vacua by using the multiplication

map by t [11,12]. The definition and discussion of the multiplication map is given in Appendix B. We also discuss this further in Section 2.4.1 where, for the specific case of $t = 2$, the multiplication map will be shown to coincide with the Belyi extending map α_2 of [55].

- *Holomorphic Invariants.* In cases when the rank of the low energy gauge group is too high, i.e. when the degree of the tree level superpotential is large, there is always at least one N_i which is equal to 1. The precise condition is $\deg W'(z) > N/2$: when this condition is satisfied, the confinement index is always one. One might naively think that there is only one branch since we have exhausted the standard order parameters. However, it is possible to show that there are many branches, all of them having Coulomb vacua. This is the problem that motivated the search for non-conventional order parameters in [12]. It turns out that the discussion that follows also applies for superpotentials of any degree.

  The new non-conventional order parameters proposed in [12] are obtained by studying relations between the vacuum expectation values of different chiral operators that can be defined in the theory. The expectation values of chiral operators become holomophic functions on the moduli space of vacua due to supersymmetry. It turns out that, at least in the examples considered in [12], these functions satisfy different polynomial constraints in different branches. The problem of whether the existence of these relations was the reason for the existence of the different branches or viceversa was left as an open question. For the present purposes, we take the former as the correct point of view. In fact, we will see that in the mathematical literature the refined valency list for trees gives very similar information as the relations between holomorphic functions found in [12].

  The chiral operators of relevance are $\mathrm{Tr}\Phi^r W_\alpha W^\alpha$, whose appropriately normalized vacuum expectation value is denoted by $t_r = -(1/32\pi^2)\langle \mathrm{Tr}\Phi^r W_\alpha W^\alpha \rangle$. In terms

of the reduced Seiberg-Witten curve $y^2 = F_{2n}(z)$, they can be computed as[11]

$$t_r = \frac{1}{2\pi i} \oint_\infty z^r \, y(z) \, dz \, . \tag{2.21}$$

The relations introduced in [12] to distinguish between different branches are polynomial equations in the t_r's.

The different branches that these relations distinguish are determined by the distribution of double zeroes of the curve

$$y^2 = P_N^2(z) - 4\Lambda^{2N} = F_{2n}(z) \, H_{N-n}^2(z) \tag{2.22}$$

in the two factors of $P_N^2(z) - 4\Lambda^{2N}$, i.e. by the pair (s_+, s_-). In other words, if we start with the factorization problem $P_N^2(z) - 4\Lambda^{2N} = F(z)H^2(z)$, we get

$$\begin{aligned} P_N(z) - 2\Lambda^N &= \tilde{R}_{N-2s_-}(z)\tilde{H}_{s_-}^2(z), \\ P_N(z) + 2\Lambda^N &= R_{N-2s+}(z)H_{s+}^2(z) \, . \end{aligned} \tag{2.23}$$

In order to derive the relations it is convenient to write

$$y(z) = \sqrt{\tilde{R}_{N-2s_-}(z)R_{N-2s+}(z)} = \frac{H_{s_+}(z)R_{N-2s_+}(z)}{\tilde{H}_{s_-}(z)} \sqrt{1 - \frac{4\Lambda^N}{H_{s_+}^2(z)R_{N-2s_+}(z)}} \, . \tag{2.24}$$

Since the integral defining the t_r's is around infinity, the computation can be carried out by expanding the square root. It is easy to see that if $0 \leq r \leq s_+ + s_- - 2$ then only the leading term in the expansion contributes. It turns out that in order to distinguish different values of (s_+, s_-) all that is needed are relations between those (restricted) t_r's. Using the fact that Λ does not appear, by matching dimensions (which for t_r is $3 + r$) and by matching the charge under the $U(1)_\Phi$ symmetry (which for t_r is r), one concludes that the polynomials must be homogeneous in the number of Φ's and the number of $W_\alpha W^\alpha$. Consider for example the case when $s_- = 1$ and $s_+ = 3$. Then one can show that $t_0 t_2 - t_1^2 = 0$.

We will see in the next section that (s_+, s_-) gives some information about the refined valency list of a dessin. However, the refined valency list contains more

[11] Strictly speaking, the curve needed for the computation is given by the matrix model curve of the Dijkgraaf-Vafa correspondence. However, in cases when none of the N_i are zero, the matrix model curve is the same as the reduced Seiberg-Witten curve.

information. In section 2.4.2 we will show by means of examples that the extra information of the refined valency list can be obtained if one keeps the next to leading order term in the expansion of the square root. In other words, in the expansion

$$\sqrt{1-\frac{4\Lambda^N}{H^2_{s_+}(z)R_{N-2s_+}(z)}}=1-\frac{2\Lambda^N}{H^2_{s_+}(z)R_{N-2s_+}(z)}+\mathcal{O}(\Lambda^{2N}/z^{2N}) \qquad (2.25)$$

the first term gives information about (s_+, s_-) while the second encodes the whole refined valency list. It would be interesting to find a combinatorial meaning of the higher order terms. It is important to mention that the extra relations we find distinguish the isolated point where the dessin appears from its neighbouring points in the $\mathcal{N}=1$ branch.

2.4 Cross Fertilization

Before we discuss some examples to illustrate our ideas, we would like to exhibit part of the dictionary between the mathematical and physical descriptions. First we show how the multiplication map [11] can be interpreted as an example of a Belyi-extending map [55]; we also show that the information about the refined valency list of trees, described in Section 2.2.6, can be recovered by studying the holomorphic invariants. Most importantly, we give a combinatorial interpretation of the confinement index introduced in [12]. We then speculate on the relation between the classification of dessins and the study of phases of gauge theories in four dimensions and formulate a few precise conjectures.

2.4.1 Multiplication Map As A Belyi Extending Map

Consider a tree with N edges. The Belyi map has the form (2.13):

$$\beta_N(z)=1-\frac{P_N^2(z)}{4\Lambda^{2N}}\,.$$

The dessin corresponds to a rigid polynomial equation, which is a special point in the parameter space of the non-rigid factorization problem

$$P_N^2(z)-4\Lambda^{2N}=F_{2n}(z)\,H^2_{N-n}(z)\,. \qquad (2.26)$$

The multiplication map [11] (with multiplication factor 2) guarantees that, if $P_N(z)$ satisfies the non-rigid factorization equation (2.26), one solution to the factorization equation

$$P_{2N}^2(z) - 4\Lambda^{4N} = F_{2n}(z)\,\tilde{H}_{2N-n}^2(z)$$

is given by (see Appendix B for details)

$$P_{2N}(z) = 2\Lambda^{2N}\,T_2\left(\frac{P_N(z)}{2\Lambda^N}\right), \tag{2.27}$$

where $T_2(x) = 2x^2 - 1$ is a Chebyshev polynomial of the first kind. Since $P_N(z)$ gives rise to a Belyi map, $P_{2N}(z)$ as defined in (2.27) also leads to a Belyi map β_{2N} whose inverse image of the interval $[0,1]$ leads to a dessin with $2N$ edges. Therefore, by applying the multiplication map, we get a new Belyi map of the form

$$\begin{aligned}\beta_{2N} &= 1 - \frac{P_{2N}^2(z)}{4\Lambda^{4N}} = 1 - \left(2\,\frac{P_N^2(z)}{4\Lambda^{2N}} - 1\right)^2 \qquad (2.28)\\ &= \frac{P_N^2(z)}{\Lambda^{2N}}\left(1 - \frac{P_N^2(z)}{4\Lambda^{2N}}\right) = 4\,\beta_N(1-\beta_N)\\ &\equiv \alpha_2 \circ \beta_N\,, \qquad (2.29)\end{aligned}$$

with $\alpha_2(y) = 4y(1-y)$. We thus find that this map coincides with the Belyi extending map mentioned in Section 2.3.1, which relates the monodromy group to the cartographical group.

In [55] the author gives a prescription to draw the dessin associated with any Belyi extending map starting from the original dessin. Roughly, the procedure consists in drawing on $\mathbb{P}^1$ the preimage through the Belyi extending map of the $[0,1]$ segment; then, one substitutes this new drawing in place of each segment of the original dessin. Let us apply this to our example. The map α_2 is of degree two, so it covers $[0,1]$ twice and we expect it to double the number of edges of the dessin. More precisely, the critical point $y = 1/2$ is mapped by α_2 to the vertex $z = 1$ of the $[0,1]$ segment. Therefore, we infer the following rule to draw the dessin obtained through the Belyi extending map α_2 :

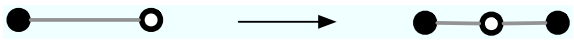

One could check that for generic t the multiplication map by t is a Belyi extending map that substitutes to each edge in the original graph a branchless tree of length t. Naively, the dessins with confinement index 2 or higher would appear to be "scaled up" versions of smaller dessins. Indeed this is what one gets if one applies the multiplication map to the rigid factorizations that lead to the dessins.

However, from the gauge theory point of view, one can also apply the multiplication map to the non-rigid problem (2.26) and *then* impose the constraints that leads to a rigid factorization problem. In other words, if $\mathcal{F}_{R/NR}$ is the set of rigid/non-rigid factorizations and if M is the multiplication map acting on the factorizations $\mathcal{F}$,

$$M(\mathcal{F}_R) \subset \Big(M(\mathcal{F}_{NR})\Big)_R, \tag{2.30}$$

where the last subscript R indicates that the factorizations are restricted to be rigid. This shows that the multiplication map is more than an operation to get new Belyi maps from old ones. Starting from a point in the moduli space of a $U(N)$ gauge theory which is *not* an isolated singularity (so that there is no associated dessin), one can apply the multiplication map by t and sometimes obtain a singular point in the moduli space of the $U(tN)$ theory where one *can* obtain a dessin. We will discuss such examples in Section 3.1. Moreoever, we will also see in Section 2.4.3 that applying the multiplication map to non-rigid factorizations is what allows us to prove that the confinement index is a Galois invariant.

2.4.2 Refined Valency Lists From (Refined) Holomorphic Invariants

We have already mentioned in Section 2.3.2 that while solving the non-rigid problem (2.1) it is convenient to classify the solutions in terms of integers (s_+, s_-), where $s_\pm$ refers to the number of double roots in either of the two factors $(P(z) \pm 2\Lambda^N)$. We now would like to relate these numbers to the refined valency list introduced in Section 2.2.6. From the definitions one can check that a given dessin with refined valency lists

$V^+ = \{u_k^+\}$ and $V^- = \{u_k^-\}$ will appear in an $\mathcal{N} = 1$ branch whose (s_+, s_-) values are given by[12]

$$s_\pm = \sum_{k=1}^{\infty} k\,(u_{2k}^\pm + u_{2k+1}^\pm)\,. \tag{2.31}$$

Recall that u_k is the number of k-valent vertices in the dessin. Clearly, the refined valency list contains more information than just the values of $s_\pm$.

From the discussion in Section 2.3.2, we have seen that the set of relations between the expectation values of chiral operators t_r's depends upon the distribution of double roots $s_\pm$, i.e. different branches are defined by the different polynomial relations between the t_r's. These chiral ring relations are satisfied at any generic point on that branch. However the dessins appear only at special points in that moduli space. A simple counting of parameters shows that at such points there will be more relations that are not generically satisfied. In the examples to be discussed in Section 3.1 we will write down explicitly these extra relations satisfied by the t_r's.

Since the generic relations seem to distinguish branches of $\mathcal{N} = 1$ vacua, it is tempting to conjecture that these special points are isolated phases. In other words, they are distinct phases from their neighbours in the $\mathcal{N} = 1$ branch. That this is the case is easy to see in some cases where the corresponding $\mathcal{N} = 1$ theory becomes superconformal in the IR. Moreover it is believed that there is always a choice of superpotential for which the resulting $\mathcal{N} = 1$ vacuum flows to an interacting superconformal theory [12, 23, 49].

2.4.3 Confinement Index As A Galois Invariant

The physical interpretation of the confinement index t was given earlier in this Section 2.3.2. We also explained how t can be computed from the periods of a particular meromorphic differential $T(z)dz$ on the Seiberg-Witten curve. The aim of this section is to give a purely combinatorial description of the confinement index t, and to show that this is indeed a Galois invariant.

Consider a given tree T, constructed as T= $\beta^{-1}([0,1])$ from a clean Belyi map

[12] In assigning a refined valency list to a dessin, there is an overall choice of sign in assigning $+/-$ to the vertices. It follows that this amounts to exchanging s_+ and s_-. The same choice is also present in gauge theory.

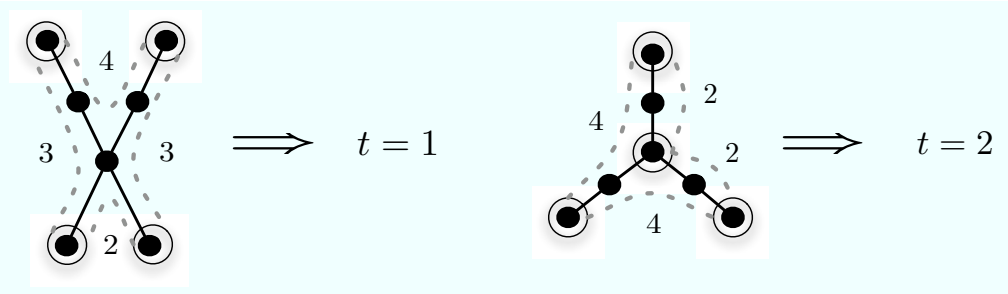

Figure 2.10: Two examples of the computation of the confinement index from combinatorial data.

$\beta(z) = 1 - P(z)^2$, where $P(z)$ is a polynomial. Let us concentrate on the preimages of 0 under β. There can be vertices with any valences. In particular, there must be vertices with valence one; this is a simple consequence of the fact that the Belyi map is clean.

The procedure for computing t is the following: circle all vertices with odd valence. Choose any of the circled univalent vertices as the starting point. Move from the chosen vertex to the next circled vertex, say going clockwise around the tree, and count the number of edges between the two circled vertices; call it h_1. Move from the second circled vertex to the next circled vertex. Again count the number of edges between the two vertices; call it h_2. The most important rule to apply when going around the tree is that each circled vertex can be used only once as a starting point and only once as an end point. Therefore, if the next vertex was used previously both as an end point and as a starting point, one should skip it and go to the next one. Continue around the tree until there are no more unused circled vertices. The prescription makes sense because there is an even number of odd-valent vertices[13].

After completing this procedure one is left with a list of integers $\mathcal{L} = \{h_1, h_2, \ldots, h_f\}$, where f is the number of odd vertices in the dessin. Then t is simply given by the greatest common divisor of the elements of $\mathcal{L}$. Two simple examples are shown in Figure 2.10.

[13]That there is an even number of odd vertices is clear from the fact that β is a polynomial of even degree.

This rule works because the vertices with odd valence are precisely the points between which one would draw the cuts in the gauge theory approach. Then, this definition can be seen to coincide with the definition of the confinement index introduced in [12]. This follows from the fact that the integral of $T(z)\,dz$ between successive vertices is 1.

Having given a purely combinatorial definition of t we proceed to show that this is indeed a Galois invariant. The proof involves concepts and terminology reviewed in Appendix A.

Let us consider all possible trees with a fixed number of edges N. If N is prime then the only possible values of t are $t = 1$ and $t = N$. The only tree with $t = N$ is the branchless tree which is a tree defined over $\mathbb{Q}$ and hence it is its own Galois orbit[14]. All other trees have $t = 1$, so there is nothing further to prove.

Consider an N which is not prime. Let $N = p_1^{r_1} \dots p_s^{r_s}$ be the prime decomposition of N. Take any p_i and consider the auxiliary polynomial $P_{p_i}(z)$. Use the multiplication map by $m = N/p_i$ to produce what we called a non-rigid curve (for more details on the multiplication map see Appendix B)

$$1 - T_m^2(P_{p_i}(z)) = (1 - P_{p_i}^2(z))U_{m-1}^2(P_{p_i}^2(z))\,. \tag{2.32}$$

This depends on the $p_i + 1$ coefficients of $P_{p_i}(z)$. As discussed in section 2.2, the new $\tilde{P}_N(z) = T_m(P_{p_i}(z))$ gives rise to a Belyi map $\beta(z) = 1 - \tilde{P}_N^2(z)$ if and only if $\tilde{P}'_N(z)$ divides the right hand side of (2.32). This is equivalent to imposing that the right hand side of (2.32) has only $N - 1$ distinct roots. These conditions will give rise to polynomial equations for the coefficients of $P_{p_i}(z) = a_0 z^{p_i} + \dots + a_{p_i+1}$. Let the set of polynomials that must vanish be $\mathcal{S} = \{f_1(a), \dots, f_j(a)\}$. Since all Chebyshev polynomials $T_m(z), U_{m-1}(z)$ have coefficients in $\mathbb{Q}$ it follows that $f(a) \in \mathbb{Q}[a_0, \dots, a_{p_i+1}]$. Therefore, there is a splitting number field $K_{\mathcal{S}}$ associated to the set $\mathcal{S}$. It is a finite normal extension of $\mathbb{Q}$ and hence is left invariant by $\mathrm{Gal}(\overline{\mathbb{Q}}/\mathbb{Q})$. This means that the solutions form full Galois orbits. From the relation between the multiplication

[14] Here what we have in mind is the branchless tree with the simplest number field, which in this case it is $\mathbb{Q}$.

map and the confinement index t it follows that all such orbits can only have values of t which are multiples of m that divide N. This means that either $t = m = N/p_i$ or $t = p_i m = N$. As mentioned above, there is a single tree with $t = N$ and therefore all other orbits must have the same value $t = N/p_i$.

Consider now $k = p_i p_j$ and the polynomial $P_k(z)$. As before, use the multiplication map by $m = N/k$. Following the same procedure we conclude that dessins arising this way can only have values of t which are multiples of m and that divide N. The only possibilities are $t = N/k, N/p_i, N/p_j, N$. As before, $t = N$ gives a single tree. We have already proven that dessins with $t = N/p_i$ or $t = N/p_j$ can only come in full Galois orbits. Therefore the remaining dessins with $t = N/k$ also arise in full Galois orbits.

One can continue this argument by induction and conclude that any two dessins in the same Galois orbit must have the same confinement index t. Thus, the confinement index is a Galois invariant.

2.4.4 Speculations About Dessins And Gauge Theory: Weak And Strong Conjectures

We now have all the ingredients we need to formulate our conjectures precisely. We have already seen that there exist $\mathcal{N} = 1$ branches in pure gauge theory that are classified by order parameters such as the confinement index. Also, as mentioned in Section 2.4.2 (and as we will show in some simple examples), at the special points where the dessins appear one has extra chiral ring relations. For an appropriately chosen superpotential, these points are believed to give rise to superconformal $\mathcal{N} = 1$ theories in the IR and thus define new phases. However, it is known that for some superpotentials, these theories might not be singular. This does not exclude the possibility that these points might be new phases, perhaps distinguished by less exotic behavior, such as extra massless states or smaller rank of the gauge group.

Given the earlier discussion regarding the theory of dessins and the phases of supersymmetric gauge theory, our first conjecture should be fairly well motivated: all points where dessins appear correspond to special phases embedded in the $\mathcal{N} = 1$ branches which we call "isolated phases".

Our second conjecture, relating the phases to Galois orbits of dessins has a weak and a strong form. The strong form is easily stated: all Galois invariants are physical order parameters that can be used to distinguish the isolated phases of supersymmetric gauge theory with a given superpotential.

On the other hand, in the examples we work out in Section 3.1 we always find that all the order parameters used to distinguish branches of gauge theories that meet a particular $U(1)$ branch, defined below, are Galois invariants. This is what we refer to as the weak form of the conjecture.

Some comments are in order. By a $U(1)$ branch we mean a branch where the low energy group is a single $U(1) \subset U(N)$. This can be called the maximally confining branch. This branch has the same dimension as the other branches [12]. Any generic branch meets these $U(1)$ branches at points where the corresponding dessin is a branchless tree with N edges.

We believe that the weak form of the second conjecture is very likely to be correct and we provide evidence for it in the examples. The strong form is on much less firm ground. In particular, it relies on the correctness of the first conjecture and on assumptions that require much more study.

It would be very important to gather more evidence for the strong form since, if true, it provides a striking connection between Grothendieck's program of unveiling the structure of $\mathrm{Gal}(\overline{\mathbb{Q}}/\mathbb{Q})$ via its action on dessins and the physics problem of classifying phases of supersymmetric gauge theories. Some of the most striking consequences would be for gauge theories with matter where physics order parameters are scarce. Almost all known Galois invariants would become new gauge theory order parameters. In the next sections, we will provide some evidence in support of these conjectures.

2.4.5 A More General $\mathcal{N} = 1$ Viewpoint And A Global $\mathcal{N} = 2$ Viewpoint

The possibility that there is always an "extremal" superpotential for which the $\mathcal{N} = 1$ $U(N)$ gauge theory at one of the isolated singular points becomes superconformal in the IR motivates the following point of view. Up to now we have studied theories with

a superpotential of a given degree. However, if we fix $U(N)$ and vary the degree of the superpotential, the theories arising at the points where a dessin D appears can go from being non singular to singular in the IR. Let us denote by $d(D)$ the smallest degree of an extremal superpotential for D. It is tempting to conjecture that two theories that arise at points corresponding to two dessins D and D' in the same Galois orbit will necessarily have $d(D) = d(D')$. In other words, $d(D)$ might be a Galois invariant. We leave this problem as an interesting direction for future work.

Finally, let us comment on yet another point of view. Suppose that we set the tree level superpotential to zero. Then we recover an $\mathcal{N} = 2$ gauge theory. The Seiberg-Witten curve of Section 2.2.3 now describes the physics in the moduli space of vacua of a single theory. The valency lists C and V introduced in Section 2.2.3 simply encode information about the masses of particles in the theory. More explicitly, C determines the distribution of masses of fundamental hypermultiplets. V determines, up to modular transformations, the charges of the various monopoles and dyons that are massless in addition to the $U(1)^N$ vector multiplets present at generic points. According to the cases studied in the literature, there is reasonable evidence to suspect that all such points are $\mathcal{N} = 2$ superconformal field theories[15].

It would be very interesting to explore the relation between the classification of dessins into Galois orbits and the classification of such $\mathcal{N} = 2$ superconformal field theories. A natural possibility, worth exploring, is that field theories giving rise to dessins in the same Galois orbit might be dual theories in some sense.

In the next chapter we will discuss some examples to explain the ideas discussed so far and support our conjectures. We will also touch briefly on the topic of $\mathcal{N} = 2$ theories with matter, corresponding to dessins with loops, that has been so far excluded from the discussion for simplicity.

[15]Of course, the point with $N - 1$ mutually local massless monopoles is not a superconformal field theory. In this case one can write down, using $S-$duality, a local lagrangian describing the full behavior of the theory in the IR.

Chapter 3

Examples

3.1 $U(6)$ Pure Gauge Theory

In this chapter we would like to illustrate by means of examples the concepts we have covered up to now. We consider pure $\mathcal{N} = 2$ $U(6)$ gauge theory broken to $\mathcal{N} = 1$ by a tree level superpotential. From the general discussion about dessins and polynomial equations, it follows that the $\mathcal{N} = 2$ moduli space contains an isolated singularity for every connected tree with 6 edges. It turns out that *all* such dessins can be obtained by just using a quartic superpotential. We discuss why higher degree superpotentials are not needed and list all dessins with their corresponding factorization problems in Appendix C.

Here, we restrict our study to a cubic superpotential. The dessins we obtain are, of course, a subset of the general quartic superpotential but they turn out to exhibit all the relevant points of the physics-mathematics dictionary we have established. All $U(N)$ gauge theories with $N = 2, \ldots, 6$ were studied in detail in [12] where one parameter solutions to the factorization problem

$$P_N(z)^2 - 4\Lambda^{2N} = F_4(z)\, H_{N-2}^2(z) \tag{3.1}$$

are listed. In fact the analysis in this section can be easily repeated for all these cases. We choose $U(6)$ because it is the simplest case that exhibits four different values of the confinement index, i.e. $t = 1, 2, 3, 6$.

The rigid factorizations corresponding to dessins are obtained by imposing suitable conditions on the solutions found in [12] along the lines we described in the introduction and in Section 2.1. In Sections 3.1.1 and 3.1.2 we classify the dessins according to the $\mathcal{N} = 1$ branches to which they belong and specify the order parameters that distinguish

the special points where the dessins appear as isolated phases.

From a mathematical point of view, in order to find the explicit Belyi maps, it is not necessary to start from the non-rigid problem (3.1). Instead, one solves the rigid problems directly. In Section 3.1.3 we will present the solution to all possible rigid factorization problems that can be derived from (3.1) along the lines of [5] by using differentiation tricks. This analysis shows explicitly the classification of trees into distinct Galois orbits. In Section 3.1.3 we will reproduce the same classification of dessins using some of the known Galois invariants. We will find that this parallels the classification of phases in gauge theory.

We mentioned in Section 2.2.7 that, both in the physics and mathematical analysis, there is the freedom to shift and scale the z variable. From a physics perspective, it is natural [12] to shift the z variable in order to bring the superpotential to the canonical form $W'_{\rm tree}(z) = z^2 - \Delta$ and then analyze the $\mathcal{N} = 1$ branches obtained by varying Δ. However, since our primary goal is to exhibit the dessins and where they appear in the gauge theory moduli space, in the examples that follow, we have followed the mathematical strategy to shift and scale z to put the solution in the simplest form possible, so that the number field associated to the tree is the simplest.

3.1.1 $U(6)$ Gauge Theory: A Physicist's Point Of View

Let us now review the solution of [12] in detail. We then specialize to rigid factorizations by tuning the one free parameter available in the solutions to (3.1).

As described in [12] one can, first of all, classify $\mathcal{N} = 1$ branches by the number of double roots in either factor $(P_6(z) \pm 2\Lambda^6)$. If we denote the number of double roots in either factor as (s_+, s_-), in our case, these can take the values $(3,1)$, $(1,3)$ and $(2,2)$. All these branches meet at vacua that have $(s_+, s_-) = (3,2)$ or $(2,3)$ at which the branchless tree discussed in Section 2.2.8 appear. The $\mathcal{N} = 1$ branches are further classified by the confinement index and the non-conventional order parameters which we defined earlier in Section 2.3.2. Let us consider each value of (s_+, s_-) in turn.

- *The* $(3,1)$ *And* $(1,3)$ *Confining Vacua*

The general factorization problem (3.1) is solved by the polynomials[1]

$$\begin{aligned} P_6(z) + 2\eta\Lambda^6 &= \big((z-a)^2(z-b) - 2\epsilon\Lambda^3\big)^2 \equiv R^2(z) \\ P_6(z) - 2\eta\Lambda^6 &= (z-a)^2(z-b)\big((z-a)^2(z-b) - 4\epsilon\Lambda^3\big) \equiv S(z) \end{aligned} \tag{3.2}$$

with $\eta^2 = 1$ and $\epsilon^2 = \eta$. These polynomials can by obtained by the "multiplication by 2" map acting on either of the polynomials $P_3(z) = (z-a)^2(z-b) \mp 2\Lambda_0^3$:

$$P_6(z) = 2\Lambda^6\kappa^2\, T_2\left(\frac{P_3(z)}{2\kappa\Lambda^3}\right), \tag{3.3}$$

with $\Lambda_0^6 = \kappa^2\Lambda^6$, $\kappa^4 = 1$ and $\epsilon = \pm\kappa$. The various signs and phases in these expressions are crucial so that all the $\mathcal{N} = 1$ vacua are taken into account. However, as discussed in Section 2.2.7, since these lead to trees in the same equivalence class, we will drop such phase factors in what follows.

The Rigid Quartic Factorization

If we require that the polynomial $R(z)$ has a double root (which is to say that its discriminant vanishes) we get the rigid factorization

$$P_6(z)^2 - 4\Lambda^{12} = F_4(z)\, H_2^2(z)\, Q_1^4(z)\,. \tag{3.4}$$

This fixes Λ to be

$$\Lambda^3 = \frac{2}{27}(a-b)^3\,. \tag{3.5}$$

Substituting this into the polynomials in (3.2) and using the shift and scaling symmetry to set $a = -5$ and $b = 10$, we get

$$\begin{aligned} R^2(z) &= (z-5)^4(z+10)^2\,, \\ S(z) &= (z+5)^2(z-10)(z^3 - 75z + 750)\,. \end{aligned} \tag{3.6}$$

From this, we see that the polynomials that solve the equation

$$P_6^2(z) - 4(250)^4 = F_4(z)\, H_2^2(z)\, Q_1^4(z) \tag{3.7}$$

[1]Refer to equation (3.47) in [12].

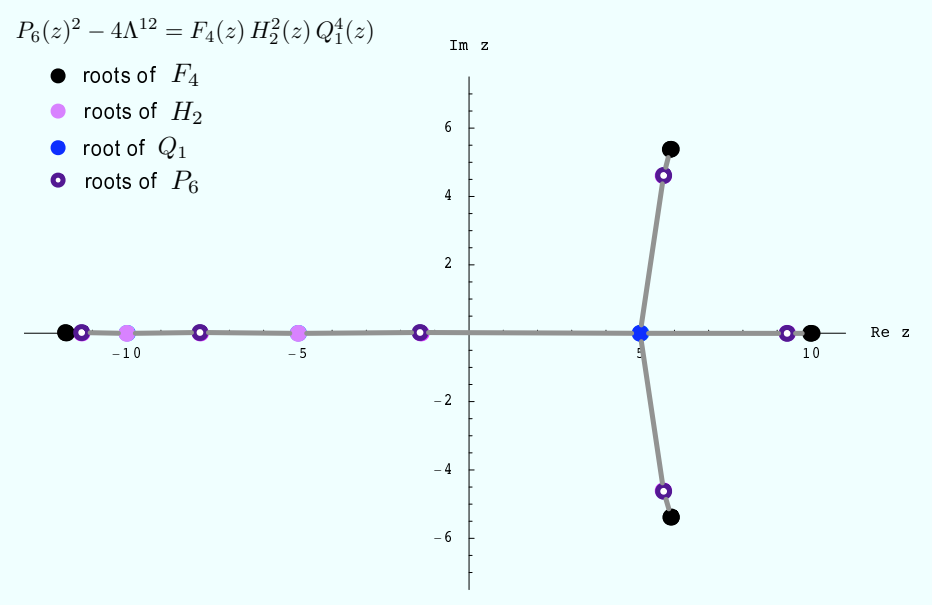

Figure 3.1: The tree obtained in the $(3,1)$ confining branch with a four-valent vertex. It has confinement index $t = 2$.

are given by

$$Q_1(z) = z - 5\,, \quad H_2(z) = (z+5)(z+10)\,, \quad F_4 = (z-10)(z^3 - 75z + 750)\,,$$
$$P_6(z) = z^6 - 150z^4 + 500z^3 + 5625z^2 - 37500z - 62500\,. \tag{3.8}$$

Plotting the zeroes of the polynomials leads to the tree in Figure 3.1. Let us make a few comments about the solution. All polynomials are defined over $\mathbb{Q}$. From the discussion in Section 2.2.4 about the action of the Galois group, we see that the tree is left invariant; in other words, it is the only element in its Galois orbit. From (3.3) we see that the tree has confinement index 2. However, observe that the tree is *not* a scaled up version of a smaller tree. This illustrates the point made in Section 2.4.1 and especially equation (2.30). One can moreover check that the combinatorial method for computing the confinement index, as explained in Section 2.4.3, also gives the correct answer $t = 2$.

The Rigid Cubic Factorization

Starting from (3.1) one can also get another rigid factorization by tuning one of

the zeroes of $F_4(z)$ to coincide with a zero of $H_4(z)$:

$$P_6^2(z) - 4\Lambda^{12} = F_3(z)\, H_3^2(z)\, Q_1^3(z)\,. \tag{3.9}$$

This leads to the condition $a = b$ in (3.2). This implies that $S(z)$ has a cubic root at $z = a$. Using the shift and scale symmetry, we can set $a = 0$ and $\Lambda = 1$. This leads to a very simple solution of (3.34) :

$$P_6(z) = z^6 - 4z^3 + 2\,, \qquad H_3(z) = z^3 - 2\,, \qquad F_3(z) = z^3 - 4 \quad \text{and} \quad Q_1(z) = z\,. \tag{3.10}$$

The tree associated to the factorization is drawn below in Figure 3.2.

Note that, unlike the quartic case, the multiplication by 2 is easily understood: this particular solution can also be obtained by first solving the rigid factorization problem

$$P_3^2(z) - 4\Lambda^6 = Q_1^3(z)\, F_3(z)\,, \tag{3.11}$$

and then applying to the resulting solution the multiplication map. The solution is once again defined over $\mathbb{Q}$ and the tree in Figure 3.2 is the lone element in its Galois orbit.

- *The* $(2, 2)$ *Confining Vacua*

In this sector, the factorization problem (3.27) is solved by the polynomials[2]

$$P_6(z) + 2\Lambda^6 = (z^2 + g - \Lambda^2)^2 (z^2 + g + 2\Lambda^2)\,, \tag{3.12}$$

$$P_6(z) - 2\Lambda^6 = (z^2 + g + \Lambda^2)^2 (z^2 + g - 2\Lambda^2)\,. \tag{3.13}$$

These polynomials are obtained by the "multiplication by 3" map; modulo phase factors, $P_6(z)$ in (3.12) is given in terms of $P_2(z) = z^2 + g$ as

$$P_6(z) = 2\Lambda^6\, T_3\left(\frac{P_2(z)}{2\Lambda^2}\right)\,. \tag{3.14}$$

The trees in this branch will therefore have confinement index 3.

[2]Refer equation (3.50) in [12].

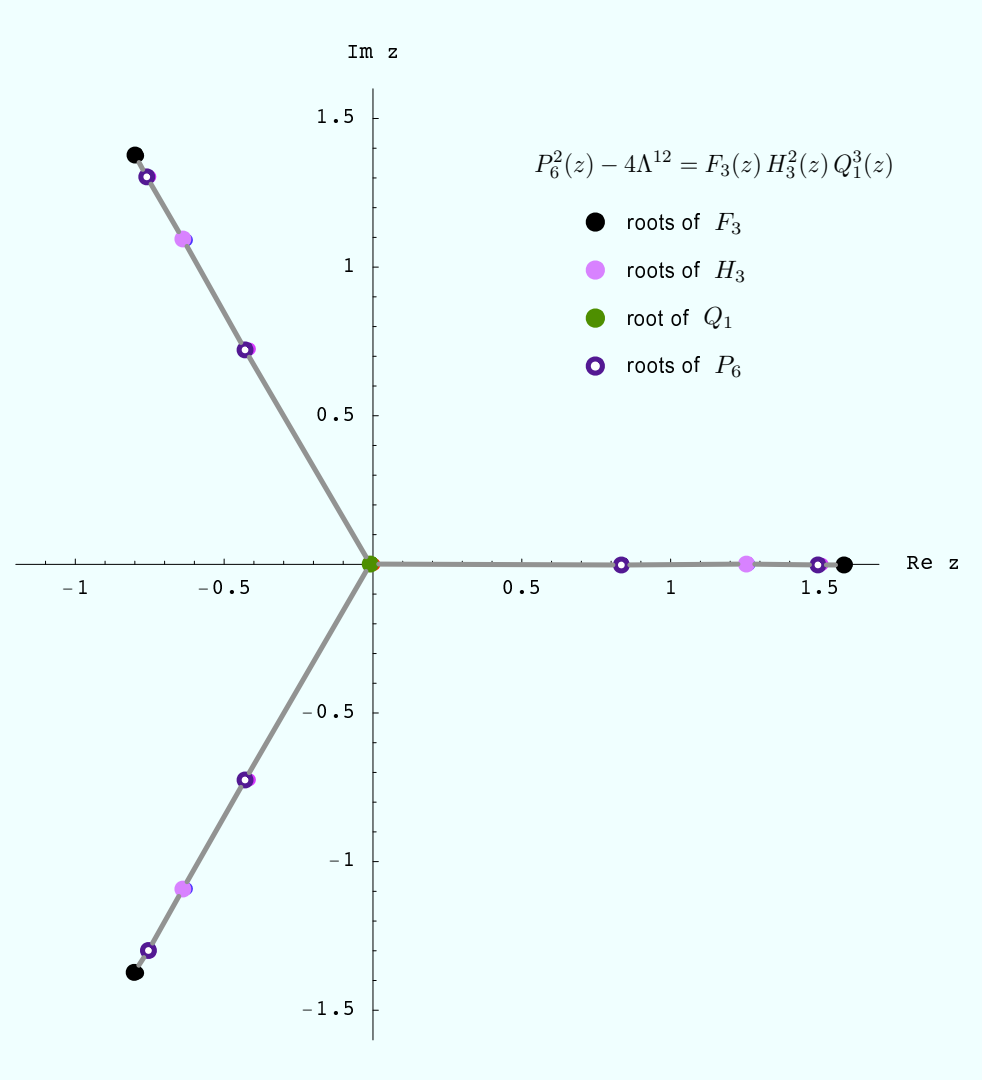

Figure 3.2: Tree obtained in the $(3, 1)$ confining branch with a trivalent vertex. It is a scaled up dessin, obtained by applying the multiplication map on a smaller dessin with 3 edges.

The Rigid Quartic Factorization

One can set $g = \Lambda^2$ to get the quartic factorization (3.27), while one can rescale z to set $\Lambda = 1$. The resulting polynomials that solve (3.27) are

$$P_6(z) = z^4(z^2+3) - 2\,, \quad H_2(z) = (z^2+2)\,, \tag{3.15}$$

$$Q_1(z) = z \quad \text{and} \quad F_4(z) = (z^2+3)(z^2-1)\,. \tag{3.16}$$

Plotting the roots of the polynomials leads, this time, to the tree in Figure 3.3. The polynomials are defined over $\mathbb{Q}$ and so the tree is the only element in its Galois orbit.

The Rigid Cubic Factorization

Note that it is not possible to get the cubic factorization equation (3.34) by tuning the available free parameter. Thus, we do not find any trivalent tree in this branch of the moduli space. One can also show this using the combinatorial definition of the confinement index by trying to construct a trivalent tree with six edges and $t = 3\,$.

- *The* $(2,2)$ *Coulomb Vacua*

The solution of the factorization problem (3.27) in this branch is parametrized as[3]

$$\begin{aligned} P_6(z) + 2\Lambda^6 &= \left[z^2 + (1+\sigma)z + \frac{(3+\sigma)(9+15\sigma-\sigma^2+\sigma^3)}{108}\right]^2 \\ &\qquad \left[z^2 - \frac{(1-\sigma)(3-\sigma)^2(3+\sigma)}{108}\right] \\ P_6(z) - 2\Lambda^6 &= \left[(z+\frac{2\sigma}{3})^2 + (1-\sigma)(z+\frac{2\sigma}{3}) + \frac{(3-\sigma)(9-15\sigma-\sigma^2-\sigma^3)}{108}\right]^2 \\ &\qquad \left[(z+\frac{2\sigma}{3})^2 - \frac{(1+\sigma)(3+\sigma)^2(3-\sigma)}{108}\right] \end{aligned} \tag{3.17}$$

[3]Refer to equation (3.53) in [12]. We have set $g \to \sigma\, h$, $z- \to z\, h$ and $\Lambda \to \Lambda\, h$ in that equation.

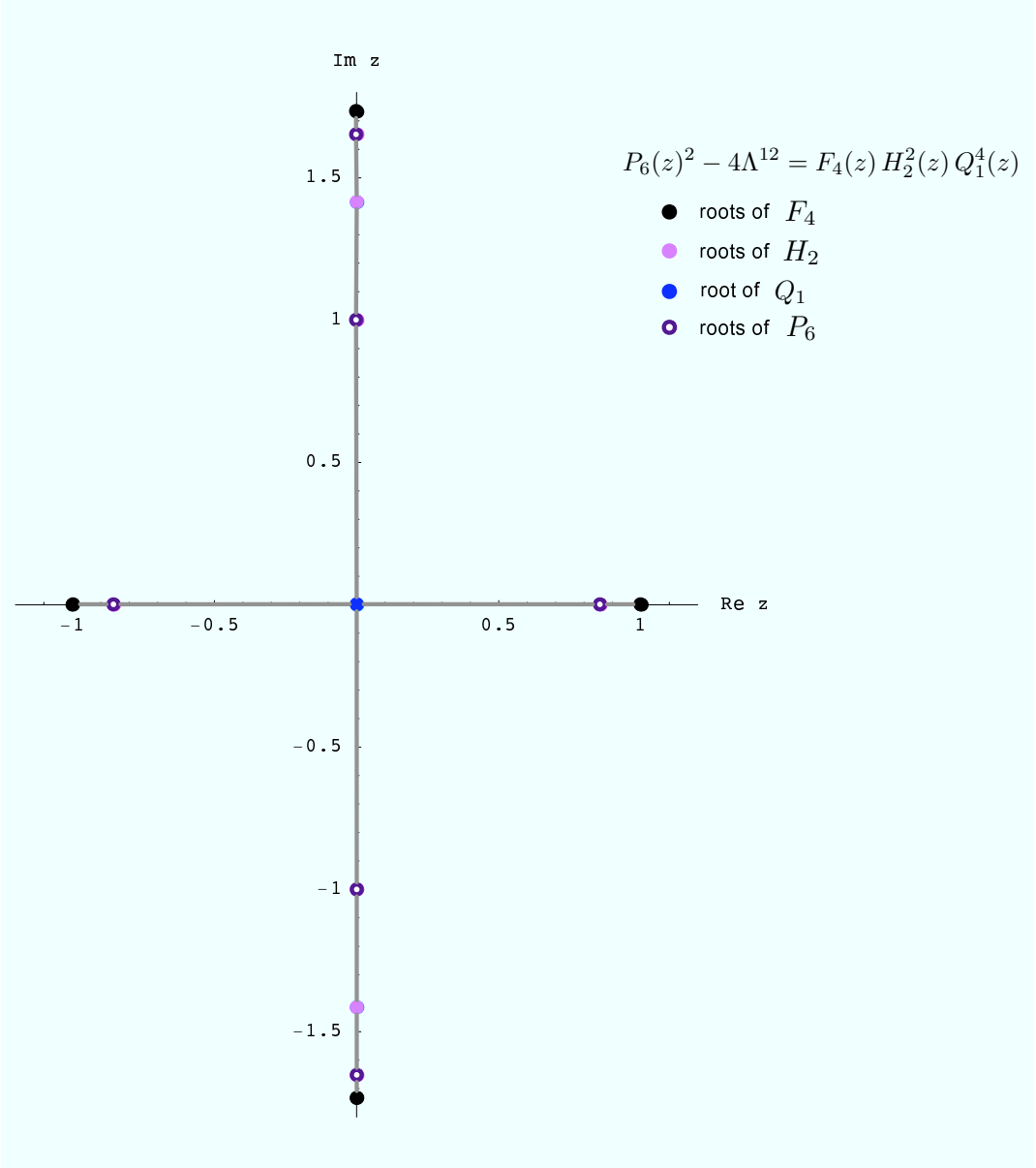

Figure 3.3: The tree obtained in the $(2, 2)$ confining branch with a four-valent vertex. It has confinement index $t = 3$.

with σ and Λ satisfying the constraint

$$\sigma^5(\sigma^2-9)^2 = 27^3\Lambda^6\,. \tag{3.18}$$

The Rigid Quartic Factorization

Requiring that the first factor in the either of the two equations in (3.17) has a double root leads to the quartic factorization (3.27). We get the condition

$$\sigma^2 - 25 = 0\,. \tag{3.19}$$

For $\sigma = 5$, the polynomials that solve the equation (3.7) are given by

$$\begin{aligned} &Q_1(z) = z-2\,, \quad H_2(z) = z^2 - \frac{2}{3}z + \frac{128}{27}\,, \quad F_4 = \left(z^2+\frac{64}{9}\right)\left(z^2-\frac{20}{3}z+\frac{332}{27}\right)\,, \\ &P_6(z) = z^6 - 8z^5 + \frac{280}{9}z^4 - \frac{800}{9}z^3 + \frac{560}{3}z^2 - \frac{2048}{9}z + \frac{3839488}{19683}\,. \end{aligned} \tag{3.20}$$

Plotting the zeroes of the polynomials lead to the tree in Figure 3.4. Since the tree is found in the Coulomb branch, it has confinement index 1. This can also be checked directly using the combinatorial definition: we get $t = GCD(3,4) = 1$. For $\sigma = -5$, we get an equivalent tree but reflected about the $\mathrm{Re}\,(z) = 0$ axis. Note that the solution in (3.20), like the ones we have obtained earlier, are polynomials defined over $\mathbb{Q}$. This is why the Galois orbits in each case consist of only a single tree. We now discuss a set of trees whose associated number field is non-trivial and therefore constitute a larger Galois orbit.

The Rigid Cubic Factorization

Requiring that the two factors in the first of the two equations in (3.17) have a root in common leads to the non-trivial condition[4]

$$\sigma^3 - 3\sigma^2 + 3\sigma + 15 = 0\,. \tag{3.21}$$

[4]The similar constraint for the second equation does not change the number field and we get the same set of trees.

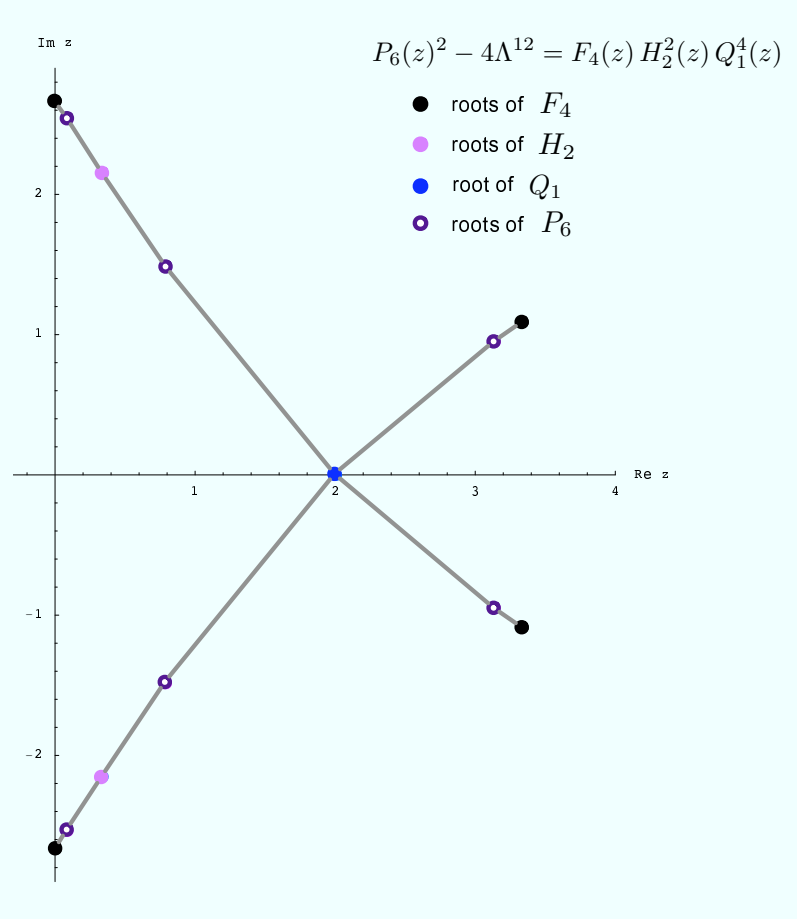

Figure 3.4: The tree obtained in the $(2, 2)$ coulomb branch with a four-valent vertex.

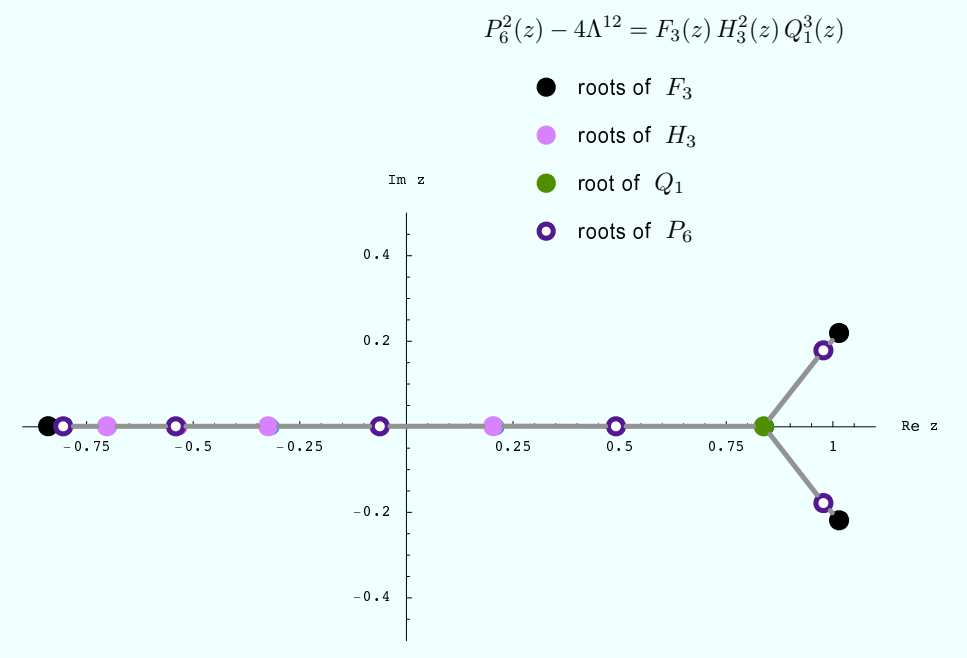

Figure 3.5: Tree for the case $\sigma^{(0)}$ in (3.22). It has $t = 1$.

Solving for σ leads to three solutions

$$\sigma = \begin{cases} \sigma^{(0)} = (1 - 2\,(2)^{\frac{1}{3}}) \\ \sigma^{(+)} = (1 + 2^{\frac{1}{3}}(1 - i\,\sqrt{3})) \\ \sigma^{(-)} = (1 + 2^{\frac{1}{3}}(1 + i\,\sqrt{3})) \end{cases} \tag{3.22}$$

Substituting these results into the polynomials and plotting their roots lead to the trees in Figure 3.5, 3.7 and 3.6 respectively. All of these have confinement index $t = 1$.

From the fact that all three trees are obtained from a single polynomial (3.21) irreducible over $\mathbb{Q}$, it follows that these three trees belong to the same Galois orbit. From (3.22), we observe that unlike the earlier solutions which were all defined over $\mathbb{Q}$, the number field associated to these trees is non-trivial.

Let us study this example in more detail. The terminology is explained in Appendix A. By inspection of (3.22), we find that $\sigma^{(0)}$ and $\sigma^{(\pm)}$ belong to the field $K = \mathbb{Q}(2^{\frac{1}{3}}, \omega)$ where $\omega = \frac{1}{2}(1 + i\sqrt{3})$ (a cube root of unity). It is easy to see

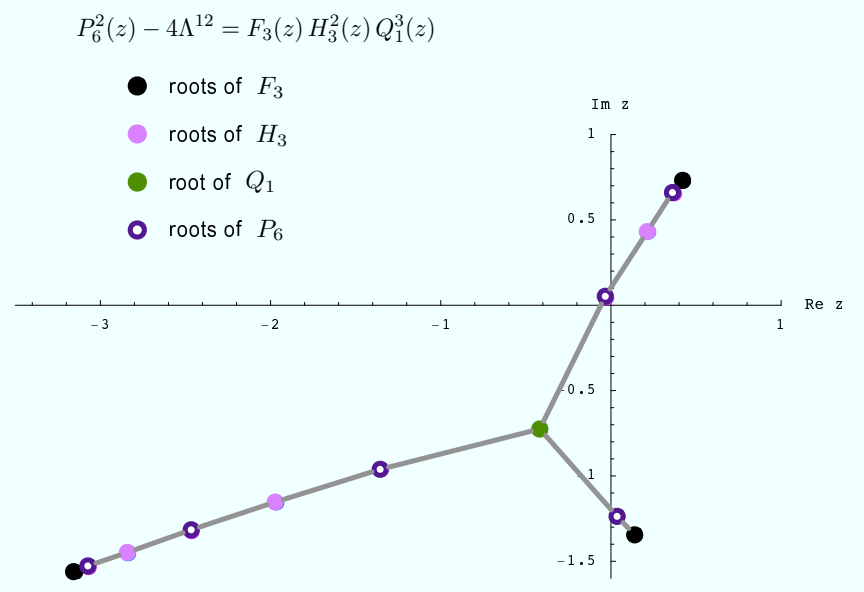

Figure 3.6: Tree for the case $\sigma^{(-)}$ in (3.22). It has $t = 1$.

that K is also the splitting field of the polynomial $x^3 - 2$, whose associated Galois group $\mathrm{Gal}(K/\mathbb{Q})$ is the group of permutations of three elements, S_3, which is non-abelian.

- *The* $(3,2)$ *And* $(2,3)$ *Vacuum*

  If two roots of $F_4(z)$ coincide in (3.1) we get the factorization problem

$$P_6^2(z) - 4\Lambda^{12} = F_2(z)H_5^2(z) = (z^2 - 4\Lambda^2)H_5^2(z)\,, \tag{3.23}$$

  where, in the second equality, we have suitably shifted and scaled z. Setting Λ to one, (3.23) is solved by the polynomials [22]

$$P_6(z) = 2\,T_6\left(\frac{z}{2}\right) \qquad \text{and} \qquad H_5(z) = U_5\left(\frac{z}{2}\right)\,.$$

  Plotting the zeroes of these polynomials leads to the branchless tree discussed in Section 2.8. In Figure 17, we show the tree that arises for the particular case of $U(6)$. As explained in the earlier more general discussion, this is the singularity at which the $\mathcal{N} = 1$ branches meet. This is the only case we consider that has one of the $N_i = 0$. Therefore this can be explained as the intersection of $U(1)$

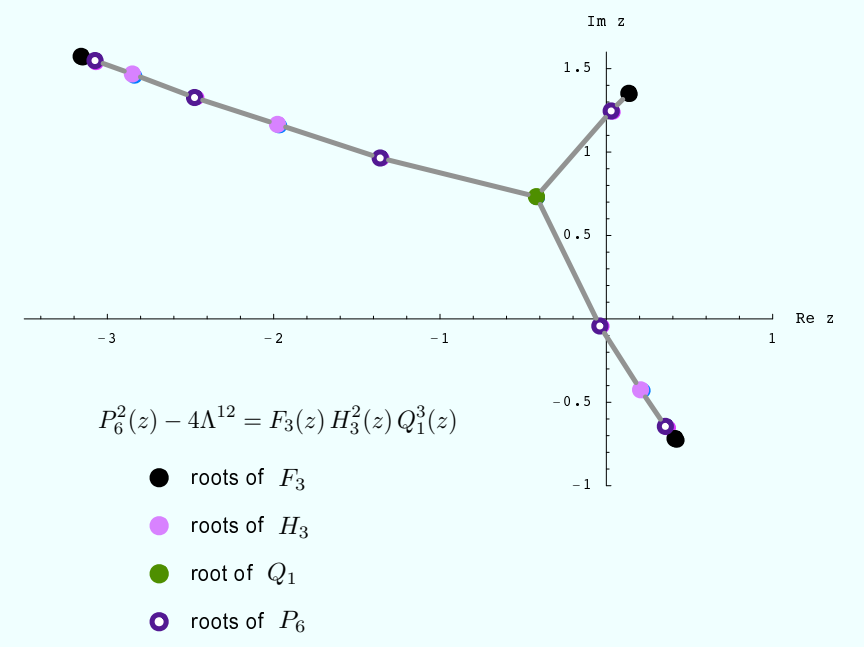

Figure 3.7: Tree for the case $\sigma^{(+)}$ in (3.22). It has $t = 1$.

and $U(1)^2$ branches. See Appendix C for a more complete discussion. From the combinatorial definition of the confinement index, the dessin has $t = 6$, the largest value for the case with $N = 6$ edges.

3.1.2 Classifying Dessins From Gauge Theory

So far we have started with the non-rigid factorization problem and tuned the parameters to get isolated singularities where dessins appear. We have seen how the dessins fall into different Galois orbits. We now classify them according to the $\mathcal{N} = 1$ branches to which they belong using gauge theory order parameters. We summarize all our findings from the gauge theory point of view in Figure 3.9. Given that the confinement index is a Galois invariant, we find each of the three trees with a 4-valent vertex to belong to distinct Galois orbits as shown in Figure 3.9. Similarly, using the confinement index, we find that the trivalent trees fall into at least two distinct Galois orbits: the trivalent dessin with $t = 2$ is left invariant under the action of $\mathrm{Gal}(\overline{\mathbb{Q}}/\mathbb{Q})$.

Note that in the $t = 1$ and $t = 2$ branches we have both trivalent and quartic dessins.

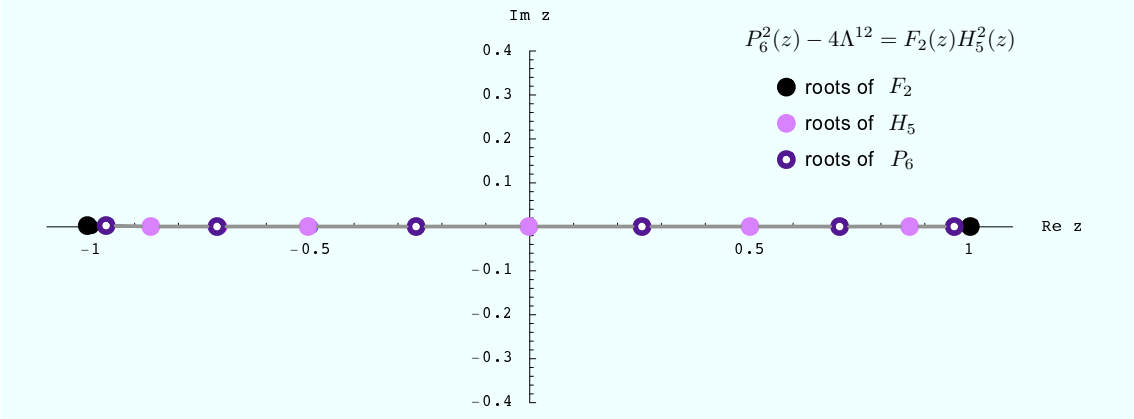

Figure 3.8: The tree obtained at the maximally confining point. It has $t = 6$.

From our discussion about valency lists, it follows that they are in distinct Galois orbits. However, in each case, they have the same value of t and of (s_+, s_-). This is where extra gauge theory criteria are needed in order to distinguish these isolated phases.

Let us concentrate on the pair of dessins with $t = 2$. A simple way to see that these correspond to two different phases is by tracing them back to the problem in $U(3)$ broken to $U(1) \times U(2)$ and then "multiplying by 2". The trivalent dessin comes from the unique dessin with three edges. Such a special point is where $P_3^2(z) - 1 = z^3(z^3 - 1)$. This is actually known to be a superconformal field theory in the IR (see [2, 49] and references therein). On the other hand, the quartic dessin comes from a generic point in the $U(3)$ theory and therefore it is a different phase.

This discussion proves that the two dessins are in different phases. However, we want to go further and show that even the theory corresponding to the quartic dessin is a distinct phase from its neighbors in the $t = 2$ branch. Recall that in Section 2.4.2 we argued that there might be extra chiral ring relations that characterize the corresponding special points within each branch. Let us see this in detail in this case.

For the quartic factorization (3.27) in the branch defined by $s_+ = s_- = 2$, we take

$$\tilde{H}_2(z) = (z - c)^2\,, \qquad R_2(z) = z^2 + \alpha z + \beta\,, \qquad H_2(z) = z^2 + \gamma z + \delta\,. \tag{3.24}$$

where we have adopted the notations in (2.23). Using these in the definition of the t_r in Section 2.3.2 we find the following chiral ring relation that is satisfied *only* at the

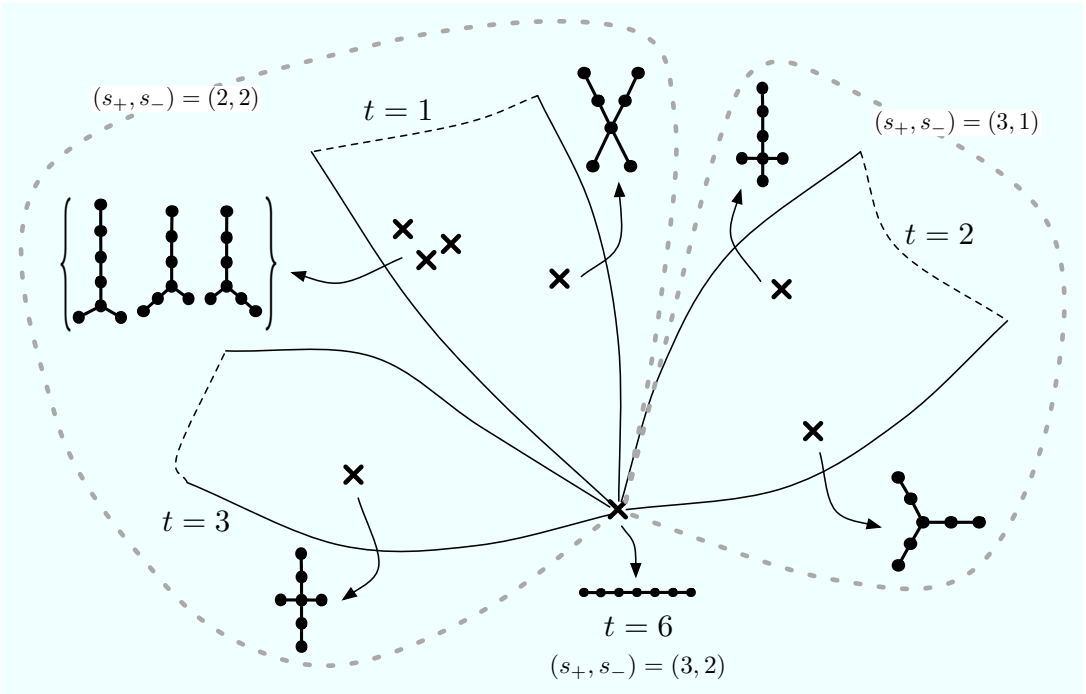

Figure 3.9: Summary of the analysis of the $U(6)$ gauge theory and the location of the trees in the various branches of the gauge theory moduli space. The dotted lines indicated a coarse-grained classification of $\mathcal{N} = 1$ branches based on the (s_+, s_-) values. In this case the branches are more finely distinguished by the confinement index t. Branches meet at the point where another monopole becomes massless.

special (quartic) point in the $\mathcal{N}=1$ branch:

$$4\,t_0\,t_2^3 - 3\,t_1^2\,t_2^2 + 4\,t_1^3\,t_3 - 6\,t_0\,t_1\,t_2\,t_3 + t_0^2\,t_3^2 - 4t_1^3\,\Lambda^6 + 6\,t_0\,t_1\,t_2\,\Lambda^6 - 2t_0^2\,t_3\,\Lambda^6 + t_0^2\,\Lambda^{12} = 0\,. \tag{3.25}$$

Note that this relation uses the Λ^6 term in (2.25). In this polynomial, each term has the same R-charge, or equivalently the same dimension, and also the same Q_Φ. To see this, note that Λ naturally has $Q_\Phi = 1$. However, in (3.25) we have set the coupling of the cubic term in the superpotential to 1. Such a coupling g is dimensionless, has $Q_\Phi = -3$ and shows up in (3.25) in the combination $g\Lambda^6$ which then has $Q_\Phi = 3$.

Our new relation (3.25) is not satisfied at any other point in the $t=2$ branch apart from the special point under consideration. At any other point in the same branch one can show that all t_r's with $r = 0, \ldots, 5$ are independent. In other words, one can at most find a relation similar to (3.25), which gives t_6 in terms of the other six. Assuming that our conjectures about the physical order parameters being Galois invariants are correct, this concludes our discussion of the trees from the physics point of view as we have, using purely gauge theory criteria, managed to classify the dessins into distinct Galois orbits.

3.1.3 $U(6)$ Gauge Theory: A Mathematician's Point Of View

We now discuss how a mathematician would tackle the same problem of classifying dessins into Galois orbits. We start with a particular valency list and find all solutions to the associated polynomial equations using differentiation methods. In the end, one generically finds a polynomial that factors over $\mathbb{Q}$. Each factor corresponds to a different Galois orbit.

For the $U(6)$ gauge theory perturbed by a cubic superpotential, there are three distinct valency lists possible for the rigid factorization problem:

- Consider the branchless tree shown in Figure 3.8. From the valency list, one gets the polynomial equation

$$P_6^2(z) - 4 = F_2(z) H_5^2(z) = (z^2 - 4) H_5^2(z)\,, \tag{3.26}$$

where, in the second equality, we have suitably shifted and scaled z. In Appendix A of [5] it is shown how to obtain the solution to this equation using the differentiating trick. The solutions are Chebyshev polynomials. Plotting the roots of the polynomials, we get back the tree in Figure 3.8.

- The trees shown in Figures 3.1, 3.3 and 3.4 have the same valency list and arise from the polynomial equation

$$P_6(z)^2 - 4 = F_4(z)\, H_2^2(z)\, Q_1^4(z)\,. \tag{3.27}$$

Differentiating (3.27) we get

$$\begin{aligned} 2\, P_6(z)P_6'(z) = H_2(z)\, Q_1^3(z)\, \Big(& F_4'(z)H_2(z)Q_1(z) \\ & + 2\, F_4(z)H_2'(z)Q_1(z) + 4\, F_4(z)H_2(z)Q_1'(z) \Big)\,. \end{aligned} \tag{3.28}$$

Since all polynomials involved are monic, it is easy to see that this leads to two equations

$$\begin{aligned} P_6'(z) &= 6\, H_2(z)\, Q_1^3(z)\,, \\ 12\, P_6(z) &= F_4'(z)H_2(z)Q_1(z) + 2\, F_4(z)H_2'(z)Q_1(z) + 4\, F_4(z)H_2(z)Q_1'(z)\,. \end{aligned} \tag{3.29}$$

After scaling and shifting the z variable, one can write

$$\begin{aligned} H_2(z) &= z^2 - 1\,, \qquad & Q_1(z) &= z + q_1\,, \\ P_6(z) &= z^6 + \sum_{i=1}^{6} p_i\, z^{6-i}\,, \qquad & F_4(z) &= z^4 + \sum_{i=1}^{4} f_i\, z^{4-i}\,. \end{aligned} \tag{3.30}$$

The first equation in (3.29) leads to linear equations for the p_i, which we can easily solve to obtain

$$\begin{aligned} p_1 &= \frac{18}{5} q_1\,, \qquad & p_2 &= \frac{3}{2}(3q_1^2 - 1)\,, \\ p_3 &= 2q_1(q_1^2 - 3)\,, \qquad & p_4 &= -9q_1^2\,, \qquad & p_5 &= -6q_1^2\,. \end{aligned} \tag{3.31}$$

Substituting this in the second of the two equations in (3.29) leads to

$$\begin{aligned} f_1 &= \frac{16}{5} q_1\,, \qquad & f_2 &= \frac{1}{25}(79q_1^2 - 25)\,, \qquad & f_3 &= \frac{2}{25} q_1(7q_1^2 - 55)\,, \\ f_4 &= \frac{1}{100}(-75 - 718q_1^2 - 35q_1^4)\,, \qquad & p_6 &= \frac{1}{100}(25 + 276q_1^2 + 7q_1^4)\,, \end{aligned} \tag{3.32}$$

such that q_1 satisfies the equation

$$q_1(q_1^2 - 25)(5q_1^2 + 3) = 0\,. \tag{3.33}$$

Each inequivalent solution of (3.33) leads to a dessin. Thus, each dessin has associated to it a specific number field [43]. In (3.33), there are solutions obtained by an overall sign flip: these do not lead to inequivalent trees.

Plotting the roots of the polynomials for each of the cases $q_1 = \{5, 0, i\sqrt{\frac{3}{5}}\}$ respectively leads to the trees in Figures 3.1, 3.3 and 3.4. Since each of the values of q_1 is a Galois orbit in itself (up to an overall sign), the three solutions lead to dessins that belong to different Galois orbits. Thus, they should have a different set of Galois invariants. That this is so can be checked by computing the monodromy groups. We will postpone further analysis to the next section.

- The trivalent trees in Figures 3.2, 3.5, 3.6 and 3.7 all have the same valency list and arise from the polynomial equation

$$P_6^2(z) - 4 = F_3(z)\, H_3^2(z)\, Q_1^3(z)\,. \tag{3.34}$$

Differentiating the equation as before leads to two equations

$$\begin{aligned} P_6'(z) &= 6H_3(z)Q_1^2(z) \\ 12P_6(z) &= F_3'(z)H_3(z)Q_1(z) + 2F_3(z)H_3'(z)Q_1(z) + 3F_3(z)H_3(z)Q_1'(z)\,. \end{aligned} \tag{3.35}$$

We can choose to parametrize the polynomials as

$$\begin{aligned} P_6(z) &= z^6 + \sum_{i=1}^{6} p_i z^{6-i}\,, \qquad & H_3(z) &= z^3 + \sum_{i=1}^{3} h_i z^{3-i}\,, \\ Q_1(z) &= z\,, & F_3(z) &= z^3 + \sum_{i=1}^{3} f_i z^{3-i}\,, \end{aligned} \tag{3.36}$$

where we have used the shift symmetry to set the constant coefficient of Q_1 to be zero. We will not discuss the solution in detail here, as the analysis is similar to the one we did for the quartic factorization. The solution set is parametrized by (h_1, h_2) that satisfy the relation

$$24\, h_1^6 - 156\, h_1^4\, h_2 + 450\, h_1^2\, h_2^2 - 625\, h_2^3 = 0\,. \tag{3.37}$$

We find two branches of solutions :

a) $h_1 = h_2 = 0$: This leads to the simple solutions

$$P_6(z) = z^6 + 2z^3 + \frac{1}{2}\,, \qquad H_3(z) = z^3 + 1\,, \qquad f_3(z) = z^3 + 2\,. \tag{3.38}$$

The tree that corresponds to this solution is shown in the Figure 3.2.

b) $h_1, h_2 \neq 0$: One can use the scaling symmetry to set $h_1 = 1$ and there are three solutions which are solutions to the cubic equation for h_2 in (3.37). These are given by

$$h_2 = \begin{cases} h_2^{(0)} = -\frac{2}{25}(-3 - 2\,(2)^{\frac{1}{3}} + 2^{\frac{2}{3}}) \\ h_2^{(+)} = \frac{1}{25}(6 + 2^{\frac{2}{3}}(1 - i\,\sqrt{3}) - 2\,(2)^{\frac{1}{3}}(1 + i\,\sqrt{3})) \\ h_2^{(-)} = \frac{1}{25}(6 + 2^{\frac{2}{3}}(1 + i\,\sqrt{3}) - 2\,(2)^{\frac{1}{3}}(1 - i\,\sqrt{3})) \end{cases} . \tag{3.39}$$

The three trees associated to $h_2^{(0)}$, $h_2^{(-)}$ and $h_2^{(+)}$ are shown in the Figures 3.5, 3.6 and 3.7 respectively. Since $h_2^{(0)}$, $h_2^{(\pm)}$ are solutions to the polynomial equation (3.37) which is irreducible over $\mathbb{Q}$, the corresponding dessins are part of the same Galois orbit. Moreover, the number field is $\mathbb{Q}(2^{1/3}, w)$ with $w^3 = 1$ as it should be from our discussion in Section 3.1.1.

For $h_2 = h_2^{(0)}$ (Figure 3.5), we present the polynomials that solve (3.35) :

$$\begin{aligned} P_6(z) &= z^6 + \frac{6}{5}z^5 + \frac{11250 + 7500\,2^{\frac{1}{3}} - 3750\,2^{\frac{2}{3}}}{31250}\,z^4 + \frac{1000 + 4500\,2^{\frac{1}{3}} - 3000\,2^{\frac{2}{3}}}{31250}\,z^3 \\ &\quad + \frac{44 + 30\,2^{\frac{1}{3}} - 51\,2^{\frac{2}{3}}}{31250} \\ H_3(z) &= z^3 + z^2 + \frac{30 + 20\,2^{\frac{1}{3}} - 10\,2^{\frac{2}{3}}}{125}\,z + \frac{2 + 9\,2^{\frac{1}{3}} - 6\,2^{\frac{2}{3}}}{125} \\ F_3(z) &= z^3 + \frac{2}{5}z^2 + \frac{-15 + 20\,2^{\frac{1}{3}} - 10\,2^{\frac{2}{3}}}{125}\,z + \frac{8 - 6\,2^{\frac{1}{3}}}{125}\,. \end{aligned} \tag{3.40}$$

By direct computation, we have therefore classified into Galois orbits the class of trees with 6 edges that we considered in Section 3.1.1. The results of the

mathematical analysis of the rigid factorizations are summarized in Figure 3.10. These coincide with the classification we obtained from the gauge theory analysis.

3.1.4 Using Galois Invariants To Classify Dessins

In the previous section, we have shown explicitly how dessins are organized into Galois orbits. We now attempt to rediscover the classification using the Galois invariants discussed in Section 2.3.1, focusing on the factorizations in (3.27) and (3.34).

•*Quartic Case*

From the direct solution of the factorization problem, we see that there are three distinct Galois orbits that correspond, respectively, to the three distinct trees in Figures 3.1, 3.3 and 3.4. These three trees can been partially distinguished by the more refined valency list introduced in Section 2.2.6 for trees. Let us see this in detail.

Depending on how one distributes the roots between the two factors $(P(z) \pm 2)$, there are two distinct possibilities:

$$P_6(z) - 2 = \begin{cases} \tilde{H}_1^2(z) Q_1^4(z) \\ \\ F_2(z) Q_1^4(z) \end{cases} \tag{3.41}$$

If we assign negative valences to each of the zeroes of the polynomials appearing on the right, then, the first choice singles out the tree in Figure 3.3 as the only possibility. On the other hand, the second possibility is satisfied by the trees in both Figures 3.1 and 3.4. We assign signs $+/-$ to the vertices in Figure 3.10 to indicate these two possibilities.

In order to distinguish the remaining two dessins, we can compute the monodromy group of the trees[5]. Here, we compute the monodromy groups of the trees with the refined bi-partite structure, as in Figure 2.7 of Section 2.2.6. Taking the difference of the two equations in (2.15) we find an auxiliary polynomial equation that leads to a non-clean Belyi map, whose pre-images of 1 are the vertices with $-$ valency and

[5]All the monodromy groups have been obtained using the GAP software downloaded from http://www.gap-system.org.

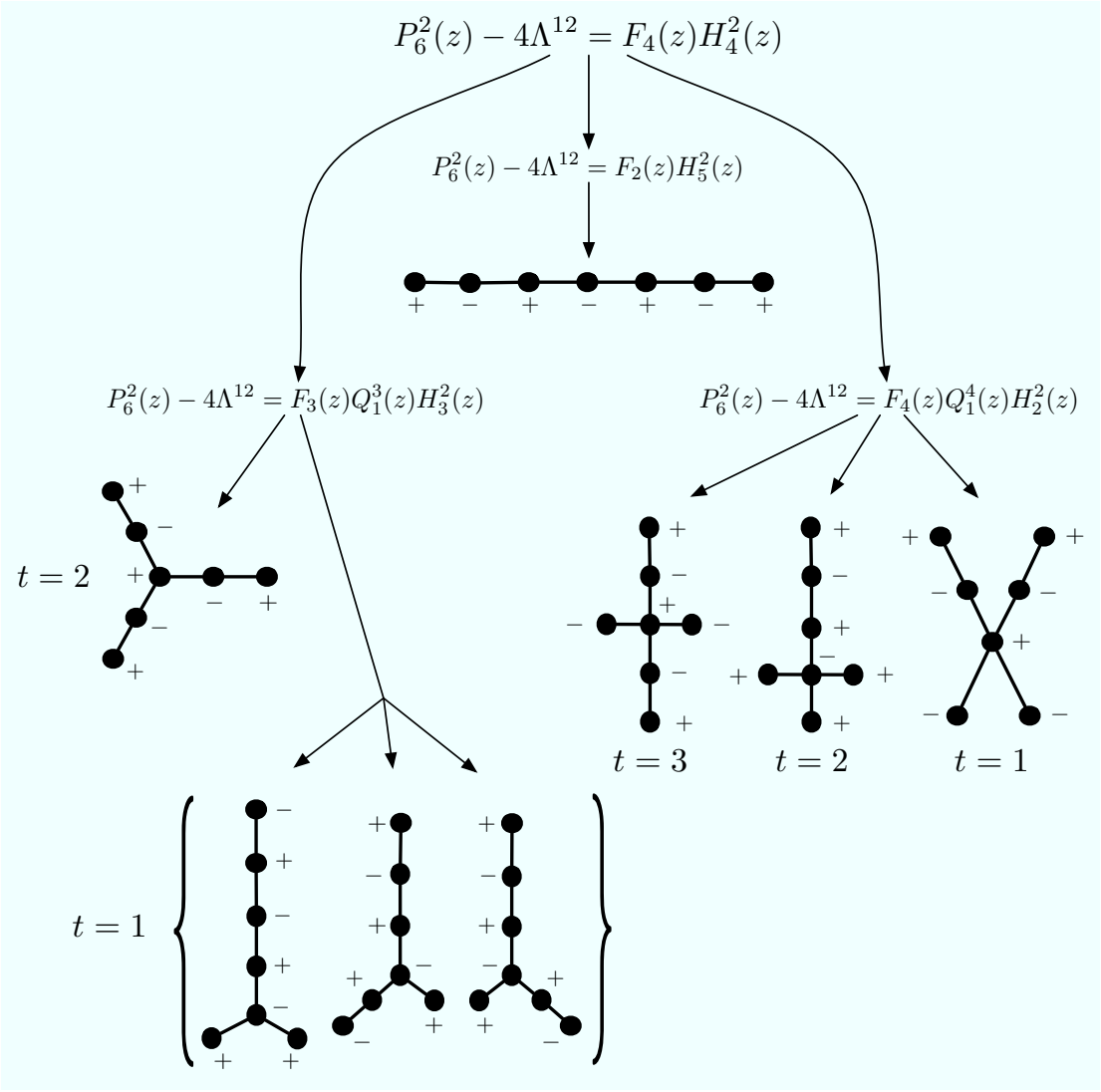

Figure 3.10: Summary of the analysis of the $U(6)$ gauge theory and the associated dessins. We have also included the results of gauge theory analysis and indicated the confinement index and refined valency list of each figure.

Figure	Monodromy Group
10	$(S_3 \times S_3) \ltimes C_2$
12	$C_2 \times S_4$
13	S_5
11	$C_3 \times S_3$
14, 15, 16	S_6

Table 3.1: Monodromy groups for dessins that occur in the pure $U(6)$ gauge theory perturbed by a cubic superpotential.

whose pre-images of 0 are vertices with + valency. The monodromy group for trees is therefore generated by $\sigma_{+/-}$, which correspond to the permutation of edges around the $+/-$ vertices respectively.

The groups of all the trees we have encountered in the $U(6)$ example have been collected in Table 3.1. S_n is the permutation group of n elements while C_n is the cyclic group of n elements. The monodromy group turns out to be different for the trees in Figures 3.1 and 3.4: for Figure 3.1, we get the monodromy group $(S_3 \times S_3) \ltimes C_2$, of order 72 , while for Figure 3.4, we get the monodromy group S_5 , of order 120 .

•*Cubic Case*

The discussion parallels the one for the quartic factorization. The two possibilities of distributing the roots

$$P_6(z) - 2 = \begin{cases} F_3(z) Q_1^3(z) \\ \\ F_2(z) \tilde{H}_2^2(z) \end{cases} \tag{3.42}$$

correspond to two distinct refined valency lists that distinguishes the tree in Figure 3.2 from any one of the trees in Figures 3.5, 3.6 or 3.7. In this case, no further invariant is required to distinguish them.

Thus, we find that the classification of dessins into Galois orbits agrees with what we obtained in Section 3.1.2 regarding the classification of isolated phases in gauge theory. So far we have only considered dessins that are trees. We now generalize our discussion and consider more general dessins. This will highlight some open questions related to the phases of gauge theories with flavour.

3.2 Gauge Theories With Flavour

In this section we turn to a discussion of gauge theories with matter. The dessins that appear at isolated singularities in the moduli space will no longer be trees. We will mostly focus on the curves that were discussed in [5], with isolated Argyres-Douglas singularities in the moduli space.

We start with a general discussion of the non-rigid factorization

$$P_N^2(z) + B_L(z) = Q_{2n}(z) H_{N-n}^2(z)\,, \tag{3.43}$$

where we have exhibited the degrees of the polynomials explicitly. This curve arises from a $\mathcal{N} = 2$ $U(N)$ gauge theory with N_f massive flavors broken to $\mathcal{N} = 1$ by a tree level superpotential

$$W_{\text{tree}} = \text{Tr} W(\Phi) + \tilde{Q}_{\tilde{f}} m_f^{\tilde{f}}(\Phi) Q^f\,, \tag{3.44}$$

where f and $\tilde{f}$ run over the number of flavors N_f and

$$W(z) = \sum_{k=1}^{n+1} \frac{g_k}{k} z^k, \qquad m_f^{\tilde{f}}(z) = \sum_{k=1}^{l+1} m_{f,k}^{\tilde{f}} z^{k-1}\,. \tag{3.45}$$

The $\mathcal{N} = 1$ vacua, as before, are those for which $Q_{2n}(z) = W'(z)^2 + f(z)$, where $f(z)$ is a polynomial such that $\deg(f) = \deg(W'(z))/2 - 1$. $m(z)$ is a matrix of polynomials of size $N_f \times N_f$.

It turns out that the only information about the superpotential $\tilde{Q}_{\tilde{f}} m_f^{\tilde{f}}(\Phi) Q^f$ which is relevant for the curve (3.43) is the polynomial [13, 31, 45]

$$B_L(z) = \det m(z)\,. \tag{3.46}$$

Clearly, plenty of choices of $m(z)$ can lead to the same $B_L(z)$.

The particular class of dessins we are interested in arise when $B_L(z)$ has only $n+1$ distinct roots. We use our shift and scale symmetry to set $B_L(z)$ to be of the form

$$B_L(z) = \alpha\, z^{m_0} (z-1)^{m_1} \prod_{j=2}^{n} (z - p_j)^{m_j}\,. \tag{3.47}$$

Two natural ways of obtaining such $B(z)$'s are the following:

- $N_f = L = \deg B_L(z)$ and $m_f^{\tilde{f}}(z)$ a constant diagonal mass matrix with m_0 masses equal to 0, m_1 masses equal to 1, and m_j masses equal to p_j.
- $N_f = n+1$ and $m_f^{\tilde{f}}(z)$ a diagonal matrix with polynomial entries z^{m_0}, $(z-1)^{m_1}$, and $(z-p_j)^{m_j}$.

The former leads to a theory with unbroken $\mathcal{N}=2$ supersymmetry if there is no $W(z)$. Moreover, it has a large flavor symmetry classically. The latter, on the other hand, has a very small number of flavors and generically no special flavor symmetry.

What we now do to obtain the Argyres-Douglas (AD) dessins studied in [5] is to further tune the masses of the flavors and the parameters of the superpotential to set

$$H_{N-n}(z) = Q_{2n}(z)\, R_{N-3n}(z)\,. \tag{3.48}$$

This leads to the rigid factorization problem [5]

$$P_N^2(z) + B_L(z) = Q_{2n}^3(z)\, R_{N-3n}^2(z)\,. \tag{3.49}$$

In the rest of the section we will focus on such factorization problems, for which many explicit solutions have been obtained in [5]. We will use these solutions to discuss some interesting issues in gauge theory.

3.2.1 $U(10)$ Gauge Theory With Flavour

Consider the specific case of dessins arising from the factorization problem of the second example in Section 2.2.3:

$$P_{10}^2(z) + \alpha z^5 (z-1)^5 (z-t)^5 = Q_4^3(z) R_4^2(z)\,. \tag{3.50}$$

This problem was completely solved in [5]. There are two inequivalent solutions to (3.50). Taking the explicit solutions from [5] one can plot the zeroes of the polynomials as before; we have drawn the corresponding dessins in Figure 3.11 and 3.12.

It turns out that the monodromy group distinguishes between the two dessins and therefore they belong to different Galois orbits. For the two dessins considered here, the relations $\sigma_1^2 = 1$ and $\sigma_0^6 = 1$ are satisfied. Let us denote the two monodromy groups

corresponding to the two dessins by M_1 and M_2 respectively. In order to explicitly write down the generators, it is useful to number the half-edges of the dessin, as in the Figures 3.11 and 3.12.

From the definitions, one can check that

- M_1 is generated by

$$\begin{aligned}\sigma_1 &= (1,2)(3,4)(5,6)(7,8)(9,10)(11,12)(13,14)(15,16)(17,18)(19,20)\\ \sigma_0 &= (1,10,11)(2,15,3)(4,5)(6,19,7)(8,9)(12,13)(14,20,18)(16,17)\,. \end{aligned} \tag{3.51}$$

  It has order 30720 and has 84 conjugacy classes.

- M_2 is generated by

$$\begin{aligned}\sigma_1 &= (1,2)(3,4)(5,6)(7,8)(9,10)(11,12)(13,14)(15,16)(17,18)(19,20)\\ \sigma_0 &= (1,10,11)(2,13,3)(4,19,5)(6,7)(8,9)(12,20,18)(14,15)(16,17)\,. \end{aligned} \tag{3.52}$$

  It has order 30720 and has 63 conjugacy classes.

Since $M_1 \neq M_2$, the two dessins belong to distinct Galois orbits. We can now ask if it is possible, from the gauge theory analysis, to distinguish between them. Note that the holomorphic invariants introduced in section 2.3.2 do not give any information in this case, as it is not possible to factorize (3.50) as $P(z) \pm f(z)$, for some polynomial $f(z)$, unlike the pure gauge theory case. This is reflected in the fact that from the mathematical point of view, it is not possible in general to define a refined valency list when the dessin is not a tree.

Similarly, although the combinatorial definition of the confinement index still makes sense, there is no sense in which confinement is a good order parameter for gauge theories with matter. So although t might still be a good Galois invariant, its physical interpretation is unclear. Some preliminary analysis of the phases have already been attempted in [7], but a more detailed study would be necessary.

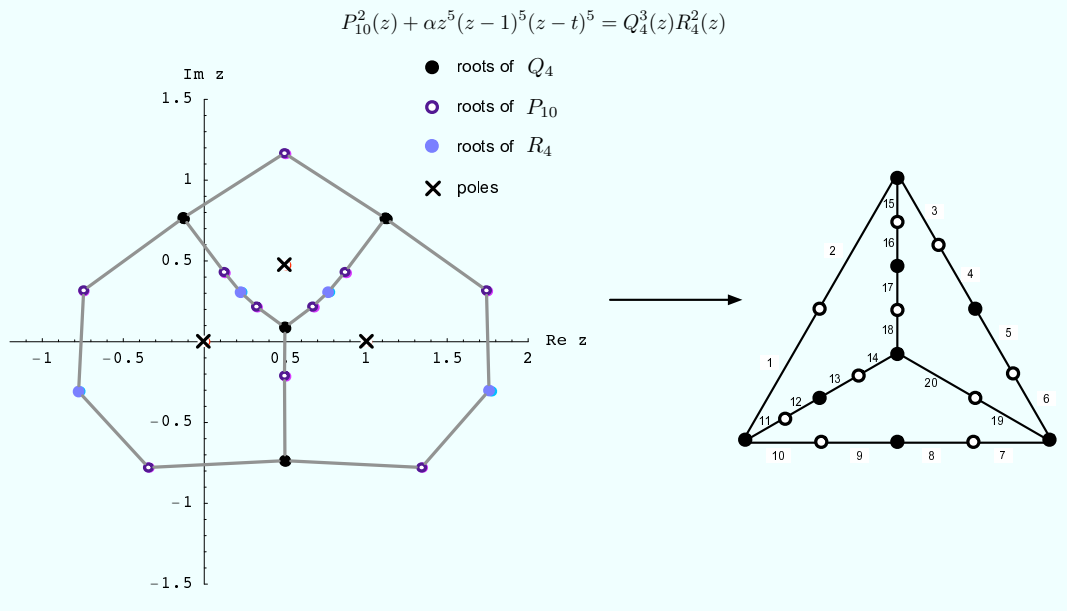

Figure 3.11: One of the two dessins arising from the factorization (3.50). Each face is bounded by three line segments containing $1, 2$ and 2 edges respectively. The figure to the right is a schematic version of the dessin, with the edges numbered to aid the computation of the monodromy group.

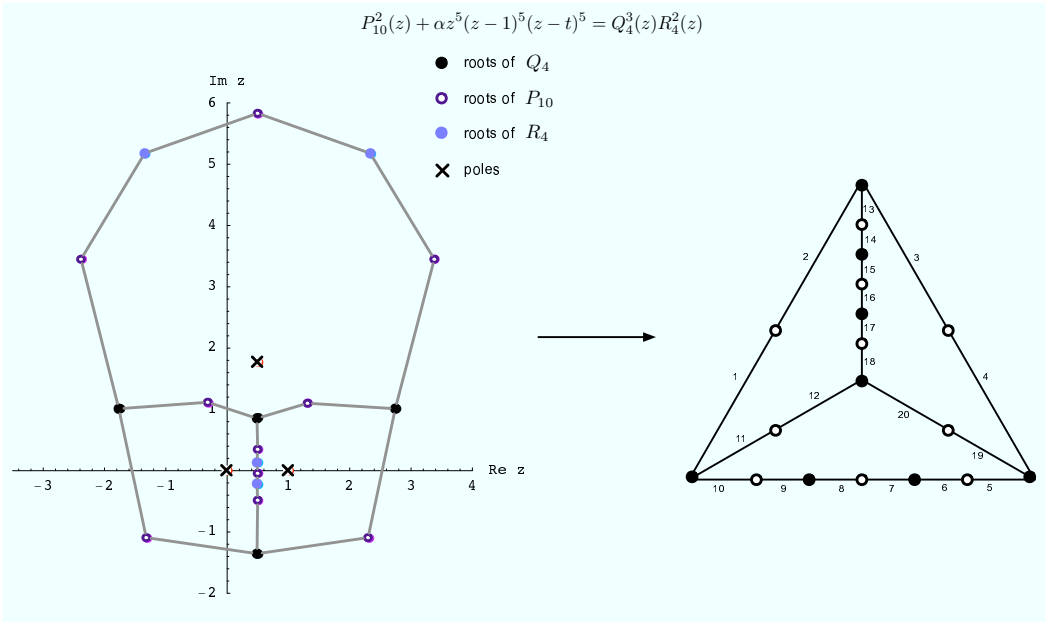

Figure 3.12: The other dessin arising from (3.50). Each face is bounded by $1, 1$ and 3 edges between trivalent vertices.

Chapter 4

Conclusions And Open Questions

The central theme of this thesis has been the relation between dessins d'enfants and supersymmetric gauge theory. In this section, we discuss some of the results we have obtained and list some of the questions and future directions of research that have emerged from our analysis.

We have seen that any clean dessin with N_c edges and $N_f + 1$ faces can be found at an isolated singularity in the moduli space of an $\mathcal{N} = 2$ $U(N_c)$ gauge theory with N_f flavours. The particular rigid factorization of the Seiberg-Witten curve that corresponds to the isolated singularity is determined by the valency lists of the dessin. Typically there are many solutions to this factorization problem. For each such solution, the rigid curve determines a rational Belyi map $\beta(z)$ whose inverse image of the $[0, 1]$ interval gives a dessin D on the sphere. Such an $\mathcal{N} = 2$ gauge theoretic perspective matches very closely the mathematical point of view of obtaining and classifying dessins into Galois orbits by direct solution of the polynomial equation.

From a physics point of view, it is also natural to study what we called the non-rigid factorizations (2.1). The solutions to these equations are interpreted as the space of vacua that preserve $\mathcal{N} = 1$ supersymmetry when the $\mathcal{N} = 2$ theory is perturbed by a tree level superpotential. One can associate to these vacua disconnected graphs (which are not dessins), that come together and join to form a dessin at any of the isolated singularities mentioned in the previous paragraph. The difference lies in the fact that these are now looked upon as $\mathcal{N} = 1$ vacua.

Interestingly, it is this $\mathcal{N} = 1$ point of view that has a nice counterpart in the more refined mathematical approach to the study of dessins, which is to define a complete list of Galois invariants that distinguish the dessins that belong to different Galois orbits.

Based on the examples we have worked out, we have been led to conjecture a relation between the mathematical programme of classifying dessins and the physics programme of classifying phases of $\mathcal{N} = 1$ gauge theory. The strongest form of the conjecture states that every Galois invariant is a physical order parameter that distinguishes different phases in the gauge theory.

One example of a Galois invariant that might give new physical information is the monodromy group associated to the dessins. In gauge theory, the group usually discussed in the context of Seiberg-Witten theory is the S-duality group: for a genus g Seiberg-Witten curve, it is an $Sp(2g, \mathbb{Z})$ group that acts on the A_i and B_i cycles of the Riemann surface. These cycles correspond to the edges that go between the filled vertices of the dessins (the pre-images of 0 under the Belyi map). However, in general the monodromy group of the dessin involves action on half-edges that go between the pre-images of 0 and 1 and involves the zeroes of $P(z)$, apart from the zeroes of y_{SW}. It is therefore different from the S-duality group, but what exactly the group signifies in the gauge theory is an open question.

In the other direction, one can ask whether the $\mathcal{N} = 1$ gauge theoretic way of finding the dessins, first by solving a more general (non-rigid) factorization problem and *then* imposing suitable constraints so that one approaches an isolated singularity in the moduli space, is useful from a mathematical point of view. From our proof that the confinement index is a Galois invariant, it seems that the answer is yes. More generally we have seen that all the order parameters have a simple interpretation in the mathematical literature as Galois invariants. We believe that in this direction the correspondence is on much firmer ground.

In Section 3.2, we discussed dessins that appear in the moduli space of a $U(N)$ gauge theory with matter. Much less is known about the possible phases of the corresponding $\mathcal{N} = 1$ vacua. We exhibited two dessins in a $U(10)$ theory with flavour, which, from the mathematical point of view belong to distinct Galois orbits as they have different monodromy groups. However, from the physics point of view, with the available order parameters, it seems that the points where the two dessins appear describe the same phase. By this we mean that none of the known order parameters are of any use to

distinguish between them. If our stronger conjecture that Galois invariants map to order parameters is correct, the monodromy group should correspond to an order parameter in physics that can distinguish the two special points where the dessins appear.

Many possible generalizations of this work present themselves. Since the dessins can be drawn on any two dimensional topological surface, it should be possible to extend the correspondence we have found to dessins drawn on genus $g \geq 1$ Riemann surfaces. On the gauge theoretic side, it would be very interesting to classify the dessins that appear in the moduli spaces of more general gauge theories, such as SO/Sp gauge groups, quiver gauge theories with products of $U(N)$ factors, etc.

The study of the $\mathcal{N} = 1$ branches in [12] uses the Dijkgraaf-Vafa relation between gauge theory and matrix models [19–21]. In this relation, two distinct hyperelliptic Riemann surfaces emerge [10]: the Seiberg-Witten curve and the spectral curve of the matrix model. In the examples considered in the text, the spectral curve was equivalent to the reduced Seiberg-Witten curve in (1.50). However this is not true in general as discussed in the examples in Appendix C. It is conceivable that one can tune the parameters of the tree level superpotential so that the spectral curve develops an isolated singularity, leading to a Belyi map. It might be very interesting to study the dessins that arise this way.

As we have stressed throughout, the main objective of this work was to provide the rudiments of a dictionary between the physics of supersymmetric gauge theory and the mathematics related to the action of the absolute Galois group on the children's drawings of Grothendieck. Much more work needs to be done to fully understand the correspondence between these two fascinating fields of study, which we hope will lead to a deeper and fuller understanding of the relevant physical and mathematical problems.

Appendix A

Field Theory And The Absolute Galois Group

The absolute Galois group $\mathrm{Gal}(\overline{\mathbb{Q}}/\mathbb{Q})$ is of central importance in many areas of mathematics. In this appendix we give a short description of the definition stated in the text: $\mathrm{Gal}(\overline{\mathbb{Q}}/\mathbb{Q})$ is the group of automorphisms of the field $\overline{\mathbb{Q}}$ of algebraic numbers that leaves $\mathbb{Q}$ fixed.

Instead of directly studying $\mathrm{Gal}(\overline{\mathbb{Q}}/\mathbb{Q})$, which is a group that cannot even be finitely generated, we will study the relevant concepts by first reviewing Galois groups of finite order. Just to give an idea of the complexity of $\mathrm{Gal}(\overline{\mathbb{Q}}/\mathbb{Q})$ it is nice to mention that mathematicians are considering the possibility that any finite group can arise as a projection of $\mathrm{Gal}(\overline{\mathbb{Q}}/\mathbb{Q})$; this is the so-called "Inverse Problem of Galois Theory"[1].

Before going into the details about the different elements that enter in the definition of Galois groups let us lay down some field theory basis. In this review we will assume familiarity with definitions of fields, rings of polynomials and basic group theory (for a very basic introduction and more details of the main example in this appendix see [25]).

Let us start by recalling some basic definitions. We say that a field E is an extension of a field F, denoted by $F \leq E$, if E has a subfield isomorphic to F. Examples of fields and extensions are $\mathbb{Q} \leq \mathbb{Q}(2^{1/4}, i) \leq \overline{\mathbb{Q}}$. Our first goal is to review the meaning of expressions such as $\mathbb{Q}(2^{1/4}, i)$.

Given a field F, a natural object to study is the ring of polynomials, $F[z]$, with coefficients in F. From now on we will assume that F is a field of characteristic zero or a finite field. This is to avoid certain pathologies that can happen otherwise. Of course, our final target, which is $\mathbb{Q}$, has characteristic zero.

---

[1] The more precise statement is that any simple group S might be the Galois group of a finite normal extension of $\mathbb{Q}$ and hence there will be a natural restriction map from $\mathrm{Gal}(\overline{\mathbb{Q}}/\mathbb{Q})$ onto S.

An element $a \in E$ is called algebraic over F if it is a zero of a polynomial $p(z)$ in $F[z]$. E is called an algebraic extension of F if all its elements are algebraic over F. We will only consider algebraic extensions from now on. It turns out that there exists a unique monic irreducible (over F) polynomial such that $p(a) = 0$ (since F is of characteristic zero or finite, a can only be a zero of order one. This is an example of one of the possible pathologies we have avoided). Since such a $p(z)$ is unique we call it $p_a(z)$. The degree of $p_a(z)$, $\deg(p_a(z)) = n$ is also called the degree of a in F.

A special class of algebraic extensions are those with the structure of a vector space with basis $\{1, a, \ldots, a^{n-1}\}$ and coefficients in F. These are called *simple extensions* and are denoted by $F(a)$. In general, if $F \leq E$ and E is of finite dimension n as a vector space over F, we say that E is a *finite extension*[2] of degree $|E : F| = n$ over F.

An example is $F = \mathbb{Q}$ and $a = 2^{1/4}$. Then $\mathbb{Q}(2^{1/4})$ is generated by $\{1, 2^{1/4}, 2^{1/2}, 2^{3/4}\}$ since $p_a(z) = z^4 - 2$ has degree $n = 4$.

Note that $z^4 - 2$ is reducible over $\mathbb{Q}(2^{1/4})$, in fact, $z^4 - 2 = (z - 2^{1/4})(z + 2^{1/4})(z^2 + 2^{1/2})$. The last factor, $(z^2 + 2^{1/2})$, is irreducible of degree 2 in $\mathbb{Q}(2^{1/4})$. So if we *adjoin* a root of $z^2 + 2^{1/2}$ to $\mathbb{Q}(2^{1/4})$ then $z^4 - 2$ *splits* over this new field.

The new element we need is $2^{1/4}i$. However, multiplying by $2^{-1/4} \in \mathbb{Q}(2^{1/4})$ we get i. Therefore, the new field is $(\mathbb{Q}(2^{1/4}))(i) = \mathbb{Q}(2^{1/4}, i)$. The latter notation shows the fact that the order in which we adjoint $2^{1/4}$ and i to $\mathbb{Q}$ is irrelevant.

We have achieved our first goal: $\mathbb{Q}(2^{1/4}, i)$ is called the *splitting field* of $z^4 - 2$. More generally, an extension E of $\mathbb{Q}$ is a splitting field if there is an irreducible polynomial in $\mathbb{Q}[z]$ such that E is the smallest field that contains all its roots.

Now we need to introduce the concept of the algebraic closure of a field F. A field K is called algebraically closed if every non-constant polynomial in $K[z]$ has a root in K. Such a K is called an algebraic closure of F if K is an algebraic extension of F, and it is denoted by $\overline{F}$. $\overline{F}$ is unique up to isomorphisms.

The next goal is to study automorphisms of fields. Splitting fields are important because given any one of them, say E such that $F \leq E \leq \overline{F}$, any automorphism of

[2]Quite nicely, in our case (with $F = \mathbb{Q}$), all finite extensions are also simple! This is called the primitive element theorem.

$\overline{F}$ that fixes F maps E onto itself and induces an automorphism of E leaving fixed F. Moreover, splitting fields are the only ones with this property. The basic automorphisms are quite simple: if a and b are roots of the same irreducible polynomial, then the map $\phi(a) = b$ with $\phi(q) = q$ if $q \in F$ is an automorphism. a and b are called conjugates and ϕ is a conjugation. Automorphisms of E that leave fixed F form a group under composition denoted by $G(E/F)$. If E is a splitting field, then $G(E/F)$ is called the Galois group of E over F and it is denoted by $\mathrm{Gal}(E/F)$.

Let E be a finite extension of F. The number of isomorphisms of E into $\overline{F}$ leaving F fixed is the index $\{E : F\}$ of E over F. It turns out that for the fields we consider

$$\{E : F\} = |E : F| = |G(E/F)| \tag{A.1}$$

where $|G(E/F)|$ is the order of the group.

The next step in any algebra book would be to define separable extensions. However, over $\mathbb{Q}$, all extensions are separable and we do not need to worry about that. A very special role is played by (separable) splitting fields which are then called *finite normal extensions*[3].

Now we are ready to discuss the *Fundamental Theorem of Galois Theory*. The theorem states that if E is a finite normal extension of F then there is a one to one correspondence between intermediate extensions of F and subgroups of $\mathrm{Gal}(E/F)$. The correspondence is the following: to each extension B of F such that $B \leq E$, one associates the largest subgroup G_B of $\mathrm{Gal}(E/F)$ that leaves B fixed. Moreover, B is a finite normal extension of F if and only if G_B is a normal subgroup. In fact, $\mathrm{Gal}(B/F)$ is isomorphic to the factor (or quotient) group $\mathrm{Gal}(E/F)/G_B$.

Let us apply this to our example $E = \mathbb{Q}(2^{1/4}, i)$. As discussed above, E is the splitting field of $z^4 - 2$. It has a basis $\{1, a, a^2, a^3, i, ia, ia^2, ia^3\}$ where $a = 2^{1/4}$.

Since $|E : \mathbb{Q}| = 8$ we must have $|\mathrm{Gal}(E/\mathbb{Q})| = 8$. It is a simple exercise to exhibit the eight automorphisms of E leaving $\mathbb{Q}$ invariant (see section 47.2 of [25]). Studying the composition table one discovers that the group is nonabelian. Moreover, $\mathrm{Gal}(E/\mathbb{Q}) = D_4$, the dihedral group (the symmetry group of a square). If we denote rotations by

[3]The parenthesis around "separable" are there to indicate that it can freely be removed.

	ρ_0	ρ_1	ρ_2	ρ_3	μ_1	δ_1	μ_2	δ_2
$a \rightarrow$	a	ia	$-a$	$-ia$	a	ia	$-a$	$-ia$
$i \rightarrow$	i	i	i	i	$-i$	$-i$	$-i$	$-i$

Table A.1: Action of the dihedral group D_4 on $E = \mathbb{Q}(2^{1/4}, i)$.

$k\pi/2$ (with $k = 0, 1, 2, 3$) as ρ_k, mirror images (reflections) as μ_i and diagonal flips as δ_i, then the identification with automorphisms is collected Table A.1 (only the action on a and i is needed).

The lattice of all subgroups of D_4 is well known (see section 47.2 of [25]). According to Galois theory there must be one and only one intermediate extension of $\mathbb{Q}(2^{1/4}, i)$ for each subgroup. This gives rise to the lattice of intermediate extensions of $\mathbb{Q}(2^{1/4}, i)$. Let K_H denote the subfield of $\mathbb{Q}(2^{1/4}, i)$ left fixed by the subgroup H of D_4. For example, it is easy to check that $K_{\{\rho_0,\rho_2\}} = \mathbb{Q}(\sqrt{2}, i)$. Note that $\mathbb{Q}(\sqrt{2}, i)$ is also a splitting field and hence a finite normal extension. One can easily check that $\{\rho_0, \rho_2\}$ is indeed a normal subgroup of D_4! Likewise, consider $K_{\{\rho_0,\mu_1\}} = \mathbb{Q}(2^{1/4})$. This is not a splitting field and one can check that $\{\rho_0, \mu_1\}$ is not a normal subgroup of D_4.

Now we can go back to our object of interest: $\mathrm{Gal}(\overline{\mathbb{Q}}/\mathbb{Q})$. Here we will follow very closely an explanation given in [30] and we will illustrate the main ideas using our example of $\mathbb{Q}(2^{1/4}, i)$. We have already explained the meaning of the algebraic closure of a field. Here $\overline{\mathbb{Q}}$ is then the algebraic closure of $\mathbb{Q}$, the field of algebraic numbers. This is clearly a complicated object that can be constructed as the union of all splitting fields over $\mathbb{Q}$, which as we know, are finite normal extensions of $\mathbb{Q}$. Let E denote a generic one, then

$$\overline{\mathbb{Q}} = \bigcup_{E \in \mathcal{E}} E \tag{A.2}$$

where $\mathcal{E}$ is the set of all such extensions. For each extension E we have the corresponding Galois group, $\mathrm{Gal}(E/\mathbb{Q})$, of E over $\mathbb{Q}$.

Consider our favorite example, $E = \mathbb{Q}(2^{1/4}, i)$. Its Galois group over $\mathbb{Q}$ is $\mathrm{Gal}(E/\mathbb{Q}) = D_4$. Consider $L = \mathbb{Q}(\sqrt{2}, i)$. As we saw, $L \leq E$. Now, every automorphism of E leaves L invariant. This is because L is a splitting field. The Galois group of L over $\mathbb{Q}$ is then

the factor group $\mathrm{Gal}(L/\mathbb{Q}) = \mathrm{Gal}(E/\mathbb{Q})/\{\rho_0, \rho_2\}$.

Now there is a natural group epimorphism $\rho_{E,L} : \mathrm{Gal}(E/\mathbb{Q}) \to \mathrm{Gal}(L/\mathbb{Q})$ given by the restriction map. That this is an epimorphism, i.e, an onto map, follows from the fact that every automorphism of L that fixes $\mathbb{Q}$ can be extended to an automorphism of E in $|E : L|$ ways. In our example $|E : L| = 2$. Consider the following automorphism of L: $(\sqrt{2}, i) \to (\sqrt{2}, -i)$. This can then be extended to E in two ways a follows: $(2^{1/4}, i) \to (\pm 2^{1/4}, i)$.

Consider now $\mathbb{Q}(i) = K_{\{\rho_0,\rho_1,\rho_2,\rho_3\}}$. This is also a splitting field. We then have the following sequence of finite normal extensions $\mathbb{Q} \leq \mathbb{Q}(i) \leq \mathbb{Q}(\sqrt{2}, i) \leq \mathbb{Q}(2^{1/4}, i)$. From this sequence we can make an observation that will be very important in the definition of $\mathrm{Gal}(\overline{\mathbb{Q}}/\mathbb{Q})$: an element (g_1, g_2) of the cartesian product $\mathrm{Gal}(\mathbb{Q}(i)/\mathbb{Q}) \times \mathrm{Gal}(\mathbb{Q}(\sqrt{2}, i)/\mathbb{Q})$ can be extended to an element of $\mathrm{Gal}(\mathbb{Q}(2^{1/4}, i)/\mathbb{Q})$ if and only if $\rho_{L,\mathbb{Q}(i)}(g_2) = g_1$. This is because if $g \in \mathrm{Gal}(\mathbb{Q}(2^{1/4}, i)/\mathbb{Q})$ is one of the possible extensions then it has to have a consistent action on each of the subfields.

The absolute Galois group $\mathrm{Gal}(\overline{\mathbb{Q}}/\mathbb{Q})$ can now be constructed in a very similar way. It is a subgroup of the cartesian product of the Galois groups of all finite normal extensions of $\mathbb{Q}$

$$\mathrm{Gal}(\overline{\mathbb{Q}}/\mathbb{Q}) < \prod_{E \in \mathcal{E}} \mathrm{Gal}(E/\mathbb{Q}) \tag{A.3}$$

consisting of all elements $(g_\mathcal{E}) \in \prod_{E \in \mathcal{E}} \mathrm{Gal}(E/\mathbb{Q})$ (this is an infinite "array" with one entry for each $E \in \mathcal{E}$) satisfying the constraint that $\rho_{K_2,K_1}(g_{K_2}) = g_{K_1}$ whenever $K_1 \leq K_2$. The identification of each $g \in \mathrm{Gal}(\overline{\mathbb{Q}}/\mathbb{Q})$ with the element $(g_\mathcal{E})$ implies that g_E is the restriction of g to E. That this set of restrictions is consistent follows from the condition involving ρ.

Finally, the action of g on $\overline{\mathbb{Q}}$ is determined by the action on each finite normal extension via g_E. This is the basic result we used in section 2.4 where we discussed the action of $\mathrm{Gal}(\overline{\mathbb{Q}}/\mathbb{Q})$ on dessins. We said that if $g \in \mathrm{Gal}(\overline{\mathbb{Q}}/\mathbb{Q})$ then η acts on a dessin by acting on the coefficients of the Belyi map. In other words, the coefficients of the Belyi map, being found as solutions to some set of polynomial equations, belong to a splitting field E and g acts via its restriction g_E.

A.1 Glossary Of Terms In The Text

- An *algebraic number* is an element $a \in \mathbb{C}$ that generates a finite extension $\mathbb{Q}(a) \geq \mathbb{Q}$.
- $\overline{\mathbb{Q}}$ is the field of all algebraic numbers and it is also the algebraic closure of $\mathbb{Q}$.
- A *number field* is a finite algebraic extension of $\mathbb{Q}$.
- A *monic polynomial* is one whose monomial of highest degree has coefficient 1.

Appendix B

The Multiplication Map As A Belyi-Extending Map

It was shown in [11,12] that once a solution to the factorization problem (2.1) is known for $U(N)$, then it is possible to construct a solution to a similar factorization problem for $U(tN)$. Let us first review this construction.

Consider the factorization problem

$$P_t^2(z) - 4\Lambda^{2t} = F_2(z) H_{t-1}^2(z)\,. \tag{B.1}$$

The solution is given by

$$P_t(z) = 2\Lambda^t \eta^t T_t\left(\frac{z}{2\eta\Lambda}\right), \quad F_2(z) = z^2 - 4\eta^2\Lambda^2\,, \quad H_{t-1}(z) = \eta^{t-1}\Lambda^{t-1} U_{t-1}\left(\frac{z}{2\eta\Lambda}\right), \tag{B.2}$$

where $\eta^{2t} = 1$. $T_t(z)$ and $U_{t-1}(z)$ are the Chebyshev polynomials of the first and second kind respectively, defined by setting $z = \cos\theta$ and

$$T_t(z) = \cos(t\theta) \qquad U_{t-1}(z) = \frac{1}{t}\frac{dT_t}{dz}(z) = \frac{\sin(t\theta)}{\sin\theta}\,. \tag{B.3}$$

This implies that they satisfy the relation

$$1 - T_t^2(z) = (1 - z^2)\, U_{t-1}^2(z)\,. \tag{B.4}$$

Now suppose we have a solution to the factorization problem

$$P_N^2(z) - 4\Lambda_0^{2N} = F_{2n}(z) H_{N-n}^2(z)\,. \tag{B.5}$$

Then we can use the solution to (B.2) to construct a solution to

$$P_{tN}^2(z) - 4\Lambda_0^{2tN} = \tilde{F}_{2n}(z)\tilde{H}_{tN-n}^2(z) \tag{B.6}$$

as follows:

$$\begin{aligned} P_{tN}(z) &= 2\Lambda^{tN}\eta^t T_t\left(\frac{P_N(z)}{2\eta\Lambda^N}\right), \quad \tilde{F}_{2n}(z) = F_{2n}(z) \\ H_{tN-n}(z) &= \eta^{t-1}\Lambda^{N(t-1)} H_{N-n}(z)\, U_{t-1}\left(\frac{P_N(z)}{2\eta\Lambda^N}\right), \qquad \Lambda_0^{2N} = \eta^2\,\Lambda^{2N}\,. \end{aligned} \tag{B.7}$$

This procedure to get exactly t solutions to the $U(tN)$ theory from a given solution of the $U(N)$ theory was referred to as the multiplication map (by t) in [11].

Let us now show that the multiplication by t map can be used to construct new Beyi maps from old ones. The simple example of $t = 2$ has already been discussed in Section 4. As discussed in that section, the main point is to use the multiplication map to define the new Belyi map as

$$\tilde{\beta}_t(z) = 1 - \frac{P_{tN}^2(z)}{4\Lambda_0^{2tN}}\,, \tag{B.8}$$

where $P_{tN}(z)$ is given by the first equation in (B.7) and $P_N(z)$ gives rise to a Belyi map

$$\beta(z) = 1 - \frac{P_N^2(z)}{4\Lambda_0^{2N}}\,. \tag{B.9}$$

We would now like to exhibit (B.8) as the composition of a Belyi-extending map with the Belyi map (B.9). For this purpose, let us define the polynomials

$$T_{2k}(z) = M_k(z^2) \qquad \text{and} \qquad T_{2k+1}(z) = z\, S_k(z^2)\,. \tag{B.10}$$

This follows from the form of the Chebyshev polynomials (B.3). If we now define the Belyi-extending maps

$$\alpha_{2k}(u) = 1 - M_k^2(1-u) \qquad \text{and} \qquad \alpha_{2s+1}(u) = 1 - (1-u)S_k^2(1-u)\,, \tag{B.11}$$

one can check that

$$\tilde{\beta}_t(z) = \alpha_t(\beta(z)) \tag{B.12}$$

is a Belyi map for all integer values of t. As for α_2, one check that geometrically, the multiplication by t replaces a given edge in a dessin by a branchless tree of length t.

Appendix C

Complete List Of Trees For The $U(6)$ Gauge Group

In this appendix we study the problem of realizing all possible connected trees with 6 edges. Along the way we will mention some interesting points about the structure of $\mathcal{N}=1$ vacua from the matrix model point of view [10].

In section 3.1, we studied examples a pure $U(6)$ gauge theory deformed by a cubic superpotential. However, a cubic superpotential does not allow enough flexibility in the non-rigid Seiberg-Witten curve to realize all possible trees with 6 edges. We mentioned in the text that if we consider a superpotential $W(z)$ of degree $n+1$, then the curve describing the $\mathcal{N}=1$ vacua of $U(N)$ is given by

$$y^2 = P_N^2(z) - 4\Lambda^{2N} = (W'(z)^2 + f_{n-1}(z))H_{N-n}^2(z) \tag{C.1}$$

where $W'(z)$ has degree n.

However, this is true only for vacua with all values of N_i different from zero. In other words, if $U(N)$ is classically broken to $U(N_1)\times\ldots\times U(N_n)$. It turns out that if $n-s$ of the N_i's are zero then the description of $\mathcal{N}=1$ vacua is more subtle and it was elucidated in [10] by using matrix model techniques inspired by the Dijkgraaf-Vafa relation [19–21]. The way to treat all cases at once is by introducing another curve, called the matrix model curve, $y_m^2 = W'(z)^2 + f_{n-1}(z)$. Then, if $U(N)$ is broken classically to $U(N_1)\times\ldots\times U(N_s)$ the factorization problems to be solved are

$$\begin{aligned} y^2 &= P_N^2(z) - 4\Lambda^{2N} = F_{2s}(z)H_{N-s}^2(z), \\ y_m^2 &= W'(z)^2 + f_{n-1}(z) = F_{2s}(z)R_{n-s}^2(z). \end{aligned} \tag{C.2}$$

This means in particular, that the $(3,2)$ vacua in Section 3.1.1 for the $U(6)$ example is the intersection of the $s=2$ branch with the $s=1$ branch, where the low energy

gauge groups are $U(1)^2$ and $U(1)$ respectively. This intersection was studied in great generality in [49].

Note however, that the trivalent and four-valent factorizations in $U(6)$ do not correspond to points where the $s = 2$ branch intersects the $s = 1$ branch. This is because both values of N_i are nonzero. More generally, it is clear that isolated singular points of a theory with $s = p$ are particular cases of those of a theory with $s = n$ for any $p < n$, since the corresponding branches can intersect.

The set of interesting values of n in the case of $U(6)$ is $n = 1, \ldots, 6$.[1] We now turn to the construction of all possible dessins associated to $U(6)$. It turns out that one only needs to consider a quartic superpotential, i.e., $n = 3$.

Let us prove that $n = 3$ suffices. Instead of starting with $n = 6$ and descending all the way to $n = 3$ it is best to use the fact that isolated singular points give rise to all possible connected trees with 6 edges. These trees must have seven vertices. All possible valency lists are the following $(6, 0, 0, 0, 0, 1)$, $(5, 1, 0, 0, 1, 0)$, $(5, 0, 1, 1, 0, 0)$, $(4, 2, 0, 1, 0, 0)$, $(4, 1, 2, 0, 0, 0)$, $(3, 3, 1, 0, 0, 0)$, and $(2, 5, 0, 0, 0, 0)$. Recall that a valence list $(u_1, \ldots, u_6)$ means that there are u_k vertices with valence k. These were obtained by requiring that the sum of all u_k's is always seven and that the sum of all u_k's times k is always 12.

The previous valence lists lead to factorization problems of the Seiberg-Witten curve of the form

$$\begin{aligned} &F_6(z)H_1^6(z), \qquad F_5(z)Q_1^2(z)H_1^5(z), \qquad F_5(z)Q_1^3(z)H_1^4(z), \\ &F_4(z)Q_2^2(z)H_1^4(z), \qquad F_4(z)Q_1^2(z)H_2^3(z), \qquad F_3(z)Q_3^2(z)H_1^3(z)\,, \end{aligned} \tag{C.3}$$

and $F_2(z)Q_5^2(z)$ respectively.

Now we can prove our claim by simple inspection. All these factorization problems are particular points in the space of curves (with $n = 3$) given by

$$y^2 = P_6^2(z) - 4\Lambda^{12} = F_6(z)H_3^2(z)\,. \tag{C.4}$$

[1] There is a subtlety when $n = 6$ which is related to the fact that tr Φ^7 in the superpotential is not an independent quantity but this will not affect our discussion (see [12] for more details).

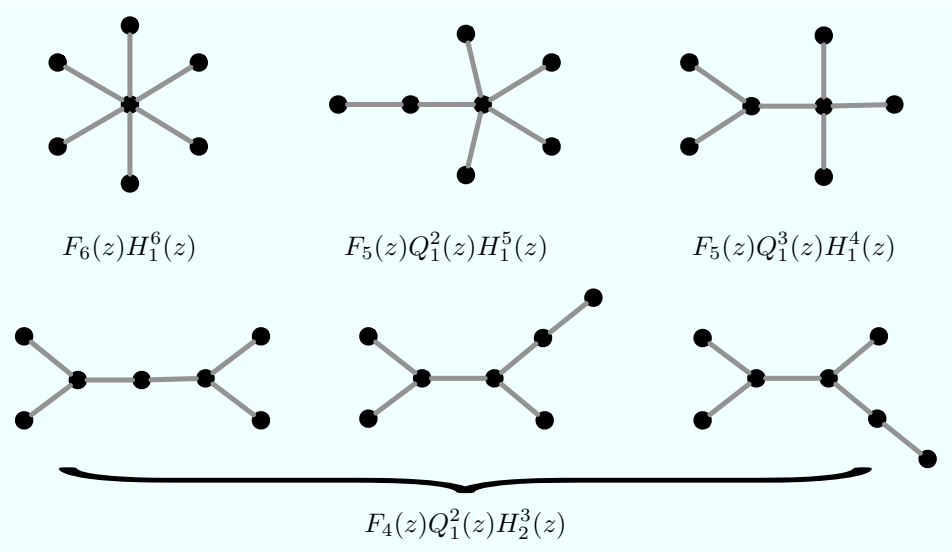

Figure C.1: All possible dessins (and the associated factorizations) that appear in the $\mathcal{N} = 2$ moduli space of the $U(6)$ gauge theory, apart from the ones already discussed in the main body of the article. We have omitted the vertices corresponding to the zeroes of $P_6(z)$.

It is also easy to check that $F_6(z)H_1^6(z)$, $F_5(z)Q_1^2(z)H_1^5(z)$, $F_5(z)Q_1^3(z)H_1^4(z)$ and $F_4(z)Q_1^2(z)H_2^3(z)$ cannot possibly be obtained from the cubic superpotential (the $n = 2$ case considered in the text), while all the other factorizations – $F_4(z)Q_2^2(z)H_1^4(z)$, $F_3(z)Q_3^2(z)H_1^3(z)$ and $F_2(z)Q_5^2(z)$ – were considered in Section 3.1.

The inherently $n = 3$ factorizations give rise to only six different trees, shown in Figure C.1.

Bibliography

[1] L. Alvarez-Gaume and S. F. Hassan, "Introduction to S-duality in N = 2 supersymmetric gauge theories: A pedagogical review of the work of Seiberg and Witten," Fortsch. Phys. **45** (1997) 159 [hep-th/9701069].

[2] P. C. Argyres and M. R. Douglas, "New phenomena in SU(3) supersymmetric gauge theory," Nucl. Phys. B **448**, 93 (1995), hep-th/9505062.

[3] P. C. Argyres and A. E. Faraggi, "The vacuum structure and spectrum of N=2 supersymmetric SU(n) gauge theory," Phys. Rev. Lett. **74** (1995) 3931 [arXiv:hep-th/9411057].

[4] P. C. Argyres, M. R. Plesser and A. D. Shapere, "The Coulomb phase of N=2 supersymmetric QCD," Phys. Rev. Lett. **75**, 1699 (1995), hep-th/9505100.

[5] S. K. Ashok, F. Cachazo and E. Dell'Aquila, "Strebel Differentials With Integral Lengths And Argyres-Douglas Singularities," hep-th/0610080.

[6] S. K. Ashok, F. Cachazo and E. Dell'Aquila, "Children's drawings from Seiberg-Witten curves," arXiv:hep-th/0611082.

[7] V. Balasubramanian, B. Feng, M. x. Huang and A. Naqvi, "Phases of N = 1 supersymmetric gauge theories with flavors," Annals Phys. **310**, 375 (2004), hep-th/0303065.

[8] G .V .Belyi, "On Galois extensions of a maximal cyclotonic field," Math. U.S.S.R. Izvestija **14** (1980), 247-256

[9] E. B. Bogomolny, "Stability Of Classical Solutions," Sov. J. Nucl. Phys. **24** (1976) 449 [Yad. Fiz. **24** (1976) 861].

[10] F. Cachazo, M. R. Douglas, N. Seiberg and E. Witten, "Chiral rings and anomalies in supersymmetric gauge theory," JHEP **0212**, 071 (2002), hep-th/0211170.

[11] F. Cachazo, K. A. Intriligator and C. Vafa, "A large N duality via a geometric transition," Nucl. Phys. B **603**, 3 (2001), hep-th/0103067.

[12] F. Cachazo, N. Seiberg and E. Witten, "Phases of N = 1 supersymmetric gauge theories and matrices," JHEP **0302**, 042 (2003), hep-th/0301006.

[13] F. Cachazo, N. Seiberg and E. Witten, "Chiral rings and phases of supersymmetric gauge theories," JHEP **0304**, 018 (2003), hep-th/0303207.

[14] F. Cachazo and C. Vafa, "N = 1 and N = 2 geometry from fluxes," hep-th/0206017.

[15] P. Candelas and X. de la Ossa, "Moduli Space Of Calabi-Yau Manifolds," Nucl. Phys. B **355**, 455 (1991).

[16] S. R. Coleman and J. Mandula, "All Possible Symmetries Of The S-Matrix," Phys. Rev. **159** (1967) 1251.

[17] J. de Boer and Y. Oz, "Monopole condensation and confining phase of N = 1 gauge theories via M-theory fivebrane," Nucl. Phys. B **511** (1998) 155 [hep-th/9708044].

[18] B. de Wit and A. Van Proeyen, "Potentials And Symmetries Of General Gauged N=2 Supergravity - Yang-Mills Models," Nucl. Phys. B **245** (1984) 89.

[19] R. Dijkgraaf and C. Vafa, "Matrix models, topological strings, and supersymmetric gauge theories," Nucl. Phys. B **644**, 3 (2002), hep-th/0206255.

[20] R. Dijkgraaf and C. Vafa, "On geometry and matrix models," Nucl. Phys. B **644**, 21 (2002), hep-th/0207106.

[21] R. Dijkgraaf and C. Vafa, "A perturbative window into non-perturbative physics," hep-th/0208048.

[22] M. R. Douglas and S. H. Shenker, "Dynamics of SU(N) supersymmetric gauge theory," Nucl. Phys. B **447**, 271 (1995), hep-th/9503163.

[23] T. Eguchi and Y. Sugawara, "Branches of $\mathcal{N} = 1$ Vacua and Argyres-Douglas Points," JHEP **0305**:063, 2003, hep-th/0305050.

[24] S. Ferrara, "Calabi-Yau Moduli Space, Special Geometry And Mirror Symmetry," Mod. Phys. Lett. A **6** (1991) 2175.

[25] John B. Fraleigh, "First Course in Abstract Algebra" Addison-Welsley, Third Edition.

[26] P. Goddard, J. Nuyts and D. I. Olive, "Gauge Theories And Magnetic Charge," Nucl. Phys. B **125** (1977) 1.

[27] P. Goddard and D. I. Olive, "New Developments In The Theory Of Magnetic Monopoles," Rept. Prog. Phys. **41** (1978) 1357.

[28] A. Grothendieck, "Esquisse d'un Programme," Preprint 1985.

[29] A. Hanany and Y. Oz, "On the quantum moduli space of vacua of N=2 supersymmetric SU(N(c)) gauge theories," Nucl. Phys. B **452**, 283 (1995), hep-th/9505075.

[30] G. Jones and M. Streit, "Galois Groups, Monodromy Groups and Cartographic Groups Geometric Galois Actions: 2. The Inverse Galois Problem, Moduli Spaces and Mapping Class Groups," London Math. Soc. Lecture Notes Series **243**, Cambridge Univ. Press 1997, 25-65.

[31] A. Kapustin, "The Coulomb branch of N = 1 supersymmetric gauge theory with adjoint and fundamental matter," Phys. Lett. B **398**, 104 (1997), hep-th/9611049.

[32] A. Klemm, W. Lerche, S. Yankielowicz and S. Theisen, "Simple singularities and N=2 supersymmetric Yang-Mills theory," Phys. Lett. B **344** (1995) 169 [arXiv:hep-th/9411048].

[33] A. Klemm, W. Lerche and S. Theisen, "Nonperturbative effective actions of N=2 supersymmetric gauge theories," Int. J. Mod. Phys. A **11** (1996) 1929 [arXiv:hep-th/9505150].

[34] W. Lerche, "Introduction to Seiberg-Witten theory and its stringy origin," Nucl. Phys. Proc. Suppl. **55B** (1997) 83 [Fortsch. Phys. **45** (1997) 293] [arXiv:hep-th/9611190].

[35] C. Montonen and D. I. Olive, "Magnetic Monopoles As Gauge Particles?," Phys. Lett. B **72** (1977) 117.

[36] G. W. Moore and N. Seiberg, "Polynomial Equations for Rational Conformal Field Theories," Phys. Lett. B **212**, 451 (1988).

[37] G. W. Moore and N. Seiberg, "Naturality in Conformal Field Theory," Nucl. Phys. B **313**, 16 (1989).

[38] G. W. Moore and N. Seiberg, "Classical and quantum Conformal Field Theory," Commun. Math. Phys. **123**, 177 (1989).

[39] V. A. Novikov, M. A. Shifman, A. I. Vainshtein, M. B. Voloshin and V. I. Zakharov, "Supersymmetry transformations of instantons," Nucl. Phys. B **229** (1983) 394.

[40] H. Osborn, "Topological Charges For N=4 Supersymmetric Gauge Theories And Monopoles Of Spin 1," Phys. Lett. B **83** (1979) 321.

[41] A. M. Polyakov, "Particle spectrum in quantum field theory," JETP Lett. **20** (1974) 194 [Pisma Zh. Eksp. Teor. Fiz. **20** (1974) 430].

[42] M. K. Prasad and C. M. Sommerfield, "An Exact Classical Solution For The 'T Hooft Monopole And The Julia-Zee Dyon," Phys. Rev. Lett. **35** (1975) 760.

[43] L. Schneps, "The Grothendieck Theory of Dessins d'Enfants," London Mathematical Society Lecture Note Series, vol 200, 1994.

[44] N. Seiberg, "Supersymmetry And Nonperturbative Beta Functions," Phys. Lett. B **206** (1988) 75.

[45] N. Seiberg, "Adding fundamental matter to 'Chiral rings and anomalies in supersymmetric gauge theory'," JHEP **0301**, 061 (2003), hep-th/0212225.

[46] N. Seiberg and E. Witten, "Electric - magnetic duality, monopole condensation, and confinement in N=2 supersymmetric Yang-Mills theory," Nucl. Phys. B **426**, 19 (1994) [Erratum-ibid. B **430**, 485 (1994)], hep-th/9407087.

[47] N. Seiberg and E. Witten, "Monopoles, duality and chiral symmetry breaking in N=2 supersymmetric QCD," Nucl. Phys. B **431**, 484 (1994), hep-th/9408099.

[48] G. Shabat and A. Zvonkin, "Plane Trees and Algebraic Numbers," in Jerusalem Combinatorics '93, 178 AMS Publications.

[49] D. Shih, "Singularities of N = 1 supersymmetric gauge theory and matrix models," JHEP **0311**, 025 (2003), hep-th/0308001.

[50] K. Strebel, "Quadratic Differentials," Springer-Verlag, 1984

[51] A. Strominger, "Special Geometry," Commun. Math. Phys. **133** (1990) 163.

[52] G. 't Hooft, "Magnetic Monopoles In Unified Gauge Teories," Nucl. Phys. B **79** (1974) 276.

[53] E. Witten, "Monopoles and four manifolds," Math. Res. Lett. **1**, 769 (1994), hep-th/9411102.

[54] E. Witten and D. I. Olive, "Supersymmetry Algebras That Include Topological Charges," Phys. Lett. B **78** (1978) 97.

[55] M. Wood, "Belyi-extending maps and the Galois action on dessins d'enfants," math.NT/0304489.

[56] B. Zumino, "Supersymmetry And Kahler Manifolds," Phys. Lett. B **87** (1979) 203.

Vita

1998-2002 *Laurea* in Phisics, Universitá di Torino, Torino, Italy.

2002-2007 Graduate studies in physics, Department of Physics and Astronomy, Rutgers University.

2002-2003 Teaching Assistantship, Department of Physics and Astronomy, Rutgers University.

2004-2007 Graduate Assistantship, Department of Physics and Astronomy, Rutgers University.

2005 Graduate Fellowship, Kavli Institute for Theoretical Physics, Santa Barbara, United States.

List of Publications

2004 S. K. Ashok, E. Dell'Aquila and D.-E Diaconescu, *Fractional Branes in Landau-Ginzburg Orbifolds*, Adv. Theor. Math. Phys., **8**, 461-513, `hep-th/0401135`.

2004 S. K. Ashok, E. Dell'Aquila, D.-E Diaconescu and B. Florea, *Obstructed D-Branes in Landau-Ginzburg Orbifolds*, Adv. Theor. Math. Phys., **8**, 515-563,`hep-th/0404167`.

2005 E. Dell'Aquila, *D-Branes in Toroidal Orbifolds and Mirror Symmetry*, JHEP, **604**, 35, `hep-th/0512051`.

2006 S. K. Ashok, F. Cachazo and E. Dell'Aquila, *Strebel Differentials with Integer Lengths and Argyres-Douglas Singularities*, `hep-th/0610080`.

2006 S. K. Ashok, F. Cachazo and E. Dell'Aquila, *Children's Drawings from Seiberg-Witten Curves*, `hep-th/0611082`.